CHARACTERIZING THE EFFECT OF CJUN ON THE EXPRESSION OF OCT4 VARIANTS AND HOW THEY CORRELATE WITH THE EXPRESSION OF GENES ASSOCIATED WITH POTENCY AND CELL FATE OF MURINE EMBRYONIC STEM CELLS

By

Kristine Teague

A Thesis Presented to

The Faculty of Humboldt State University

In Partial Fulfillment of the Requirements for the Degree

Master of Science in Biology

Committee Membership

Dr. Amy Sprowles, Committee Chair

Dr. John W. Steele, Committee Member

Dr. Jacob P. Varkey Punnamkuzhyil, Committee Member

Dr. Bruce A. O'Gara, Committee Member

Dr. Erik S. Jules, Program Graduate Coordinator

December 2018

ABSTRACT

CHARACTERIZING THE EFFECT OF CJUN ON THE EXPRESSION OF OCT4 VARIANTS, POTENCY AND CELL FATE OF MURINE EMBRYONIC STEM CELLS

Kristine Teague

cJun is a transcription factor associated with proliferation and growth. Recent evidence has shown it plays a role in cell fate decision making of embryonic stem cells and correlates with changes in Oct4 expression, an important marker for pluripotency. There are multiple Oct4 isoforms that arise from alternative splicing and alternative translation. Oct4A is the variant most frequently associated with pluripotency, while evidence suggests that Oct4B variants have roles in potency as well as stress responses.

We aimed to study the effect of cJun over expression in murine embryonic stem cells on *Oct4* gene expression through two methods: transient transfection of a pLVX cJun plasmid and treatment with nocodazole. We hypothesized that *cJun* expression would be increased with both of these methods and that these increases would affect *Oct4* gene expression, which would affect the expression of the potency markers *Nanog* and *Sox2* and possibly the expression of germ layer markers *Brachyury, Sox1, Gata6, and Gata4*. The unphosphorylatable cJun mutant L40/42A was also transfected to assess the role of cJun transcriptional activity on these processes. Our results revealed a trend where increased *cJun* correlated with changes in *Oct4* variant expression that correlate with

cJun transcriptional activity. *Nanog* expression appeared unaffected by transfection, but decreased with nocodazole treatment. *Sox2* expression appeared to increase slightly with transfection, but remained relatively unaffected by nocodazole treatment. cJun overexpression through transfection increased endoderm markers *Gata6* and *Gata4*, which correlates from other data in our laboratory that shows overexpression of cJun increases cardiomyocyte differentiation of mES cells (Brewer 2017). Further studies will better elucidate the relationship between cJun, the Oct4 variants, and their effect on potency and cell fate.

ACKNOWLEDGEMENTS

It has been a journey to get to this point. My time at HSU has been varied and I have met many amazing people along the way who have made this thesis possible. First, and most importantly, I'd like to thank my advisor Dr. Amy Sprowles for providing me with an opportunity to do research and to do it well. She is a constant inspiration and I am extremely grateful she was there for me. I'd also like to thank my committee members for supporting my decisions throughout this master's program and for their advice and patience.

I was also very fortunate to have amazing support from the staff, Susan Wright and David Baston. Both of them went above and beyond to provide me access to materials I needed. I'd like to specifically thank Susan for going the extra mile personally, to not only be a professional resource, but also to be my therapist and friend. She is a superhero and champion for all students and I am glad she was there for me.

Last, but not at all least, I'd like to thank all the friends I've made along the way, my family and my husband for supporting me throughout this process. They have all played the part of therapist, devil's advocate, and sounding board to help me process one thing or another. This whole experience would be meaningless without their presence.

TABLE OF CONTENTS

LIST OF TABLES

LIST OF FIGURES

LIST OF APPENDICES

INTRODUCTION

Cellular potency is the term used to describe the ability of undifferentiated cells to differentiate into multiple cell types. As cells become directed towards a particular cell fate, their potency decreases. Embryonic stem cells (ESCs) are derived from the inner cell mass (ICM) of the blastocyst and have the ability to form all the cells of the organism, as evidenced by their ability to contribute to all the tissues of a chimeric organism when placed into a blastocyst (Martin 1981). Therefore, they are described as pluripotent. The pluripotency of ESCs make them useful in studying the molecular and cellular mechanisms of organismal development and disease. Through an understanding of these processes, cellular-based therapies can be developed to provide targeted treatment options (reviewed in Pan et al. 2002, Romito and Cobellis 2016, Chen et al. 2017).

Cellular potency is controlled by a complex network of molecular mechanisms that regulate gene expression, beginning with chromatin regulation. The open and varied structures of chromatin in ESCs lead to expression of genes necessary for the pluripotent state, in comparison to more differentiated cells (Meshorer et al. 2006, Efroni et al. 2008, Barrero et al. 2010). Additionally, ESCs are characterized as having increased expression of chromatin remodeling factors (Ho et al. 2009) and hypomethylated promoters which facilitate gene expression (Grabole et al. 2013). In addition to open and active promoter regions, expression of developmental genes, such as those involved in lineage commitment, are regulated by bivalent promoter regions that suppress gene expression,

while leaving the machinery poised for transcription. These regions are characterized by H3K27me3 and H3K4me3 modifications (Azuara et al. 2006, Bernstein et al. 2006) which are antagonistic histone modifications, the presence of CpG islands (Fouse et al. 2008, Meissner et al. 2008), and the presence of RNA polymerase II at transcription initiation sites of many developmental genes (Guenther et al. 2007).

The three main transcription factors involved in maintaining pluripotency are Oct4, Sox2, and Nanog (reviewed in Chambers and Smith 2004, Takahashi and Yamanaka 2006, Okita et al. 2007, Chen et al. 2017). Generally, the three proteins work together to regulate expression of their own genes as well as others important to maintaining pluripotency (reviewed in Shi and Jin 2010). They also occupy many of these bivalent regions in various combinations, which suggests that they regulate the repression of developmental genes (Boyer et al. 2005). While these three factors are the main transcription factors, they work in cooperation with each other, and other transcription factors, to form a regulatory network that maintains pluripotency and self-renewal until a developmental signal initiates a differentiation program that changes the chromatin landscape (Wang et al. 2006, Pardo et al. 2010). Overexpression of the three together is sufficient for reprogramming terminally differentiated cells (Takahashi and Yamanaka 2006, Okita et al. 2007). Additionally, Oct4 is the only one which cannot be substituted with any other member of the Octamer binding protein family (reviewed in Jerabek et al. 2014).

The Role of Oct4 in Pluripotency and Development

Oct4/Pou5f1 is part of the POU, or Pit-Oct-Unc, family of transcription factors and is essential for the maintenance and self-renewal of pluripotent stem cells. The protein consists of a POU specific DNA binding domain, POU homeodomain, and C-terminal and N-terminal transactivation domains (reviewed in Shi and Jin 2010). Expression of the Oct4 protein is high in early development and is necessary for the pluripotency of the ICM during the blastocyst stage, as deletion of Oct4 in embryos during the transition from morula to blastocyst removes the ability of the embryo to differentiate toward primitive endoderm or epiblast tissues (Le Bin et al. 2014). Not only is Oct4 capable of actively maintaining potency through activation of potency genes, it also plays a role in lineage commitment and development. The loss of Oct4 results in the inability of the ICM to develop into the three germ layers required for development and instead becomes trophectoderm tissue (Nichols et al. 1998, Velkey and Sue O 'shea 2003). Oct4 levels must be kept at specific levels to maintain potency (reviewed in Shi and Jin 2010). A less than two-fold over expression of Oct4 can lead to differentiation into primitive endoderm and mesoderm tissues, more specifically, derivatives of those germ layers, such as the cardiac cell lineage in mouse ESCs and embryos in the early stages of differentiation (Zeineddine et al. 2006, Rodriguez et al. 2007), while a reduction of Oct4 expression by one-half leads to trophoblast tissue (Niwa et al. 2000).

A balance of enhancing and inhibiting factors function in combination with each of the three core pluripotency transcription factors to facilitate the cell fate decision making process that enables differentiation (Boyer et al. 2005, reviewed in Jerabek et al.

2014). Oct4 has been shown to be a key factor this process. When Oct4 is overexpressed in murine embryonic stem cells, it switches from the Sox2 promoter region to that of Sox17. This results in a change in chromatin structure from one that favors pluripotency to one that drives cells to mesoendoderm and ultimately cardiomyocyte-like cell fate (Aksoy et al. 2013, Abboud et al. 2015). Additionally, Oct4 regulates Fgf4 signaling which acts as a paracrine signal from ICM cells to the trophectoderm and directly activates expression of Gata6, predisposing it toward a primitive endoderm fate (reviewed in Jerabek et al. 2014). As a paracrine signal, Ffg4 initiates the upregulation of Sox17 and Gata4 in progenitor cells of the primitive endoderm, but the loss of Oct4 causes a complete loss of Gata6 four days post coitum (dpc) and the Fgf4-dependent gene expression of primitive endoderm genes is compromised and only minimally rescued with exogenous Fgf4.

Oct4 gene expression is regulated by a GC rich, TATA-less, and hypomethylated promoter which is critical to the maintenance and self-renewal of stem cells (Hattori et al. 2004; Feldman et al. 2006; reviewed in Hackett and Surani 2012). As it is conserved over a number of mammalian species, regulation of its expression and how it correlates with the stages of development has been well studied in the murine system (reviewed in Jerabek et al. 2014). There are two enhancer elements, distal and proximal, which drive transcription of *Oct4* in a tissue and developmentally specific manner. The proximal promoter is responsible for activity during the epiblast stage, while the distal enhancer functions prior to implantation and is then restricted to germ cell lineages following

implantation (reviewed in Jerabek et al. 2014). Multiple transcription factor proteins directly bind the *Oct4* promoter to control its transcription and external factors such as leukemia inhibitory factor (LIF), Wingless-related integration site (Wnt), and TGF-β/bone morphogenic protein (BMP) signaling influence *Oct4* expression. BMP works with LIF synergistically to maintain potency through activation of the JAK/STAT3 and phosphophatidylinositol 3-kinase (PI3K)/ AKT signal pathways to activate *Oct4* transcription (reviewed in Jerabek et al. 2014). *Oct4* transcription can also be increased through Wnt/ β-catenin signaling, which activates the TCF/LEF complex bound at three specific sequences in the *Oct4* promoter (Li et al. 2012). Examples of other molecules that regulate *Oct4* transcription include steroidogenic factor-1, estrogen-related receptor b (Esrrb), Sall4, Tcf3, HIF, CDK2, and germ cell nuclear factor (GNFC) (reviewed in Shi and Jin 2010 and Jerabek et al. 2014).

Oct4 activity is also regulated through mRNA splicing and alternative translation. The human *OCT4* gene, *POU5F1*, can produce 3 different mRNAs through alternative splicing: *OCTA*, *OCTB* and *OCT4B*1. OCT4A is the main variant involved in pluripotency and typically expressed at higher levels than *OCT4B* in nuclei of pluripotent cells (reviewed in Wang and Dai 2010 and Jerabek et al. 2014). The OCT4B splice variant contains an internal ribosomal entry site (IRES) and a different start codon that allows it to produce 3 different gene products through alternative translation: OC4B-265, OCT4B-190 and OCT4B-164. These variants only differ in their N-terminal transactivation domains: OCT4B-190 and -164 do not have N-terminal transactivation

domains and OCT4-265 has a domain that differs from OCT4A. All of the OCT4B isoforms have a nuclear localization signal, however they tend to localize in the cytoplasm. OCT4B-190 appears to respond to heat and cell stress and its overexpression protects against apoptosis following heat shock, while OCT4B-265 increases with genotoxic stress and is correlated with an increase in apoptosis (reviewed in Jerabek et al. 2014). The OCT4B1 variant is a putative stemness marker, because its expression pattern is high in undifferentiated cells and decreases upon differentiation, mimicking OCT4A expression throughout development (Atlasi et al. 2008, Papamichos et al. 2009). This was demonstrated in 59 human ESC lines as well as a significant correlation with NANOG expression in undifferentiated cells and a strong negative correlation to genes upregulated upon differentiation (Atlasi et al. 2008, Papamichos et al. 2009).

The mouse Oct4 homologue also produces Oct4A and Oct4B transcripts through alternative splicing. Cells in the neuroblastic layer of mice were found to express these Oct3/4 variants and to have both stem cell-like characteristics and those of differentiated neurons, providing a case for Oct4 expression in somatic tissues (Mizuno and Kosaka 2008). Oct4B can be translated into multiple isoforms: Oct4B-247aa, Oct4B-190aa and Oct4B-164aa (Guo et al. 2012). Mouse Oct4B is very similar to the human OCT4B. Oct4B localizes in the cytoplasm, increases expression upon heat shock or oxidative stress and many of the amino acids in the N-terminal domain are identical to the human OCT4B N-terminal domain. The expression of various isoforms appears to correlate to

different environmental and developmental functions, however Oct4A seems to have a larger role in development and pluripotency.

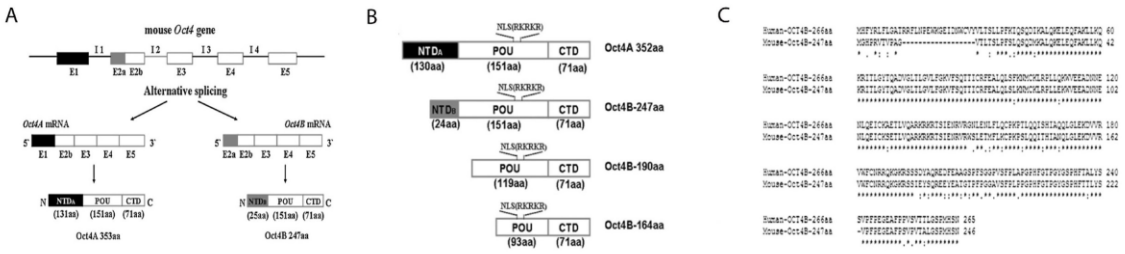

Figure 1. Mouse Oct4 produces two mRNA transcripts (A.) and four protein isoforms (B. and C.). These figures were originally published in Guo et. al 2012.

More recently Liu et al. have demonstrated new transcript and protein variants in mouse Oct4B (2017). They observed the same Oct4A and Oct4B transcripts seen previously, with the addition of four other transcript variants (**Figure 2**). These new Oct4B mRNAs vary in the number and size of introns retained. Oct4B and Oct4B' differ in the number of nucleotides spliced out of intron 1, while the remaining variants contain intron 2 (Oct4B1), introns 2 and 4 (Oct4B2), or introns 2 through 4 (Oct4B3). Because NIH3T3 cells do not produce endogenous Oct4 variants, protein variants were assessed through transient transfection with four constructs: Oct4b (pOb), Oct4b' (pOb'), Oct4b2 (pOb2), and Oct4b3 (pOb3). Protein analysis after 36 hours post transfection showed that Oct4b' produced one 189aa band, while the others produced three bands: Oct4B-246aa, -221aa and -189aa (**Figure 2**). Interestingly, these three bands are produced for Oct4b2

and 3 despite premature stop codons. Additionally, the 163aa product previously described by Mizuno and Kosaka (2008) was not seen in this study.

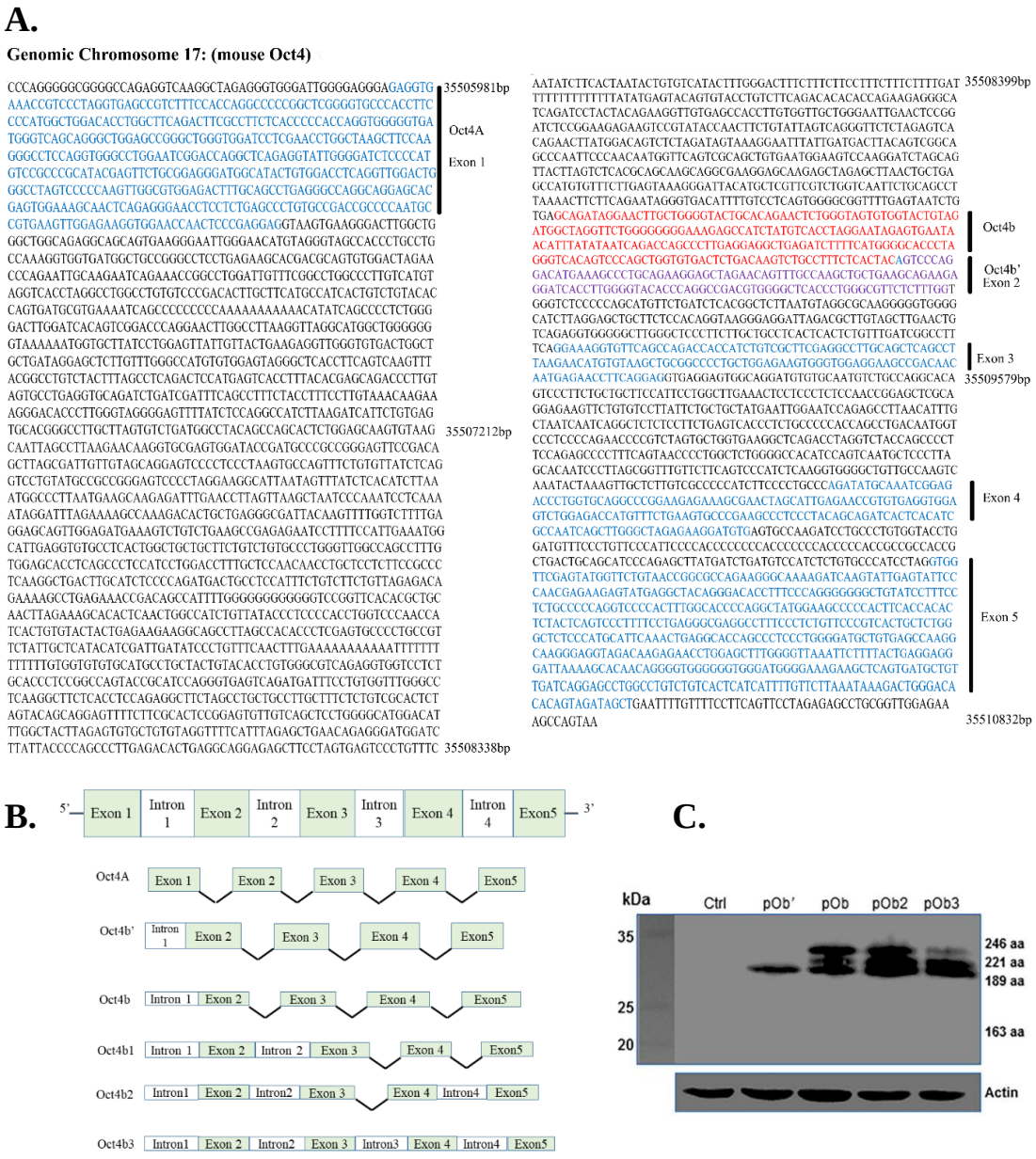

Figure 2: Mouse Oct4 produces six mRNA transcripts and multiple protein products. A. Analysis of mouse chromosomal 17 sequence shows the different exons for each variant in color and indicated by the bars to the right of the sequence. Oct4A mRNA consists of exon 1-5 with text in blue. The beginning sequence for Oct4b is highlighted in red text and the beginning of Oct4b' is highlighted in purple text. All exons and variants can also be determined by the bars to the right of the sequence. **B.** A graphical representation of the six mRNA transcripts. **C.** Western blot analysis of Oct4B protein from transiently transfected NIH3T3. Oct4b' (pOb')constructs produced one band at 189aa, while Oct4b (pOb), Oct4b2 (pOb2), and Oct4b3 (pOb3) each

Regulation of Oct4 Expression Through c-Jun

cJun is a dimeric transcription factor belonging to the activator protein 1 (AP-1) family. An immediate early gene, transcription of cJun is increased by mitogen stimulation (reviewed in Curran and Franza 1988). The transcriptional activity of cJun is increased through phosphorylation of serine-63 and serine-73 (reviewed in Shaulian and Karin 2002, Czaja 2003) primarily performed by mitogen activated protein kinase (MAPK) family member Jun N-terminal kinase (JNK) (reviewed in Shaulian and Karin 2002 and Eferl and Wagner 2003). cJun expression can also be increased through alternative translation pathways activated through cytoskeletal disrupting drugs such as nocodazole (Polak et al. 2006, Blau et al. 2012). Nocodazole increases cJun protein expression in cell culture, but this is independent of mitogen activation and does not increase cJun transcript levels (Polak et al. 2006). Rather, the alternative translation of cJun was shown to be regulated by an IRES in the cJun 5' UTR (Polak et al. 2006).

cJun has been shown to provide a variety of functions during cellular cycling and development. It regulates cellular progression from G to S1 of the cell cycle, apoptosis, and oncogenic transformation (reviewed in Jochum et al. 2001and Shaulian and Karin 2002). Additionally, cJun plays a role in development. cJun deficient mice, which contain a mutation in the cJun locus, die 11-12 days post coitum (dpc) (Johnson et al. 1993) and these fetuses present with defects in the interventricular septum of the heart and incomplete separation of aorta and pulmonary artery, suggesting lethality is a result of impaired cardiovascular function (Eferl et al. 1999). cJun deficient ESCs were able to

contribute to all tissues in a chimeric mouse, except for the liver (Hilberg et al. 1993) and cJun deficient fetal hepatocytes have an increased incidence of apoptosis and decreased proliferation (Eferl et al. 1999). Loss of cJun in hepatocytes, postnatally, did not result in any abnormalities other than impaired regeneration following a partial hepatectomy (Behrens et al. 2002). cJun was also expressed almost ubiquitously throughout development, however heightened expression was noted within rapidly dividing cells (Wilkinson et al. 1989). A more recent study showed cJun expression promoted axon growth in central nervous system neurons, independently of other target genes thought to be essential for cJun to promote axon growth (Lerch et al. 2014). It has also been demonstrated that cJun inhibits the expression of potency genes such as *Nanog*, *Sall4*, and *Oct4* in mouse embryonic stem cells, while upregulating genes that lead to endoderm lineage like *Gata6* and *Gata4* (Liu et al. 2015).

cJun transcriptional activity can regulate *Oct4* transcription and transient expression of cJun has shown a decrease in pluripotency in mESCs (Liu et al. 2015, Veluscek et al. 2016, Hosawi et al. *in prep*). Our lab has located a putative AP-1 binding site within the proximal promoter of the *Oct4* gene. Using a polyclonal antibody generated from the first 138 amino acids of the human Oct 4 protein, we have shown an increase in endogenous phosphorylated cJun. This correlates with an increase in protein containing amino acids from the Oct4A and Oct4B isoforms in murine embryonic stem cells (mES) cells treated with anisomycin, a JNK activator, or transfected with a GFP cJun construct (Hosawi 2016). Overexpression of cJun in mES cells prevented the

formation of insulin secreting clusters (Hosawi 2016), increased Gata4 protein expression, and correlated with increased cardiomyocyte differentiation (Brewer 2017). Our lab also demonstrated that cJun can up-regulate transcription of the *Oct4* promoter through luciferase assays (Brewer 2017). Chromatin immunoprecipitation data shows cJun physically associates with the Oct4 promoter (Varkey unpublished data). In light of these data, we are interested in determining whether cJun can affect Oct4 variant expression and if that affects the expression patterns of genes involved in murine embryonic stem cell potency and cell fate decision making required in early embryonic development.

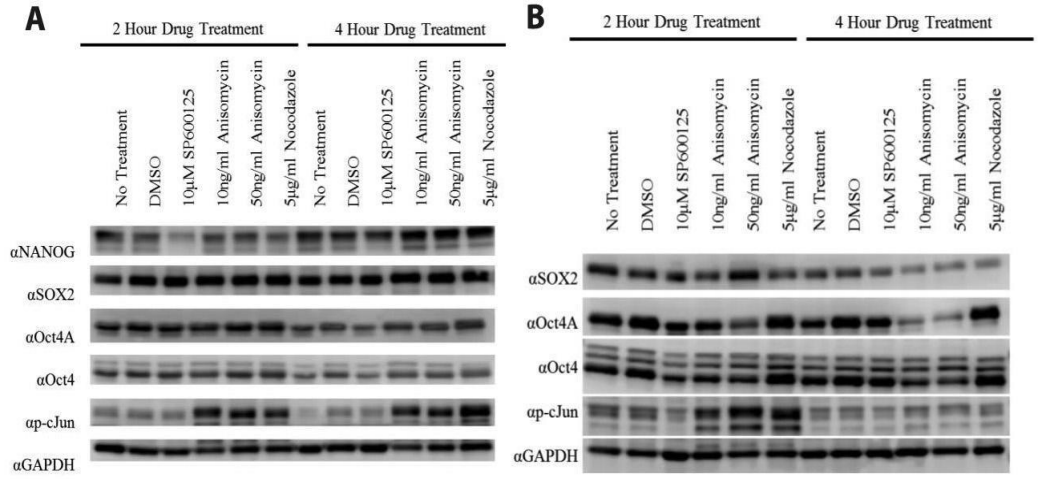

Figure 3. Immunoblot of nuclear protein from cells treated with SP600125, Anisomycin, and nocodazole. A. Following nocodazole treatment for 2h and 4h, cJun protein expression is increased. While Oct4A expression also increases upon treatment with nocodazole for 2h and 4h, Oct4all protein expression shows little change. **B.** Immunoblot data for a different replicate which shows an increase in cJun following 2h treatment with nocodazole, however no changes in cJun expression are seen at 4h. Additionally, Oct4all and Oct4A expression do not appear to change drastically, despite the differences in cJun expression at 2h and 4h.

Statement of Aims

This project aims to elucidate the role of cJun in regulating *Oct4* expression and its effects on the regulation of genes involved in pluripotency and early embryonic development. Data generated by others in our lab with an Oct4 variant-specific antibody suggested that cJun increased expression of the Oct4A and Oct4B, however it remains unclear whether this occurs at the transcriptional or translational control. If overexpression of cJun changes the expression of Oct4 in murine embryonic stem cells, we predict cell fate decision making could be affected. Finally, it is unknown if

cytoskeletal-induced translation of cJun occurs in murine embryonic stem cells and, if so, whether or not this mechanism affects Oct4 transcription and/or protein expression. We intend to address these questions through the following aims:

Specific Aim #1: Define the role of cJun in the regulation of mRNA expression of Oct4 and other pluripotency genes.

In order to test if cJun affects Oct4 expression at the transcriptional level, we have characterized the levels of Oct4 mRNA in mES cells that were transiently transfected with GFP cJun, the transcriptionally inactive cJun mutant GFP cJun L40/42A, and GFP alone. RNA was isolated from these cells, reverse transcribed to cDNA and screened by qPCR to see if there was a change in the transcript levels of *Oct4*A by using primers designed to amplify exon 1. We amplified *Oct4*B variants using primers for exon 2 (Oct4all_E2), which do not amplify *Oct4*A sequences, and all *Oct4* variants using primers for exon 5 (Oct4all_E5), which is present in all variants. Primers specific to the GFP cJun construct, pLVXcJun primers, were designed and used to establish levels of the ectopically expressed cJun mRNA above that of endogenous cJun (Appendix B). The expression of each gene was normalized to *Gapdh* and compared, using relative quantification, for each sample: no treatment (NT), empty vector (GFP), and a transcriptionally inactive cJun (L40/42) controls, as well as the GFP cJun overexpression construct. Because we have previously demonstrated that an increase in cJun correlates to an increase in a mixed pool of protein containing Oct4A, Oct4B or Oct4B1, we expected to see an increase in these transcripts if this correlation was transcriptionally regulated. If increases in cJun and/or Oct4 variants change the potency of the cells, we might also see

a modification in the mRNA levels of *Sox2* and *Nanog*. Therefore, qPCR was used to quantify those transcripts as well.

Specific Aim #2: Determine the effect of cJun overexpression on germ layer gene expression

If overexpression of cJun changes the amount of Oct4 protein in murine embryonic stem cells, we predicted the cells may be directed towards a specific cell fate. As a specific level of Oct4 protein is necessary to maintain pluripotency or initiate differentiation, an increase in Oct4 would lead to a change in expression of genes associated with germ layer formation, which we assessed through RT-qPCR. The cDNA generated from the mESCs transfected with GFP, GFP cJun, or GFP cJun L40/42A was analyzed for the expression of germ layer markers *Brachyury* (mesoderm), *Gata6* (endoderm), *Gata4* (endoderm), and *Sox1* (ectoderm). The gene expression for all genes and each sample was normalized to *Gapdh* and quantified using relative quantification.

Specific Aim #3: Determine if nocodazole treatment increases cJun protein in murine embryonic stem cells and if that increase correlates with changes in Oct4 protein expression

Immunoblot data in our lab demonstrates the addition of nocodazole to mESCs can increase the phosphorylation of cJun. It can also affect the levels of Oct4 protein, however the mechanism is unknown and our result is inconsistent (Figure 3).We are curious to know if the increased Oct4 isoforms observed are associated with the increased expression of cJun, or if the alternative translation pathway induced through cytoskeleton disruption would also affect Oct4 translation. As a preliminary test, we addressed the effect of nocodazole on Oct4 levels through RT-qPCR and immunocytochemistry (ICC)

assays. Cells were previously treated with nocodazole for two hours and stored for later RNA extraction. RNA was extracted from nocodazole treated cells, NT, and DMSO controls and evaluated for changes in the *Oct4* transcript. In addition, mESCs were treated with nocodazole and stained for cJun, Oct4 and Oct4A/B. While by no means a conclusive test, if increased cJun expression co-localizes with increased Oct4A expression, that would support a hypothesis that cJun overexpression is related to Oct4 expression.

METHODS

Basic Cell Culture of J1 Murine Embryonic Stem Cells

Murine Embryonic cell line J1 (American Type Culture Collection (ATCC) (Cat# SCRC1010, Manassas, VA) were grown on a feeder layer of murine embryonic fibroblasts treated with mitomycin C (MEFs, CytoSpring LLC, Mountain View, CA) and plated at 30,000 cells/cm^2 in culture dishes that have been pre-treated with a 0.1% gelatin solution (STEMCELL Technologies Inc, Vancouver, BC, Canada). Prior to mESC plating, these MEFs were incubated in MEF media consisting of 10% fetal bovine serum (Life Technologies, Carlsbad, CA) in 1X DMEM base media (Life Technologies, Carlsbad, CA). Mouse ESCs were grown in mESC media containing DMEM, 15% FBS, 1% 2.0mM L-Alanyl-L-glutamine (STEMCELL Technologies Inc, Vancouver, BC, Canada), 0.1 mM 2-mercaptoethanol (Sigma- Aldrich, Louis, MO), 1% 1X nonessential amino acids (Life Technologies, Carlsbad, CA), and 50 units/ml LIF (EMD Millipore, Temecula, CA). All cells were incubated at 37℃ and 5% CO_2 and passaged at approximately 50% confluency. Each time cells were passaged, cells were washed with sterile DPBS (Life Technologies, Carlsbad, CA), treated with 0.05% trypsin to remove adhered cells, spun down at 1400 x g for 5 minutes at room temperature and resuspended in warmed fresh mESC media. Cells were quantified and viability assessed with a trypan blue assay and all cells were plated at 30,000cells/cm^2.

.

Immunocytochemistry

MEFs were plated to glass coverslips coated in 2 µg/ml fibronectin (Sigma-Aldrich, Louis, MO) and incubated in MEF media described above until mESC plating. mESCs were plated on MEF coated coverslips at 30,000 cells/cm^2 and incubated in mESC media at 37°C and 5% CO_2 for 48h. Following this incubation, cells were treated with nocodazole at a final concentration of 5µg/ml or a 0.1% DMSO control for 2 or 4 hours. After drug treatment, cells were rinsed with DPBS and fixed in 0.5ml 4% paraformaldehyde in PBS per well for 5 minutes at room temperature. After fixation, the cells were washed five times in two-minute incubations with DPBS. The cells were then permeabilized with 2 ml of 1% NP-40 (Sigma- Aldrich, Louis, MO) in DPBS in each well and incubated at room temperature for 30 minutes. Next, blocking buffer containing 1.0% normal goat serum (Thermo Fisher Scientific, Waltham, MA) and 0.1% TX-100 (Sigma- Aldrich, Louis, MO) in DPBS was added to each well and incubated at room temperature for 30 minutes. The first primary antibody was added to their respective wells (Table 1): Anti-cJun (Abcam119944), Anti-Oct4 (Abcam ab19857) or Anti-Oct4A (Cell Signaling Technologies 2840S). A no primary control coverslip was treated with blocking solution instead of primary antibody and these cells were incubated at room temperature for 1h. The coverslips were washed three times, for 5 minutes each, with DPBS and the appropriate secondary antibody listed in Table 1 was added at the appropriate dilution to each well and incubated for 60 minutes at room temperature, in the dark. Coverslips were washed three times with DPBS, five minutes each, in the dark

and then placed back in block solution and incubated in the dark at room temperature for 30 minutes. Following this incubation, the second primary antibody was added to the appropriate wells, with block solution added to the no primary control, and incubated in the dark at room temperature for 60 minutes. While remaining in the dark, the cells were rinsed three times with DPBS, five minutes each, and the appropriate secondary antibody added (Alexafluor 488 or Texas Red, Table 1) (Molecular Probes, Life Technologies, Grand Island, NY).

Table 1. Antibodies and dilutions used in ICC analysis. Stem cells treated with nocodazole will be incubated with cJun and either Oct4 or Oct4A/B antibodies. This determined the relative expression of Oct4 or Oct4A/B in reference to cJun within the same cell.

Antibody	**Company and catalog number**	**Dilution**
Mouse anti-cJun	Abcam1ab 19944	1/200
Rabbit anti-Oct4	Abcam ab19857	1/200
Rabbit anti-Oct4A/B	Cell Signaling Technologies 2840S	1/200
Alexafluor 488: Goat IgG to mouse IgG	Life Technologies A11001	1/500
Texas Red: Goat IgG to rabbit IgG	Life Technologies T6391	1/200

Cells were incubated in the dark at room temperature for 60 minutes and rinsed three times with DPBS, five minutes each. Each coverslip was then be mounted on a glass slide with 7µl of DAPI mounting media (Molecular Probes, Life Technologies, Grand Island, NY) and allowed to cure overnight at room temperature, covered. The coverslips were then surrounded by nail polish, allowed to dry, and stored covered at 4°C

for long term storage. The cells were imaged using a Zeiss Axio Observer Z1 microscope.

RNA Isolation, cDNA Generation and Quantitative PCR

RNA was isolated from several stored samples, mentioned above, according to a protocol adapted from the Fisher Bio Reagents SurePrep TrueTotal RNA Purification Kit (Cat# BP2800-50). Briefly, cells were lysed with 350µl lysis solution containing beta-mercaptoethanol and vortexed for 15 seconds. 200µl of 95-100% ethanol was added and each sample vortexed for 10 seconds. The lysate solution was placed on column and centrifuged at 14000 x g for 1 minute. The flow-through was discarded and 400µl of wash solution was applied to the column and centrifuged at 14000 x g for 1 minute. The flow-through was discarded and this step was repeated once more. A third wash was done with 400µl of wash solution and spun down at 14000 x g for 2 minutes to dry the column. The collection tube was discarded with the flow-through and the column placed in a 1.5ml Eppendorf tube. Elution buffer (50µl) was added directly to the column and incubated at room temperature for one minute. This was centrifuged at 200 x g for two minutes, followed by a one-minute spin at 13,000 x g. The eluent was placed back on column and the step repeated. The concentration of the final product was determined using the NanoDrop 1000 Spectrophotometer (ThermoScientific, Waltham, MA). The RNA product was stored at -80℃ until needed.

Following extraction, 300ng of mRNA product was treated with 0.5-1U DNaseI (Invitrogen, Carlsbad, CA) for 15 minutes at room temperature and 1µl 25mM EDTA was added. The DNaseI was heat inactivated at 65°C for 10 minutes. This product was transcribed to cDNA using Applied Biosystems High Capacity cDNA Reverse Transcription Kit (Applied Biosystems, Foster City, CA) and a sample with reverse transcriptase enzyme (+RT) as well as a control sample without enzyme (–RT), were created for each sample according to the manufacturer's protocol. Once the reactions were loaded in the appropriate tubes, the reaction was run in a thermocycler with the following parameters: 25℃ for 10 minutes, 37℃ for 2 hours, 85℃ for 5 minutes and held at 4℃ until collection. These samples were stored at -20℃ for future use.

The PCR cocktail was prepared for a final volume of 20µl containing SYBR Advantage qPCR Master Mix at a final concentration of 1X, a ROX-LSR reference dye (Clonetech, Mountain View, CA) and 0.2µM of the appropriate primers (Table 2)**.** Oct4A and Oct4 variant expression were assessed with a probe-based assay (IDT). Cocktails were made according to manufacturer's protocol. Following this, samples were treated the same as the other primer sets. Template or water was added to the cocktail in its respective tube. cDNA samples were run in triplicate and three no template controls (NTCs) created for each gene. A control cDNA sample was serially diluted to create standard curves for each gene and the efficiency of each primer set was determined. The PCR reaction was set up using the software for the Applied Biosystems 7300 qPCR Machine. The reaction was carried out as follows: initial denaturation for 2 minutes at

95℃, denaturation at 95℃ for 40 cycles at 5 seconds each, annealing at 60℃ for 40 cycles at 30 seconds each, extension at 70℃ for 40 cycles at 30 seconds each and dissociation at 95℃ for 15 seconds, 60℃ for 1 minute, 95℃ for 15 seconds and 60℃ for 15 seconds. The annealing temperature varied depending on the primer set (

Appendix B). The results were analyzed with Applied PCR 7300 Analysis software.

To analyze the PCR product, a 2-3% agarose gel was prepared and run with 1X TAE Buffer. Loading dye was added to each PCR product to give a final concentration of 1X. Half of this volume was loaded into subsequent wells and run at 70 volts for one to two hours, stained in ethidium bromide and rinsed in dH_2O. Stain and rinse incubation times varied depending on the amount of agarose. The gel was imaged using the AlphaImagerHP MultiImage II (Alpha Innotech).

Data Analysis

Gene expression data for each gene was normalized to *Gapdh* expression and relative expression determined using a modified Michael W. Pfaffl equation which accounts for varied primer efficiencies (Pfaffl 2004). These data are given as Mean ± Standard Error (SE). Additionally, dissociation curves were produced for each sample to account for the decreased specificity of SYBR. This was not performed for the probe-based assays. The significance of these data was determined by performing a one-way ANOVA in R Studio for each gene. Tukey's HSD analysis was performed on ANOVA

results which produced p-values less than 0.05. All ICC images were processed identically to ensure they were comparable and co-localization was assessed using the ZEN imaging software from Carl Zeiss (Zeiss).

RESULTS

Characterizing cJun Over Expression in mESCs Transiently Transfected with PLVX-GFPcJun and PLVX-GFP L40/42A

If cJun regulates Oct4 variant expression, one would expect ectopic overexpression of the cJun protein would affect Oct4 mRNA levels. Furthermore, if cJun regulates transcription of the Oct4 mRNA directly, cells in which the transcriptionally inactive cJun mutant L40/42A is expressed should have a different effect on Oct4 mRNA levels when compared to control cells than those overexpressiong wild type cJun. To test these hypotheses, pLVXGFP, pLVX GFP cJun and the pLVX GFP cJun L40/42A mutant plasmids were transfected into mES cells with Lipofectamine 3000, plated onto gelatin and harvested 36 hours post transfection, after transfection efficiency was confirmed by flourescent microscopy of GFP. mRNA was isolated and converted to cDNA. To identify for biological variation, the transfections were performed in triplicate 3-4 times.

As immunoblot data from our lab demonstrates that endogenous cJun is expressed in J1 mES cells cultured on irradiated MEFs in LIF media (Figure 3 and not shown) and transfection efficiency was relatively low (< 20%), we developed two qPCR primer sets for cJun mRNA quantitation. One was directed to transcripts produced by the cJun loci in the genomic DNA as well as those from the pLVXcJun and L4042 plasmids (cJun primers). The second set was designed such that the forward primer was

complimentary to pLVX sequences 5’ of the cJun coding sequence in the plasmid (pLVXcJun primers).

When *cJun* cDNA was quantified using the cJun primers and compared to cJun transcript levels in untransfected control cells, the expression levels normalized to NT showed a 41.45±8.44 fold increase in cells transfected with the pLVX cJun plasmid and a 32.81±14.54 fold increase in those transfected with pLVXL4042. These were significantly higher than expression levels seen in cells transfected with pLVXGFP, which had a fold change of 1.13±0.34. When the pLVX cJun primers were used to quantify cJun cDNA levels, the fold change expression of pLVX cJun transcripts compared to untransfected controls was 650.93±314.5 for cJun, 154.3±61.53 for L40/42A and 4.92±3.22 and for GFP. Unlike the products produced by the cJun primers, only one band of the appropriate size was generated in these reactions. (Figure 4 and Table 2)

The slightly increased expression of cJun in the cells expressing GFP alone suggested the plasmid transfection appeared to have an effect on gene expression in general. Knowing the GFP plasmid did not contain endogenous cJun, we evaluated the levels of cJun normalized to GFP expression. The GFP normalized cJun expression data generated with the cJun primers were 38.96±16.16 and 31.97±13.18 for cells transfected with cJun plasmid and L40/42 respectively. The GFP normalized cJun expression data generated with the pLVXcJun primers was 199.28±52.73 and 61.87±29.9 for cJun and L40/42 transfected cells, respectively. A one-way ANOVA was performed on these data

and found that cJun expression normalized to NT alone varried significantly ($p<0.05$, $n=3$, $F(3,8)= 6.306$). Tukey's HSD determined that cJun expression varied significantly between cJun transfected cells and NT or GFP samples ($p<0.05$, $n=3$,). One way ANOVA did not show any statistically significant difference between treatments with cJun data normalized to GFP. Plasmid expression normalized to both NT and GFP were significant by one-way ANOVA, $p<0.05$ and $p<0.01$ for NT($F(3,12)= 3.673$) and GFP normalized ($F(2,9)= 9.747$), respectively ($n=4$).Tukey's HSD showed that plasmid expression normalized to NT was not as significant with $p<0.1$($n=4$) for cJun transfected cells compared to NT or GFP samples. Plasmid expression normalized to GFP were significant for cJun samples compared to NT ($p<0.05$) and GFP ($p<0.01$) by Tukeys HSD test ($n=4$). Gel analyses of these samples showed that cJun and L40/42 transfected samples produced multiple bands, however dissociation curve analysis did not always produce multiple peaks for cJun primers (Figure 4 and **Table 2**). Although the pLVXcJun primers produced multiple dissociation peaks, gel analysis demonstrated only one prominent band at the predicted size of 70bp (Figure 4). Because of this, we utilized pLVX expression as an analog for transfection efficiency and thus a marker for cJun over expression.

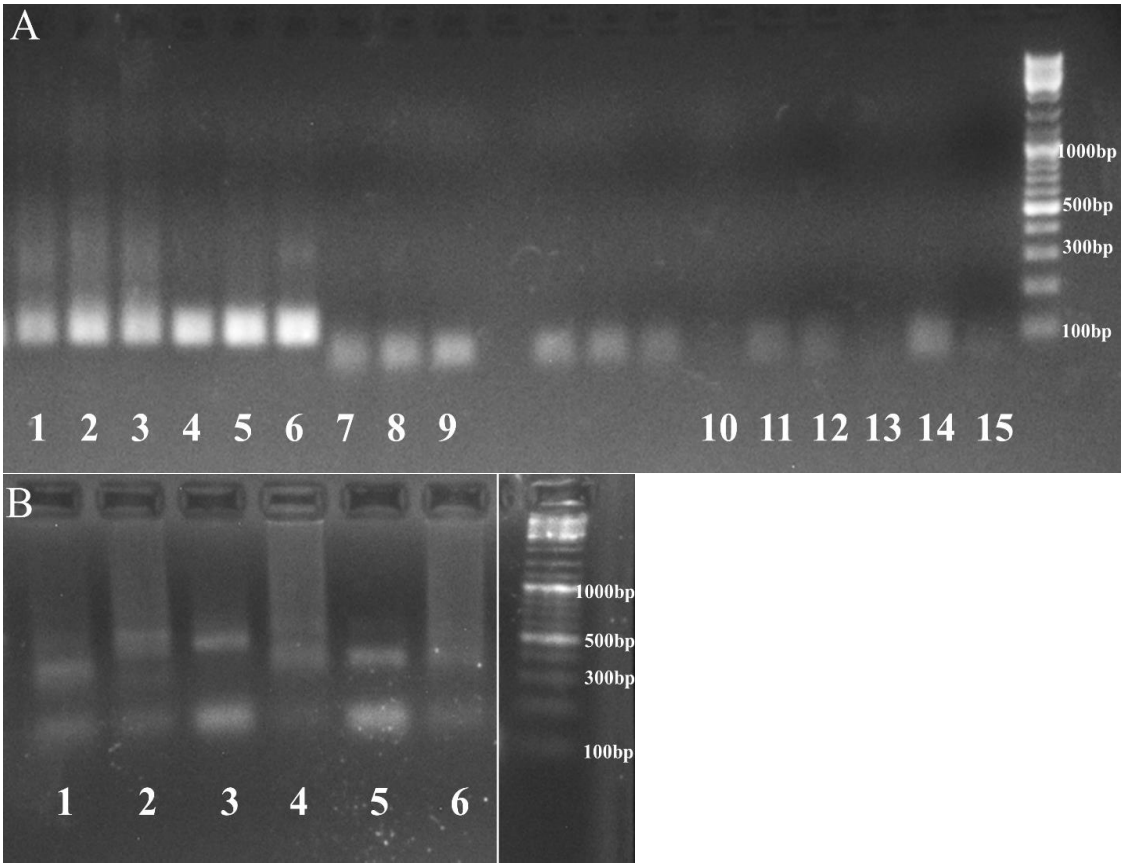

Figure 4. cJun primers produced multiple bands upon agarose gel analysis while pLVX primers produced singular bands. A. A representative image of both cJun and pLVXcJun PCR products. Dissociation curve analysis of cJun primers produced multiple peaks and multiple bands on the gel (lanes 4-6). One sample did produce a dissociation curve with one clear peak, but still showed multiple bands on the gel (lanes 1-3). This could be due to amplification of the transfected plasmid resulting in single strands. The pLVXcJun primers always produced one band at 70bp, but almost all replicates had dissociation curves with 2 peaks (lanes 10-12 and 13-15). Two replicates had one dissociation peak, but only one was analyzed on a gel and also produced one band at 70bp (lanes 7-9). The second dissociation peaks were small and could be due to GC or AT rich regions in the sequence that would cause a small secondary peak once it dissociated. **B.** An example of the multiple bands seen with cJun primers. Here more distinct bands can be seen and each sample had dissociation curves with multiple peaks. Lanes are labeled with replicate date, then sample as follows: 1-3) 32 L40/42, 4) 32 cJun, 5) 510L40/42, and 6) 530 L40/42. These data are also summarized in table 2.

Table 2. List of cJun and pLVXcJun samples, Ct value, approximate dissociation temperatures, number of each triplicate affected and number of bands present on agarose gel. Only samples transfected with the L40/42 cJun mutant or GFP cJun produced variable data. Upon gel analysis, all cJun samples showed multiple bands for all triplicates, however dissociation curve analysis did not always show multiple peaks for those triplicates. Ct values were all within 1 Ct value, demonstrating that expression was not greatly affected by the additional bands. In contrast to cJun expression, amplification with plasmid primers produced dissociation curves with multiple peaks, but only one band upon gel analysis. The multiple dissociation peaks were inconsistent and did not affect all triplicates. Asterisk indicates samples not used in data analysis.

Replicate	Treat-ment	Primer set	Average Ct value	Approximate dissociation temperature (ºC)	# of triplicate	Bands present	Fold change express-ion normal-ized to NT or GFP
1	GFP	cJun	14.29	85	3	No gel run	NT: 262.99*
1	L40/42	cJun	18.08	87	3	No gel run	NT: 8.65*, GFP:0.03*
1	cJun (plasmid)	cJun	16.61	87	3	No gel run	NT: 30.57*, GFP:0.13*
2	GFP	cJun	23.12	85	3	No gel run	NT: 0.57
2	L40/42	cJun	17.67	84 and 87	3	118bp, 290bp, 500bp	NT: 29.96, GFP: 53.01
2	cJun (plasmid)	cJun	18.45	84 and 87	1	118bp, 190bp, 290bp	NT: 48.79, GFP: 86.35
3	GFP	cJun	20.85	85	3	No gel run	NT: 1.1
3	L40/42	cJun	21.77	84 and 87	1	118bp, multiple bands of indeterminant size in the 190-700bp range	NT: 9.17 GFP:8.3

Replicate	Treat-ment	Primer set	Average Ct value	Approximate dissociation temperature (ºC)	# of triplicate	Bands present	Fold change express-ion normal-ized to NT or GFP
3	cJun (plasm id)	cJun	16.88	85 and 87	3	Multiple bands of indeterminant size between 118-190bp	NT:24.62 GFP:22.27
4	GFP	cJun	20.95	85	3	No gel run	NT:1.75
4	L40/42	cJun	16.69	84 and 87	1	118bp, bands of indeterminant size ≥ 500bp	NT:59.31 GFP:33.98
4	cJun (plasm id)	cJun	17.28	85	3	bands of indeterminant size between 118-190bp and 300-500bp	NT:50.95 GFP: 29.19
1	GFP	pLVXc Jun	40	78, 84	3	No gel run	NT: 0.77
1	L40/42	pLVXc Jun	34.53	82	3	No gel run	NT: 21.81 GFP:28.98
1	cJun (plasm id)	pLVXc Jun	32.47	82	3	No gel run	NT:119.64 GFP: 168.51
2	GFP	pLVXc Jun	40	79, 89, 88	3	No gel run	NT: 0.72
2	L40/42	pLVXc Jun	33.20	82	3	70bp	NT: 107.84 GFP:149.2
2	cJun (plasm id)	pLVXc Jun	32.37	82	3	70bp	NT:239.43 GFP: 331.28
3	GFP	pLVXc Jun	38.1	71,76,86	3	No gel run	NT:3.89
3	L40/42	pLVXc Jun	30.61	76 and 82	1	70bp	NT:174.46 GFP: 44.85

Replicate	Treat-ment	Primer set	Average Ct value	Approximate dissociation temperature (ºC)	# of triplicate	Bands present	Fold change express-ion normal-ized to NT or GFP
3	cJun (plasm id)	pLVXc Jun	30.76	76 and 82, 76 and 90	2	70bp	NT: 740.68 GFP: 190.42
4	GFP	pLVXc Jun	36.642	70,78	3	No gel run	NT:14.3 4
4	L40/4 2	pLVXc Jun	32.68	76 and 82	1	70bp	NT:313. 41 GFP: 21.86
4	cJun (plasm id)	pLVXc Jun	31.07	76 and 82	2	70bp	NT: 1504.03 GFP: 104.89

Overexpresion of cJun Has a Varied Effect on mRNA Expression of Oct4A and Pluripotency Markers Nanog and Sox2

Having varified transfection of PLVXcJun and PLVXL4042/A leads to over expression of cJun in each of the four experimental replicates, we were interested in measuring *Oct4* cDNA levels to determine the effect of cJun overexpression on this important pluripotency marker. As the level of Oct4 protein affects cellular potency, we also determined gene expression for two other pluripotency factors, *Nanog* and *Sox2*. Primer sets were validated by amplifying both cDNA from mESCs and DNA, correct amplicon size confirmed, and sequenced for correct amplicon sequence. The gels for this can be seen in Figure 5 and produced the following amplicon sizes: 230bp (*Gapdh*),

118bp (*cJun*), 70bp (GFPcJun plasmid), 364bp (*Nanog*), 207bp (*Sox2*), and 111bp (*Oct4*A).

When normalized to untransfected cells (NT), *Oct4*A cDNA was 1.52±0.3 fold higher in pLVX cJun transfected cells , 1.62±0.86 fold higher in PLVX L40/42 transfected cells and 1.36±0.4 fold higher in cells transfected with PLVX GFP. When normalized to *Oct4*A levels in cells expressing GFP, fold expression was 1.29±0.31 and 1.5±0.9 higher for cells expressing with cJun and L40/42 respectively. *Nanog* gene expression was 1.54±0.7, 1.22±0.43, and 1.17±0.42 for cJun, L40/42, and GFP transfected cells respectively. GFP normalized data were 1.15±0.28 and 1.02±0.17 for cJun and L40/42 respectively. Similarly, *Sox2* gene expression was 2.20±1.27, 3.61±2.75, and 1.45±0.67 for cJun, L40/42, and GFP transfected cells respectively. GFP normalized data were 1.31±0.32 and 1.72±0.62 for cJun and L40/42 respectively (Figure 5). One-way ANOVA analyses of NT and GFP normalized data produced no statistically significant difference between treatment for any gene ($p>0.05$, $n=4$). The affect of cJun over expression is variable and may be due to variations in transfection efficiency in each replicate. While not statistically signifcant, as changes in Oct4 expression of 1.5 fold have been demonstrated by others to have biological affects (Niwa 2000), the increases seen in the presence of cJun and L4042 are expected to effect potency. Therefore, it is possible the mild increases in *Nanog* and *Sox2* expression could also have biological implications.

A.

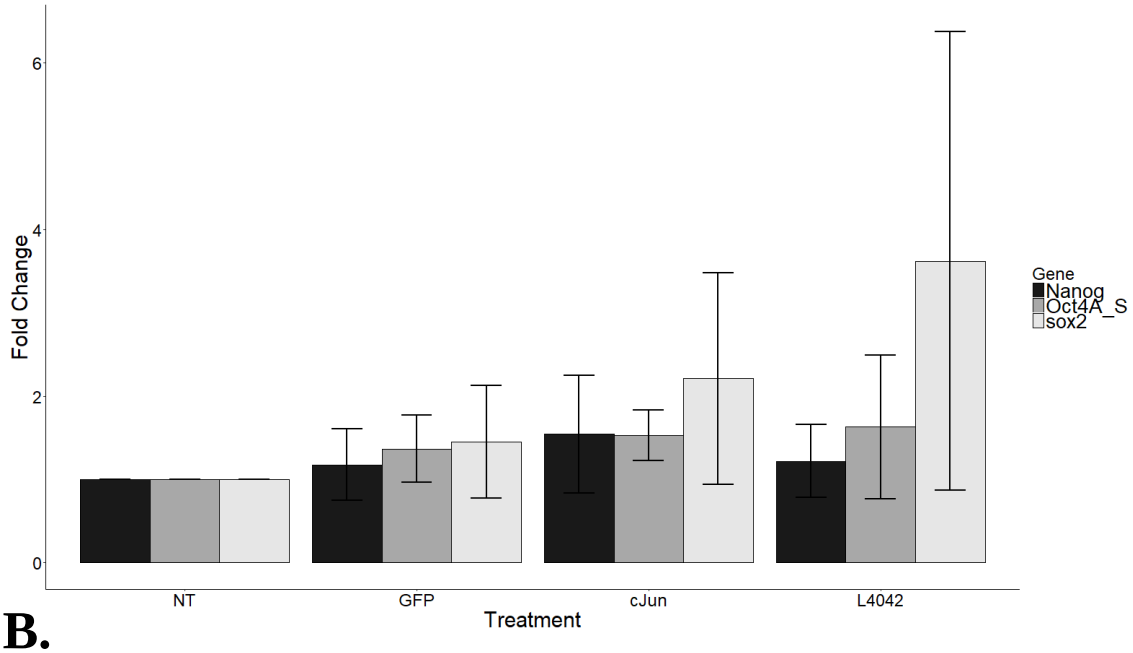
Fold Change
0
2
4
6
NT
GFP
cJun
L4042
Treatment
Gene
Nanog
Oct4A_S
sox2

B.

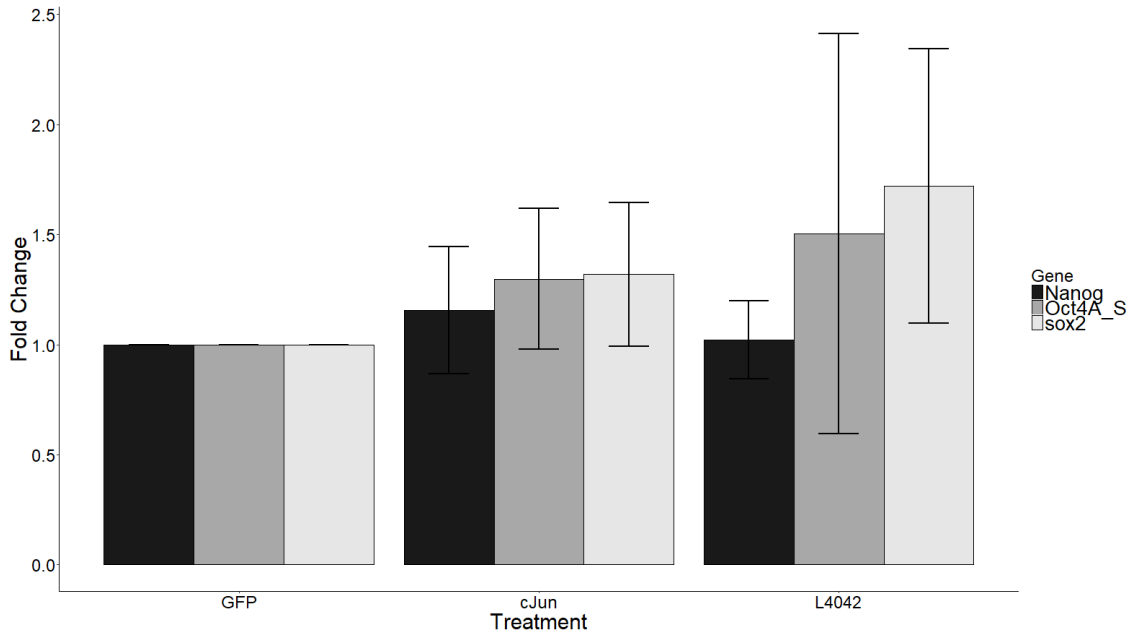
Fold Change
0.0
0.5
1.0
1.5
2.0
2.5
GFP
cJun
L4042
Treatment
Gene
Nanog
Oct4A_S
sox2

C.

Gene amplified	Treatment	Normalization	Average fold expression ± standard error
cJun	NT	NT	1
cJun	GFP	NT	1.138623±0.341253
cJun	cJun	NT	41.45499±8.442246
cJun	L40/42	NT	32.81479±14.54462
Plasmid	NT	NT	1
Plasmid	GFP	NT	4.929819±3.22303
Plasmid	cJun	NT	650.9483±314.5663
Plasmid	L40/42	NT	154.3834±61.53322
cJun	GFP	GFP	1
cJun	cJun	GFP	38.96696±16.16434
cJun	L40/42	GFP	31.97933±13.18219
Plasmid	GFP	GFP	1
Plasmid	cJun	GFP	199.2868±52.73759
Plasmid	L40/42	GFP	61.87357±29.93148

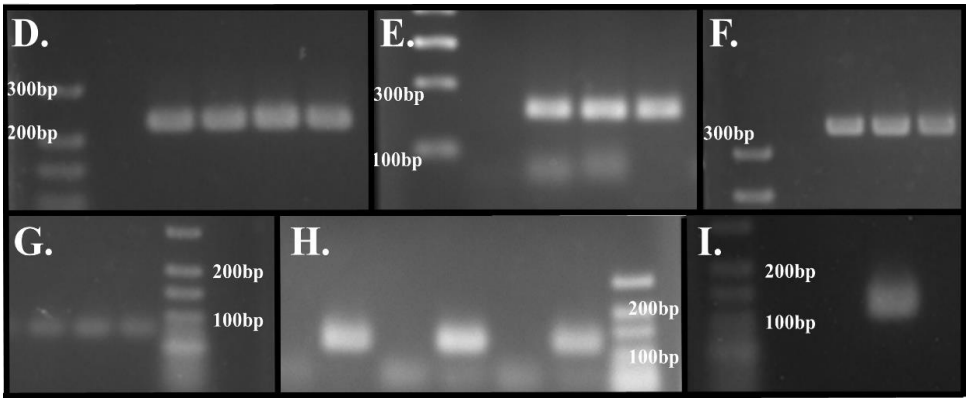

Figure 5. Overexpression of cJun affects expression levels of Sox2, and Oct4A. A. A graph of NT normalized expression data for *Oct4*A, *Nanog* and *Sox2*. **B.** Graph of the same expression data normalized to GFP. **C.** Table showing gene expression of cJun and plasmid (pLVXcJun primers) to demonstrate *cJun* over expression and plasmid transfection efficiency. Because transfection efficiency varied between replicate and between treatments, plasmid expression will be used as a marker for overexpression, in place of cJun expression. **D-I.** Gels of PCR amplified cDNA to confirm the correct amplicon size for each gene: *Gapdh* (D), *Sox2* (E), *Nanog* (F),

Because the *Oct4* gene produces multiple mRNA variants, we used a previously validated probe-based assay (Integrated DNA Technologies, Skokie, Illinois) to see if transfection with cJun affected variant expression. *Oct4*A gene expression was measured with a primer and probe set designed to bind exon 1, which is only present in the *Oct4*A

mRNA variant. These primers did not amplify genomic DNA under the experimental conditions, despite the presence of the forward and probe sequences in exon1 and the reverse in exon 2. The intron 1 sequence is a little over 2,300bp, which cannot be amplified in the 30sec annealing and elongation steps. The primer probe combination used to analyze exon 2 recognizes five *Oct4*B variants, *Oct4b', Oct4b, Oct4b1, Oct4b2,* and *Oct4b3*:. These primers did not initially amplify cDNA from mESCs, but did amplify from genomic DNA as well as cDNA generated from embryoid bodies (EBs). Finally, we used a primer and probe set which amplified exon 5, which is conserved over all *Oct4* mRNA variants. The exon 5 primers were designed to not amplify genomic DNA with a probe that spans an intron sequence, ensuring an trace amounts of genomic contamination would not be quantified (Figure 7). These data were normalized to untransfected (NT) and then to GFP in the same manner as the previous genes. When normalized to NT expression levels, Exon 1 expression was 1.73 ±0.36 fold higher for cJun transfected cells, 0.96±0.35 for the L40/42 and 1.58±0.63 for GFP transfected cells. The fold change for GFP normalized data was 1.35±0.19 and 0.94±0.47 for cJun and L40/42 respectively. Exon 2 expression was 2.71±1.1, 16.91±16.5, and 1.23 ±0.72 for cJun, L40/42, and GFP transfected cells. Expression for GFP normalized data were 5.97±4.73 and 74.21±73.51 for cJun and L40/42, respectively. Exon 5 gene expression was 1.51±0.25 for cJun transfected cells and 1.33±0.58 and 0.69±0.28 for the L40/42 and GFP controls. GFP normalized data were 4.13±2.2 and 6.5±5.2 for cJun and L40/42, respectively.

Dispite the large differences in *Oct4* expression levels seen in the presence of cJun and L40/42, a one-way ANOVA of these data, both NT and GFP normalized, did not show any significant difference in fold change between treatment for any gene ($p>0.05$, $n=4$) (Figure 6), likely due to the large standard error among the averaged samples. To see if the difference in Ct values were the result of irregular qPCR amplification among the replicates, these samples were run on agarose gels to confirm the expected base pair sizes of 111bp, 91bp, and 135bp for exon 1, exon 2, and exon 5 respectively (Figure 5 A-C). We found that exon 2 and exon 5 produced additional bands and smears, while exon 1 produced this result to a lesser extent. Upon analysis of new transcript sequences the new expected base pair band became 91bp (Oct4b'), 296bp (Oct4b2 and Oct4b3), and 297bp (Oct4b and Oct4b1) for exon 2. New expected sizes for exon 5 were 135bp for Oct4A, Oct4b', Oct4b, and Oct4b1 and 274bp for Oct4b2 and Oct4b3. Additional bands seen by agarose gel were between 100-900bp for exon 2, with the brightest bands at 296bp, indicating amplification of either Oct4b2, Oct4b3, Oct4b, or Oct4b1. Bands for exon 5 were between 135-800bp, with bright bands at the expected

135bp, indicating less expression of Oct4b2 and Oct4b3. Exon 1 produced only one band on the gel at the expected 111bp size (Figure 7 and

Figure 7. Exon 1 primers produce one amplicon, while exons 2 and 5 produce multiple bands from various Oct4B variants. A. Agarose gel of exon 1. Only one band is seen at the expected 111bp. There do appear to be very faint bands below these, which are assumed to be primer dimers or other noise, as they also appear in the –RT samples. Lanes 1-24 are triplicates for each treatment of one replicate and are consistent between treatments. Lanes 4-6 are NT, GFP are lanes 10-12, L40/42 are lanes 16-18, and cJun transfected samples are lanes 21-24. The remaining lanes are the corresponding –RT samples. **B.** Agarose gel of Exon 5. NT samples are in lanes 4-6., GFP in 10-12, L40/42 in 16-18, and cJun samples in lanes 21-24. You can see multiple bands in all samples. **C.** Agarose gel of exon 2. Lanes 4-6 are NT samples, 10-12 are GFP, 16-18 are L40/42, and 21-24 are cJun samples. Multiple bands can be seen in GFP, L40/42 and cJun samples. The bands in the L40/42 and cJun treatments are more abundant and varied in size. Additionally, cJun and L40/42 samples contain the largest band at about 1000bp and 900bp, respectively. These upper bands, denoted by the two white arrows, are faint but distinct. **D.** Agarose gel analysis of all the Oct4 primers off cDNA (lane2) and genomic DNA (lane 3). Exon 1 did not amplify in the no template control (NTC) sample (lane 1) or the genomic DNA. Similarly, exon 5 did not amplify the NTC (lane 7) or genomic DNA (lane 9), but did amplify cDNA (lane 8). Exon 2 only amplified the genomic DNA (lane 6). Because of this EB cDNA was used. **E.** Agarose gel analysis of exon 2 primers amplifying cDNA from embryoid bodies (EBs). Lane 1 shows the primers amplify genomic DNA and lane 3 shows they will amplify cDNA from EBs. Lane 2 shows the primers will not amplify the –RT sample.

Table 3). Because exon1 primers only produced one band and the probe sequence removes background qPCR signal, we assumed the extra bands seen on the gel for exon 2 and exon 5 only affect the calculated expression data if the bands contain the probe sequence and are variations on the known *Oct4*B variants.

A.

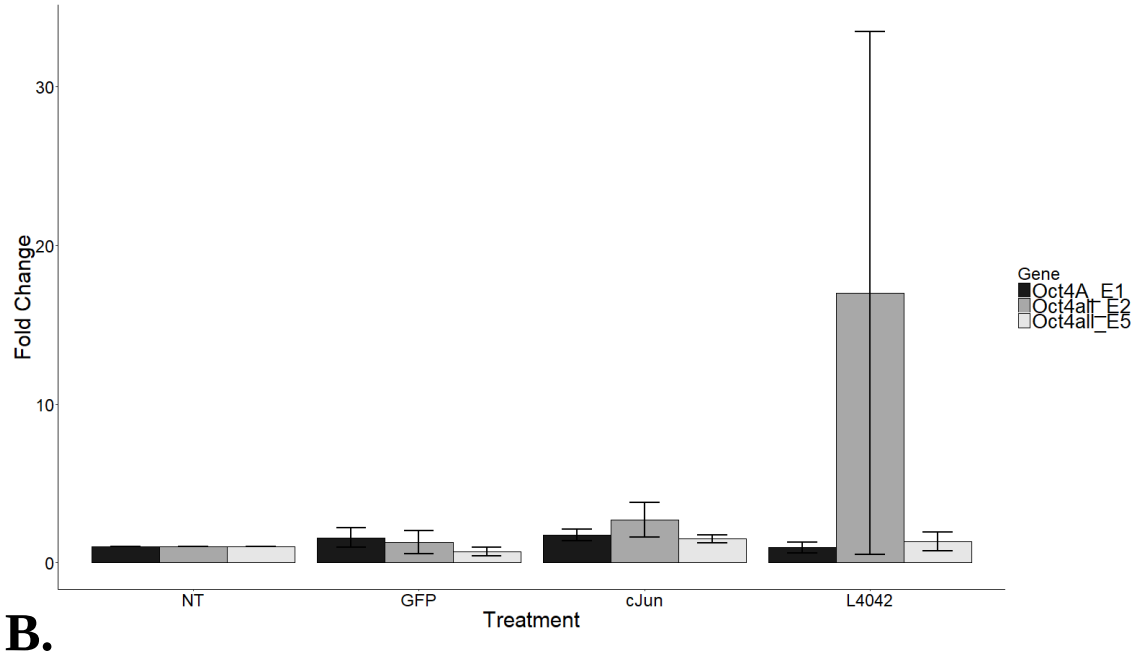
30
20
10
0
Fold Change
NT
GFP
cJun
L4042
Treatment
Gene
Oct4A_E1
Oct4alt_E2
Oct4alt_E5

B.

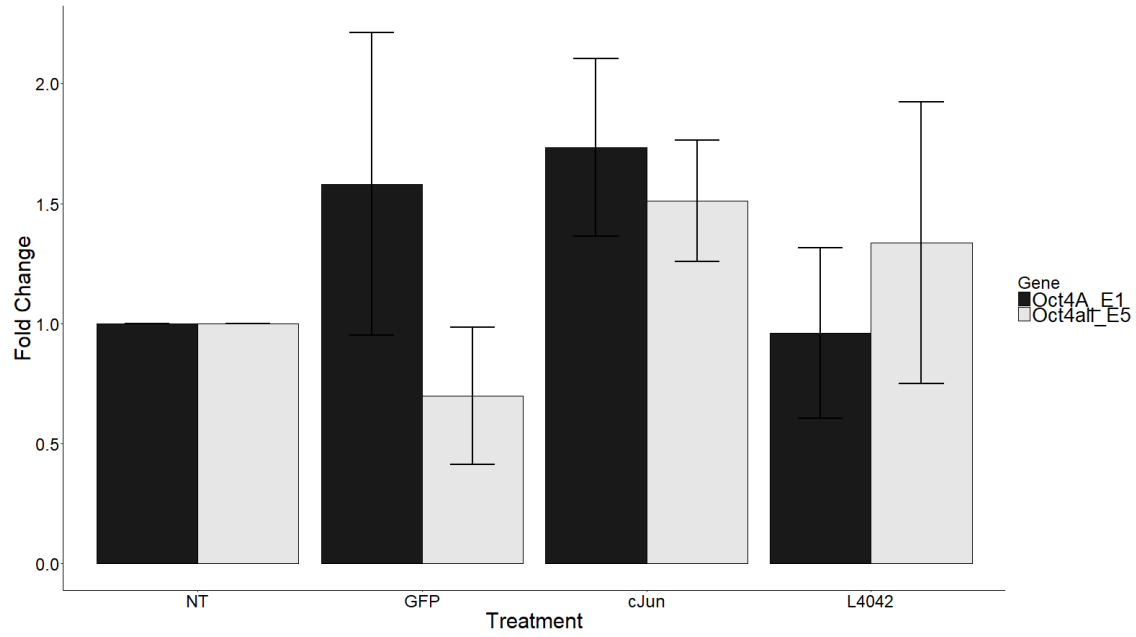
2.0
1.5
1.0
0.5
0.0
Fold Change
NT
GFP
cJun
L4042
Treatment
Gene
Oct4A_E1
Oct4alt_E5

C.

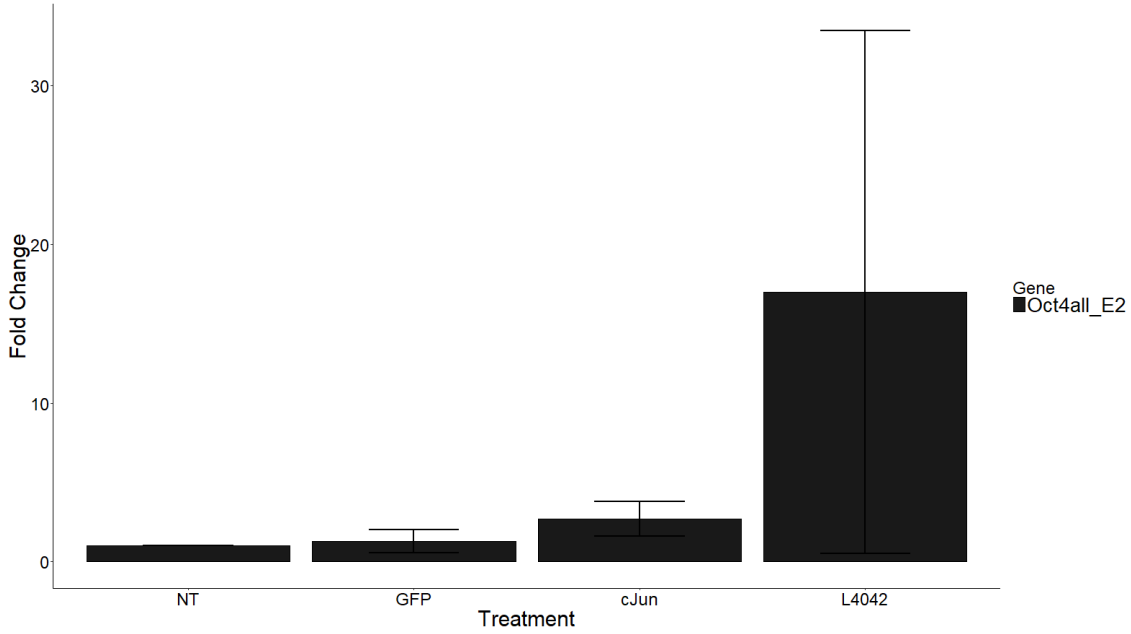
30
20
10
0
Fold Change
NT
GFP
cJun
L4042
Treatment
Gene
Oct4all_E2

D.

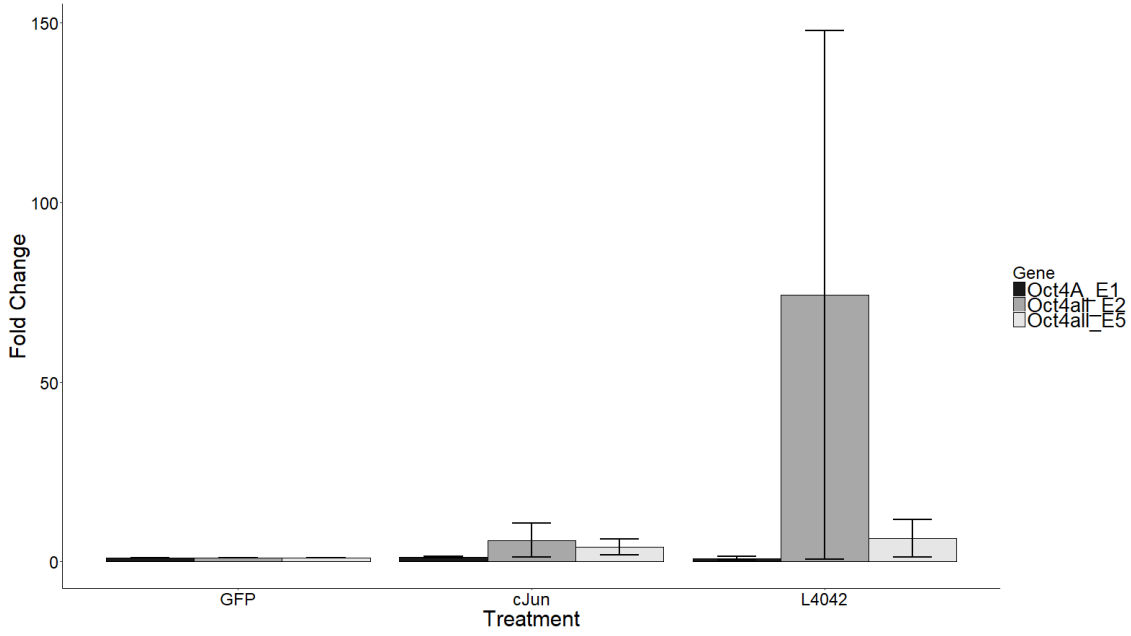
150
100
50
0
Fold Change
GFP
cJun
L4042
Treatment
Gene
Oct4A_E1
Oct4all_E2
Oct4all_E5

E.

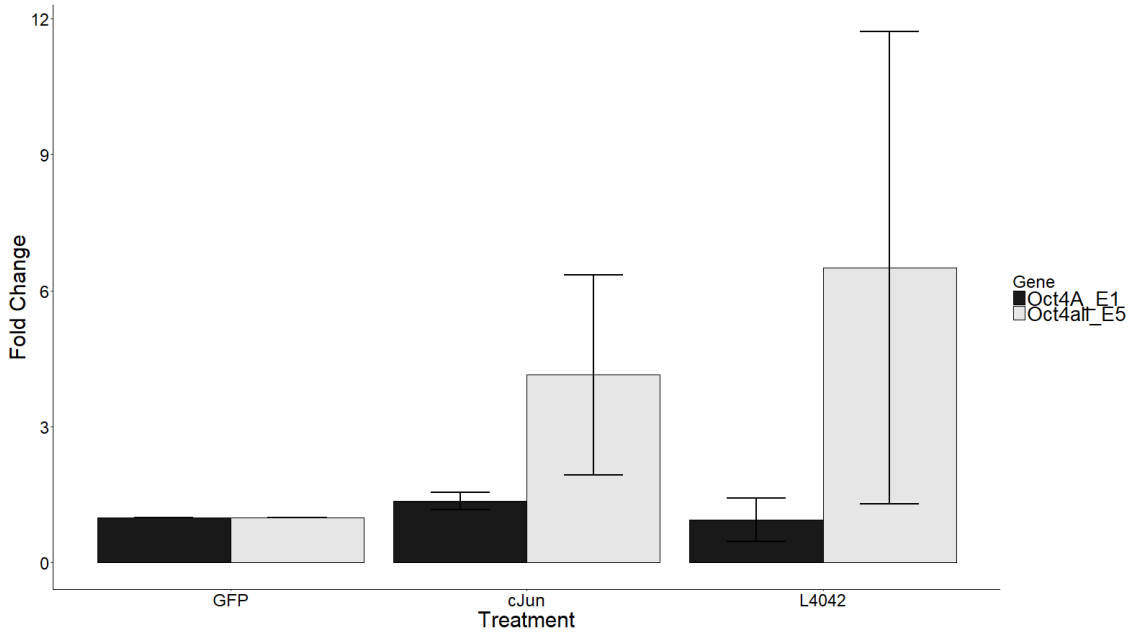
12
9
6
3
0
Fold Change
GFP
cJun
L4042
Treatment
Gene
Oct4A_E1
Oct4all_E5

F.

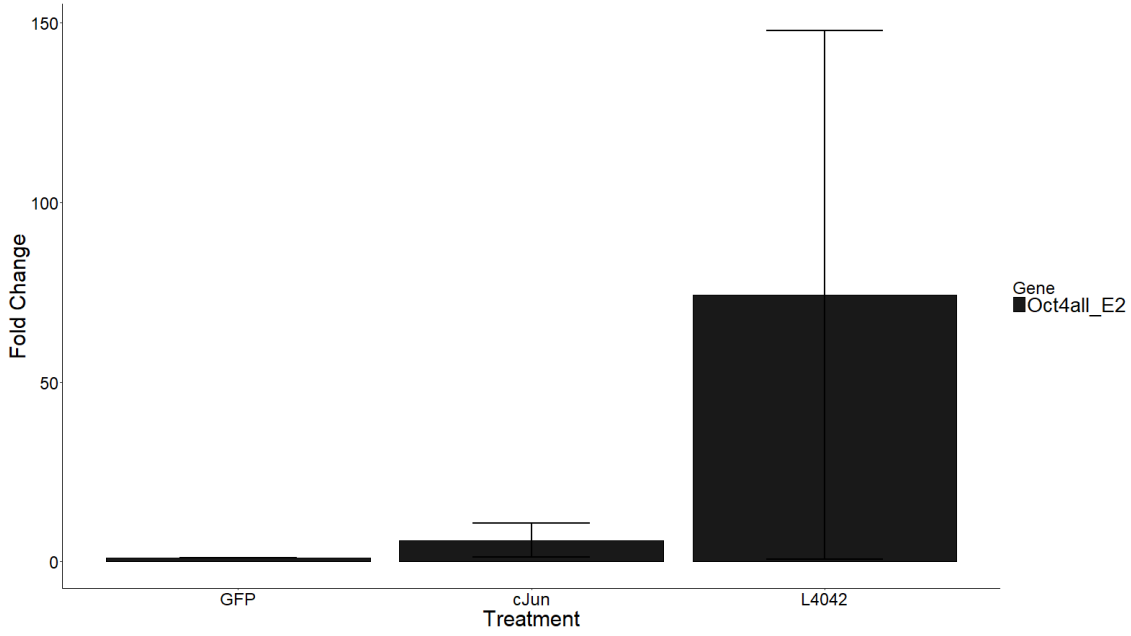
150
100
50
0
Fold Change
GFP
cJun
L4042
Treatment
Gene
Oct4all_E2

G.

Gene amplified	Treatment	Normalization	Average fold expression ± standard error
Plasmid	NT	NT	1
Plasmid	GFP	NT	4.929819±3.22303
Plasmid	cJun	NT	650.9483±314.5663
Plasmid	L40/42	NT	154.3834±61.53322
Plasmid	GFP	GFP	1
Plasmid	cJun	GFP	199.2868±52.73759
Plasmid	L40/42	GFP	61.87357±29.93148

Figure 6. cJun over expression increases gene expression of Oct4B variants. A. NT normalized graph of exons 1, 2, and 5. Exon 2 data were much larger than exon 1 or 5 so it was removed and graphed separately (**C.** and **F.**). **B.** NT normalized data of exons 1 and 5. **C.** NT normalized data for exon 2. **D.** GFP normalized data for all exons. **E.** GFP normalized data for exons 1 and 5. **F.** GFP normalized data for exon 2. **G.** Table of plasmid expression from figure 5, for reference.

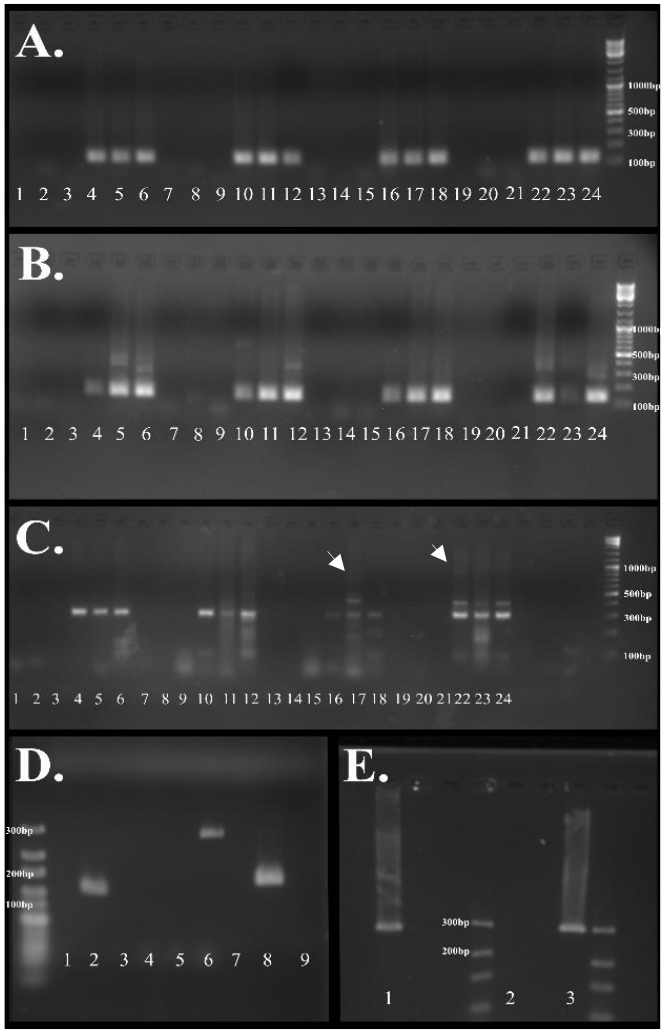
A.
1000bp
500bp
300bp
100bp
1 2 3 4 5 6 7 8 9 10 11 12 13 14 15 16 17 18 19 20 21 22 23 24
B.
1000bp
500bp
300bp
100bp
1 2 3 4 5 6 7 8 9 10 11 12 13 14 15 16 17 18 19 20 21 22 23 24
C.
1000bp
500bp
300bp
100bp
1 2 3 4 5 6 7 8 9 10 11 12 13 14 15 16 17 18 19 20 21 22 23 24
D.
300bp
200bp
100bp
1 2 3 4 5 6 7 8 9
E.
300bp
200bp
1 2 3

Figure 7. Exon 1 primers produce one amplicon, while exons 2 and 5 produce multiple bands from various Oct4B variants. A. Agarose gel of exon 1. Only one band is seen at the expected 111bp. There do appear to be very faint bands below these, which are assumed to be primer dimers or other noise, as they also appear in the –RT samples. Lanes 1-24 are triplicates for each treatment of one replicate and are consistent between treatments. Lanes 4-6 are NT, GFP are lanes 10-12, L40/42 are lanes 16-18, and cJun transfected samples are lanes 21-24. The remaining lanes are the corresponding –RT samples. **B.** Agarose gel of Exon 5. NT samples are in lanes 4-6., GFP in 10-12, L40/42 in 16-18, and cJun samples in lanes 21-24. You can see multiple bands in all samples. **C.** Agarose gel of exon 2. Lanes 4-6 are NT samples, 10-12 are GFP, 16-18 are L40/42, and 21-24 are cJun samples. Multiple bands can be seen in GFP, L40/42 and cJun samples. The bands in the L40/42 and cJun treatments are more abundant and varied in size. Additionally, cJun and L40/42 samples contain the largest band at about 1000bp and 900bp, respectively. These upper bands, denoted by the two white arrows, are faint but distinct. **D.** Agarose gel analysis of all the Oct4 primers off cDNA (lane2) and genomic DNA (lane 3). Exon 1 did not amplify in the no template control (NTC) sample (lane 1) or the genomic DNA. Similarly, exon 5 did not amplify the NTC (lane 7) or genomic DNA (lane 9), but did amplify cDNA (lane 8). Exon 2 only amplified the genomic DNA (lane 6). Because of this EB cDNA was used. **E.** Agarose gel analysis of exon 2 primers amplifying cDNA from embryoid bodies (EBs). Lane 1 shows the primers amplify genomic DNA and lane 3 shows they will amplify cDNA from EBs. Lane 2 shows the primers will not amplify the –RT sample.

Table 3. Summary of bands present on agarose gel for exon 1, exon 2, and exon 5 and the corresponding treatment condition they were located. A comparison of expected amplicon sizes with the amplicons seen on agarose gel. While many bands were expected for the Oct4B variants, there were additional bands that were not expected. These may be additional sequences as of yet unidentified. They may or may not have contributed to the expression data, as dissociation curves cannot be run on probe assays.

Primer set	**Expected bands**	**Bands present**	**Treatment**
Exon 1	1 band-111bp	1 band- 111bp	All
Exon 2	Oct4b': 91bp	296 or 297bp	All
	Oct4b2 and 3: 296bp	350bp	cJun and L40/42
	Oct4b and b1: 297bp	900bp	L40/42
		1000bp	cJun
		multiple indistinct bands of indeterminate size in the range of 100-296bp.	GFP, L40/42, and cJun
Exon 5	Oct4A, Oct4b', Oct4b and Oct4b1: 135bp	135bp	All
		300bp	
	Oct4b2 and 3: 274bp	350bp	
		400bp	cJun and L40/42
		500bp	cJun and L40/42

cJun Over Expression Increases Gene Expression of Endoderm Markers

As the changes Oct4 variant expression and the increased *Sox2* cDNA levels presents in cJun and L40/42 overexpressing cells are expected to affect potency, we measured transcript levles of germ layer markers *Brachyury, Sox1, Gata4, and Gata6* to determine whether a shift in gene expression of pluripotency factors would initiate expression of these germ layer markers and if there was a bias towards one germ layer or another. Expression of the mesoderm marker *Brachyury* was 1.02±0.38, 0.83±0.06, and

1.24±0.35 fold higher for cJun, L40/42, and GFP transfected cells. GFP normalized data were 1.04±0.42 and 0.88±0.27 for cJun and L40/42 samples. The ectoderm marker, *Sox1*, showed 1.14±0.48, 1.49±0.44, and 1.05±0.37 fold changes in expression for cJun, L40/42, and GFP, respectively. Expression for cJun and L40/42 samples normalized to GFP were 1.01±0.4 and 3.66±2.76, respectivley. *Gata4* expression, a marker for endoderm, was 1.39±0.37, 1.39±0.61, and 0.97±0.12 for cJun, L40/42, and GFP samples. GFP normalized data were 1.41±0.34 and 1.43±0.61 for cJun and L40/42, respectively. Primative endoderm marker, Gata6, produced a fold change of 2.54±0.69 in cJun transfected cells and 2.3±1.12 and 1.52±0.31 for L40/42 and GFP transfected samples, respectively. These data normalized to GFP were 1.63±0.39 and 1.46±0.53 for cJun and L40/42 (Figure 8). One-way ANOVA analyses of NT and GFP normalized data did not produce statistical significance between treatment for any gene ($p>0.05$, $n=4$). While samples were not analyzed by gel electrophoresis, they were validated in the same manner as previously mentioned and produced the expected amplicon sizes: 134bp (*Sox1*), 117bp (*Brachyury*), 225bp (*Gata4*), and 182bp (*Gata6*) (Figure 8).

A.

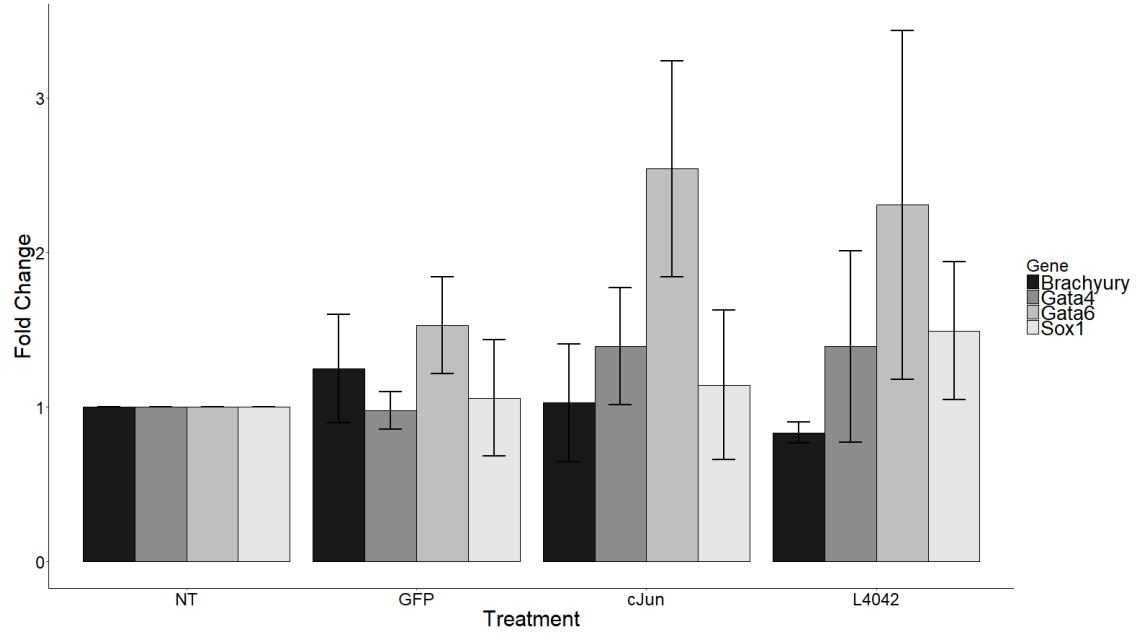
Fold Change
0
1
2
3
NT
GFP
cJun
L4042
Treatment
Gene
Brachyury
Gata4
Gata6
Sox1

B.

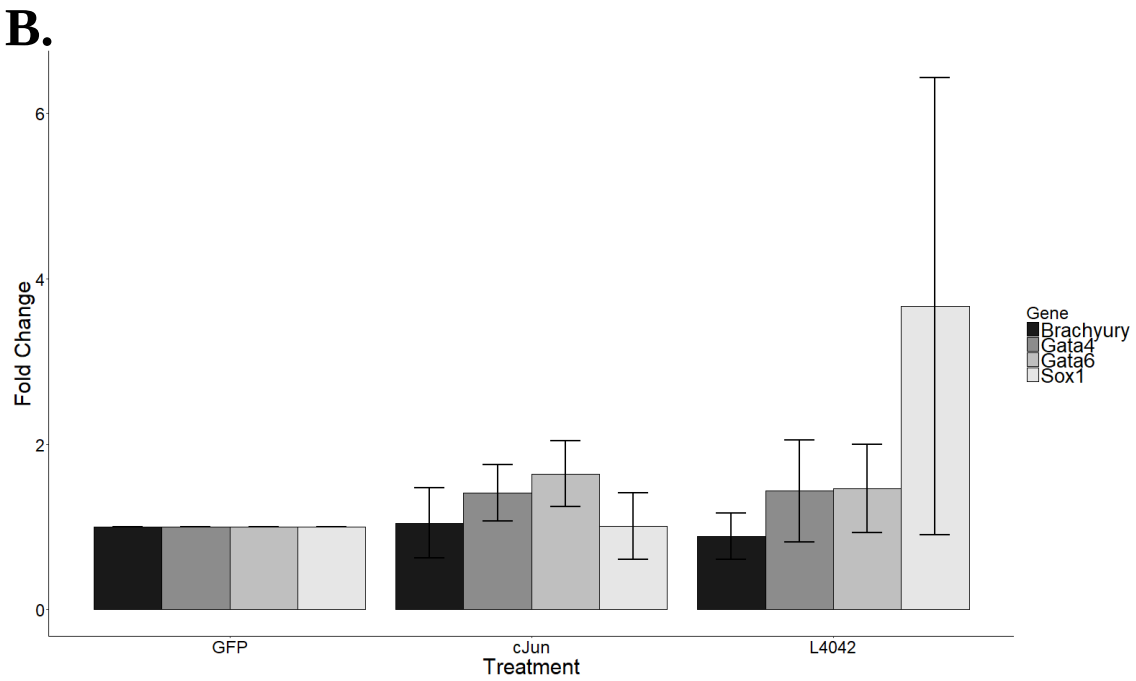
Fold Change
0
2
4
6
GFP
cJun
L4042
Treatment
Gene
Brachyury
Gata4
Gata6
Sox1

C.

Gene amplified	Treatment	Normalization	Average fold expression ± standard error
Plasmid	NT	NT	1
Plasmid	GFP	NT	4.929819±3.22303
Plasmid	cJun	NT	650.9483±314.5663
Plasmid	L40/42	NT	154.3834±61.53322
Plasmid	GFP	GFP	1
Plasmid	cJun	GFP	199.2868±52.73759
Plasmid	L40/42	GFP	61.87357±29.93148

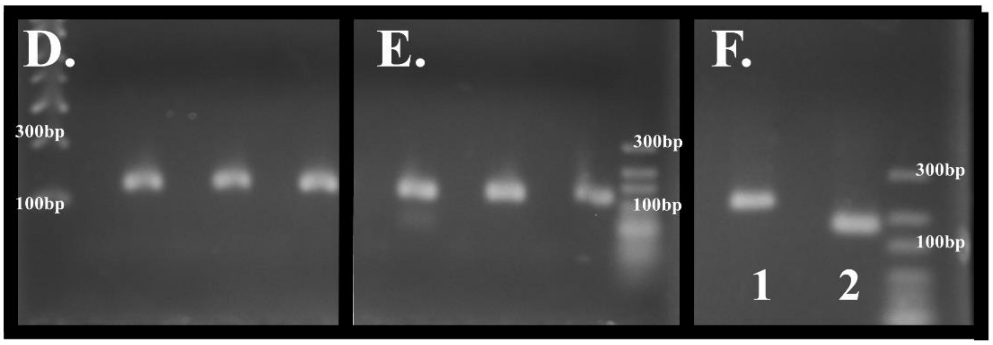

Figure 8. Figure 8. Over expression of cJun increases expression of Gata6 and Gata4. A. NT normalized expression data. **B.** GFP normalized expression data. **C.** Table of plasmid expression for reference. **D.** Agarose gel of Sox1, which produced the expected 134bp band. **E.** Agarose gel of Brachyury, which produced the correct 117bp amplicon. **F.** Agarose gel of Gata4 (lane 1) and Gata6

Nocodazole Increases cJun Gene Expression and Effects Oct4 Variant Gene Expression in mESCs

Nocodazole treatment of cells was shown to increase in cJun protein expression through an alternative translation pathway without a proportional increase in mRNA expression (Polak et al. 2006, Blau et al. 2012, unpublished data Sprowles Lab). Furthermore, the cJun proteins produced through this mechanisms have different transcriptional targets than those generated from increased transcription (Blau et al. 2012). We used SYBR qPCR assays to quantify cDNA levels of *cJun*, *Oct4*A, *Nanog*,

Sox2. Overall, cJun expression was increased with nocodazole treatment (**Table 4**). However, the range of cJun cDNA between replicates was highly variable, so a one-way ANOVA performed on these data and was not statistically significant ($p > 0.05$, $n=3$). The large variation in expression data (data not shown) could be due to the small replicate number of 3, but because DMSO also exhibits a varied effect on expression, the variation may be due to a dosage effect from both DMSO and nocodazole. Nonetheless, there are trends observed when relative levels of cJun are taken into account.There is a general decrease in *Nanog* expression with decreasing cJun for both nocodazole and DMSO treatment. Expression of *Sox2* does not seem to have any relation to cJun expression due to nocodazole or DMSO. Expression of *Oct4* using SYBR varies wildy with nocodazole treatment, while the same primers in the probe assay does not (**Table 4**). Interestingly, Oct4A expression does not vary greatly in DMSO samples, despite one replicate containing multiple dissociation peaks and 2 bands upon gel analysis (Figure 9). The additional band between 1200bp and 1500bp could be a product of a currently unknown mechanism as a reaction to DMSO and may be dose dependent as no other replicate treated with DMSO produced the same effect. The expression pattern for *Nanog*, *Sox2*, and *Oct4*A was similar with DMSO normalized data, however the variance is slightly decreased.

Table 4. Increases in cJun expression associate with increases in *Oct4* variants and decreases in *Nanog* expression. A. NT normalized data for each gene assayed by both SYBR and probe-based assays**. B.** DMSO normalized data for each gene evaluated by STBR and probe-based assays. For both tables, expression values associated with nocodazole treated samples are in aqua, while the values associated with DMSO treatment are in peach.

A.

Replicate	Treatment	*cJun*	*Oct4*A SYBR	*Nanog*	*Sox2*	*Oct4*A exon 1	*Oct4*B exon 2	*Oct4*all exon 5
1	NT	1	1	1	1	1	1	1
1	DMSO	0.29	3.45	0.74	3.94	2.00	2.41	1.82
1	Nocodazole	50.67	538.76	0.35	3.53	3.24	3.08	30.03
2	NT	1	1	1	1	1	1	1
2	DMSO	1.20	2.88	0.91	1.20	1.41	2.38	7.55
2	Nocodazole	51.84	4.72	0.36	0.75	3.72	0.39	2.85
3	NT	1	1	1	1	1	1	1
3	DMSO	0.69	6.98	2.89	0.57	0.19	1.08	0.23
3	Nocodazole	1.84	1335.16	1.89	0.46	0.24	1.07	0.30

B.

Replicate	Treatment	*cJun*	*Oct4*A SYBR	*Nanog*	*Sox2*	*Oct4*A exon 1	*Oct4*B exon 2	*Oct4*all exon 5
1	DMSO	1	1	1	1	1	1	1
1	Nocodazole	169.89	155.79	0.47	0.89	1.62	1.27	16.48
2	DMSO	1	1	1	1	1	1	1
2	Nocodazole	43.10	1.63	0.40	0.62	2.63	0.16	0.37
3	DMSO	1	1	1	1	1	1	1
3	Nocodazole	2.65	191.17	0.65	0.80	1.23	0.99	1.31

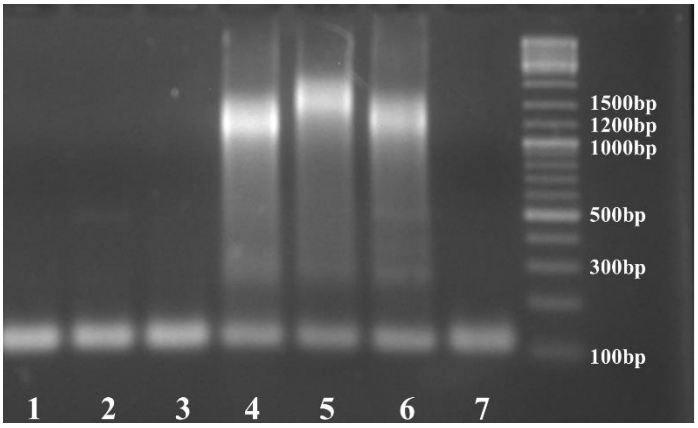

Figure 9. DMSO produces multiple bands in one replicate amplified by Oct4A primers. Exon 1 primers used in sybr assays produced multiple dissociation peaks (data not shown) and produced multiple bands on a gel. The expected 111bp band is clearly seen in all samples, but there is a large and bright band between 1200-1500bp. This does not appear to affect the expression data for this replicate, as it is similar to another replicate with similar cJun expression. Lanes 1-3 are NT, 4-5 DMSO, and lane 7 is one triplicate of the nocodazole sample for the same replicate. Both NT and nocodazole samples produced one clear dissociation peak.

Similar to transfection data, we assessed the expression of the Oct4 mRNA variants using a probe-based assay. Generally, when there was an increase in cJun expression from either DMSO or nocodazole, there was an increase in *Oct4* expression. DMSO appears to affect *Oct4*B variants, while nocodazole appears to have an increased effect on *Oct4*A versuses the other variants. These tentative relationships appear to be dose dependant, as intermediate cJun levels produce an intermediate effect on *Oct4* expression (Table 4). Additionally, when *Oct4*A increases the *Oct4*B variants decrease. These trends are weak, but are potentially affected by the low sample size and the multiple bands seen by agarose gel electrophoresis. Like the transfected samples, mulitple bands were seen for the *Oct4* variants. Exon 1 primers produced the expected 111bp band and 2 additional bands at 200bp and 400bp. The additional bands are only

seen in DMSO and nocodazole samples for all replicates and indicate an unaticipated effect of both DMSO and nocodazole on *Oct4*A expression. Exon 5 produced multiple bands in all treatments, however NT only contains the expected 135bp and 274bp bands. Additional bands seen in DMSO and nocodazole treated samples were approximately 350bp and 450bp. This could be due to differences in splicing as yet to be defined. Similar to exon 1, exon 2 produced multiple unexpected bands in DMSO and nocodazole samples. NT samples produced one clear band at approximately 296-297bp, which corresponds to the Oct4b and Oct4b1-3 variants. The expected 91bp band for Oct4b' may be the faint bands below, but could also be primer dimers as this band is also seen occasionally in the –RT and NTC samples, which showed no amplification on qPCR analysis. DMSO samples produced the 296-297bp band as well, but also produced a 550bp band and multiple bands between 250-90bp. Nocodazole produced the expected band as well as more clear bands at 250bp and 90bp (Figure 10).These variations in band sizes could explain the variation in expression data as band intensities and number of additional bands varied slightly between each replicate.

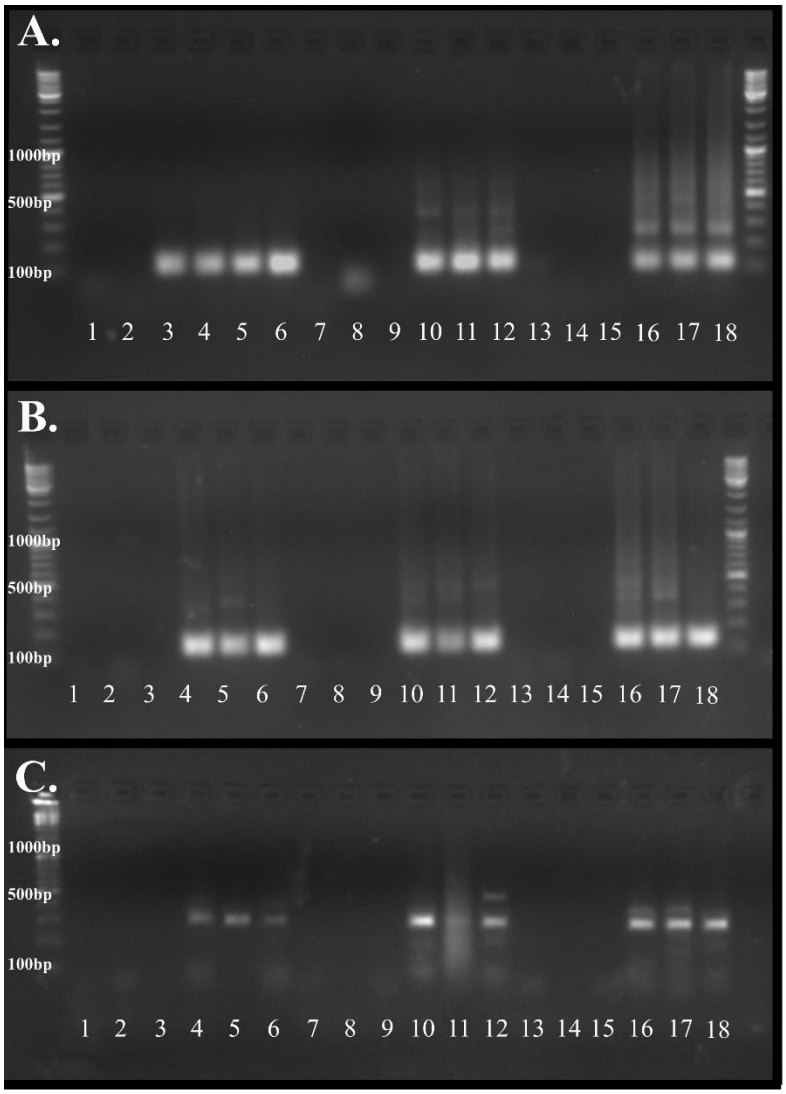
A.
1000bp
500bp
100bp
1 2 3 4 5 6 7 8 9 10 11 12 13 14 15 16 17 18
B.
1000bp
500bp
100bp
1 2 3 4 5 6 7 8 9 10 11 12 13 14 15 16 17 18
C.
1000bp
500bp
100bp
1 2 3 4 5 6 7 8 9 10 11 12 13 14 15 16 17 18

Figure 10. DMSO and nocodazole treatment have an effect on Oct4 variant expression. A. A representative agarose gel of exon 1. DMSO and nocodazole treatment have a clear effect on Oct4A expression, producing bands that were not expected at about 300bp and 400bp. Lane 3-6 are NT, Lanes 10-12 and 16-18 are DMSO and nocodazole samples respectively. Remaining lanes are corresponding –RT samples which did not amplify on qPCR analysis. **B.** A representative gel of exon 5. Multiple bands are seen in all samples, however additional bands that were unexpected were seen only in DMSO and nocodazole samples. Two bands are expected for exon 5 primers at 135bp and 274, which cover all known Oct4 variants. These are seen in all samples, but additional bands at 350bp and 450bp are seen in DMSO and nocodazole treated samples. Lanes 4-6 are NT, lanes 10-12 are DMSO and lanes 16-18 are nocodazole samples. Remaining lanes are corresponding –RT samples. **C.** Representative gel of exon 2. Like exon 1, only one band is seen in the NT sample approximately 297bp, indicating any of the four Oct4B variants, Oct4b and Oct4b1-3. Oct4b' at 91bp may or may not be the faint lower bands seen. DMSO and nocodazole samples have clear bands at approximate 297bp, but also have additional bands. Nocodazole produces multiple bands around 250bp and 90bp, while DMSO produces these and others of indeterminate size in that range of 250-90bp. DMSO produces an additional clear band at approximately 550bp. Lanes 4-6 are NT, lanes 10-12 are DMSO, and lanes 16-18 are nocodazole samples. Remaining lanes are corresponding –RT samples.

Because Oct4A is essential in maintaining potency of stem cells and because variations in protein expression can direct cell fate, indentifying whether or not the changes in gene expression are seen as changes in protein expression in the same cell will further support the hypothesis that cJun directly regulates the expression of Oct4A. The use of ICC allowed for localization of the either cJun and Oct4A or cJun and Oct4all (all Oct4 protein variants) to the individual cell level. If the signals were co-localized, this would indicate that cJun is regulating expression of Oct4 variants and suggests that increases in cJun correlate to increases in Oct4 within the same cell, which may lead to changes in potency and cell fate. ICC analysis of these data showed variation in cJun,

Oct4A/B and Oct4all protein expression between and within replicates. Despite this, there are some trends that suggest cJun and Oct4 expression are affected by nocodozole.

Generally, nocodazole appears to increase cJun and Oct4A/B expression, with overlap within the bright spots (**Error! Reference source not found.**). Like the qPCR data, there is an increase in DMSO treatment, but nocodazole increases the trend, with the largest cellular co-localization of cJun and Oct4 A/B/B' occuring 4h post-nocodazole treatment. Where bright Oct4A/B/B' points are seen, there are corresponding spots of cJun signal, however the Oct4A/B/B' spots do appear to be smaller (**Error! Reference source not found.**). Analysis of these spots using the Zeiss co-localization software seemed to support these findings. The replicate data were pooled (n=3) and analysed as a number of spots out of the total identified. There were approximately 1-3 cell colonies per image and increases in co-localized spots did not appear to increase with colony number. For cJun and Oct4A images, there were an average of 2.05 ± 0.29 colonies for NT, 1.94 ± 0.47 for 2h DMSO treatments, 2.1 ± 0.23 colonies for 4h DMSO, and 2.04 ± 0.23 colonies and 1.67 ± 0.17 colonies for 2h and 4h nocodazole treatments, respectively.

When cJun protein expression was compared to that of all Oct4 protein isoforms within the cells, there are few spots identified per colony of cells imaged, but the ratio of identified co-localization to total number of colonies evaluated for each treatment gradually increases with nocodazole treatment. The greatest difference in this ratio is seen between NT and 4h nocodazole treated samples, however the increase is not as large when looking at co-localizations that had both a strong Pearson's coefficient (≥0.1) and a

strong Mander's coefficient (≥0.98) or higher, as defined by Zinchuk et. al (2007). Aproximately 48% of all co-localized spots had at least a strong Pearson's and a strong Mander's in NT samples, but only 51% were seen with samples 4h post nocodazole treatment. Interestingly, 2h post nocodazole treatment had 81% of co-localized spots with these criteria (Table 5). This indicates that nocodazole treatment increases cJun co-localization with Oct4A, but a stronger degree of co-localization is seen in 2h nocodazole samples compared to the 4h samples.

A.

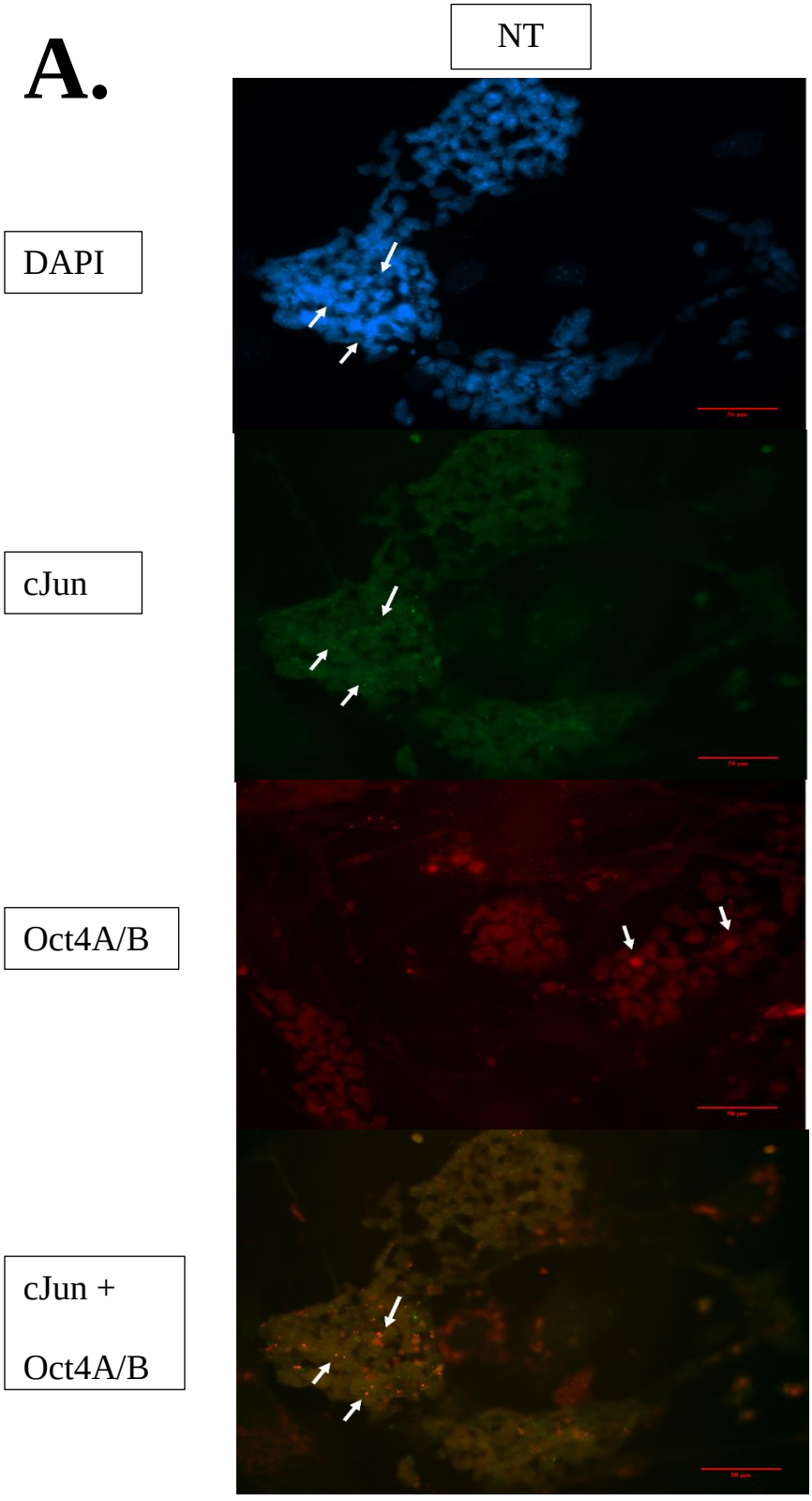

B.

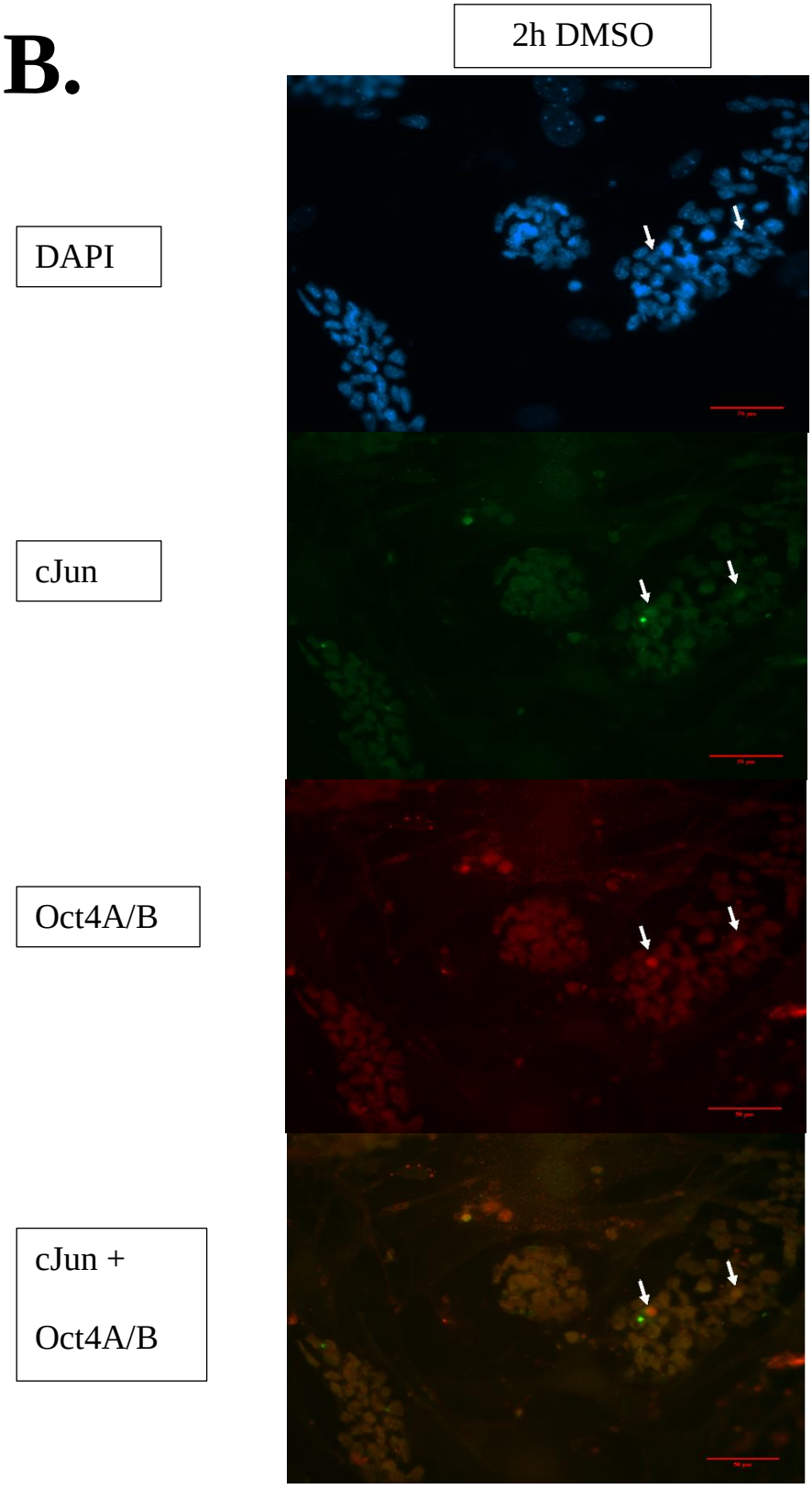

C.

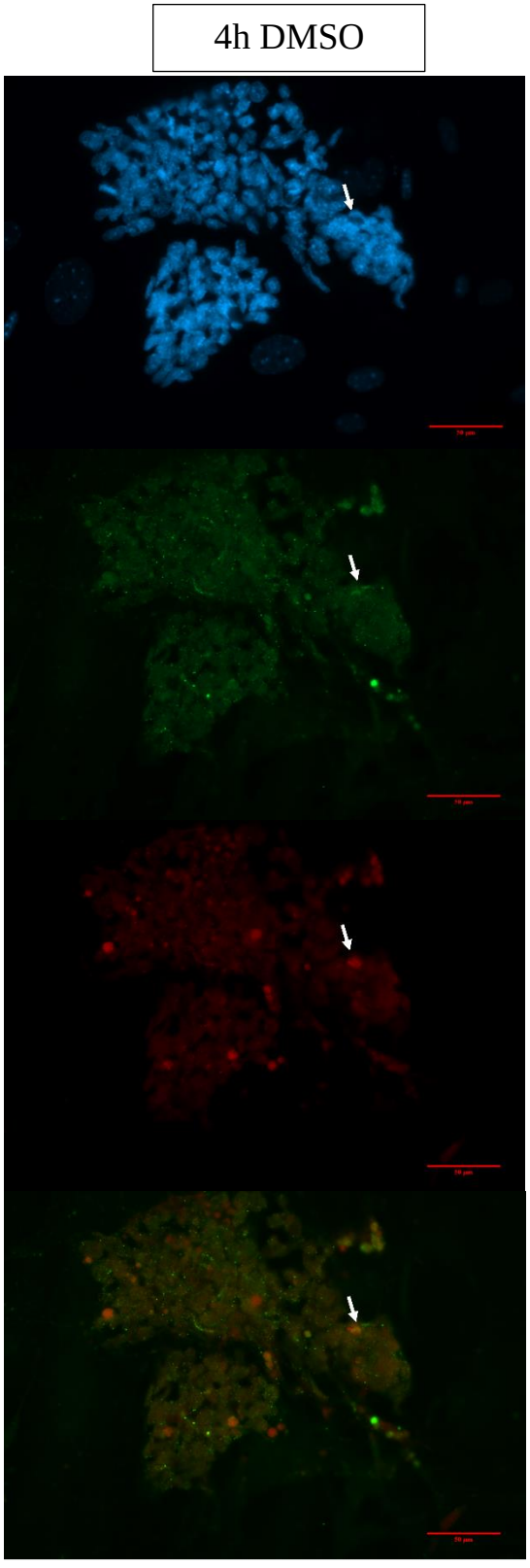

D.

2h Nocodazole (5ug/ml)

DAPI

cJun

Oct4A/B

cJun +

Oct4A/B

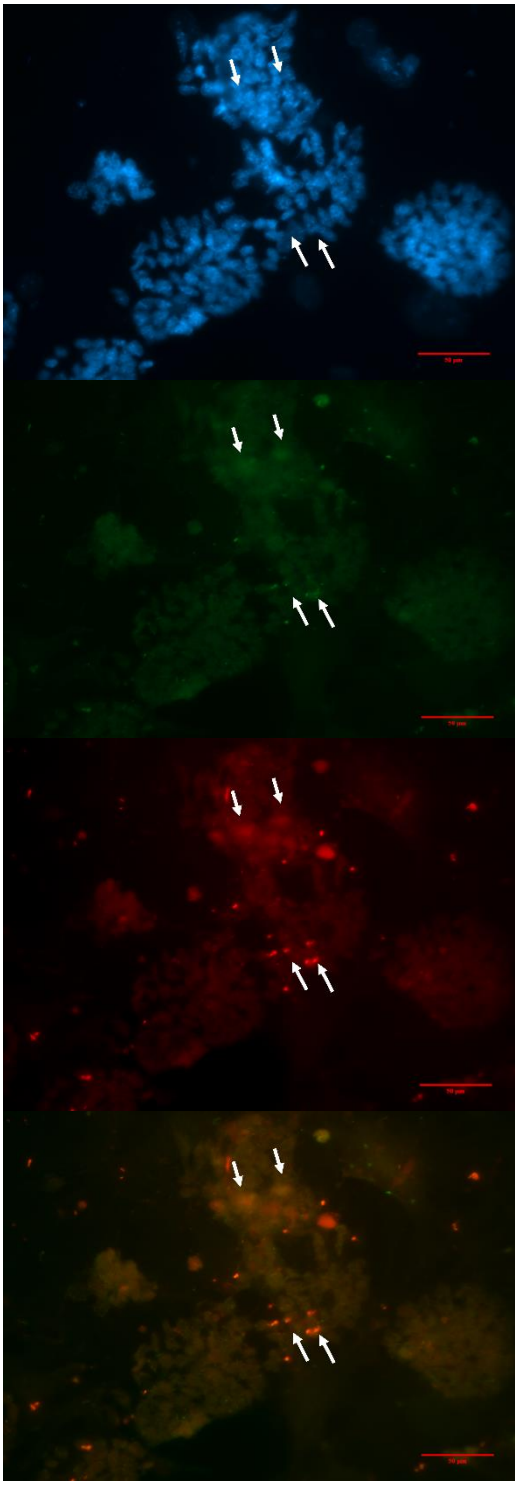

E.

4h Nocodazole (5ug/ml)

DAPI

cJun

Oct4A/B

cJun +

Oct4A/B

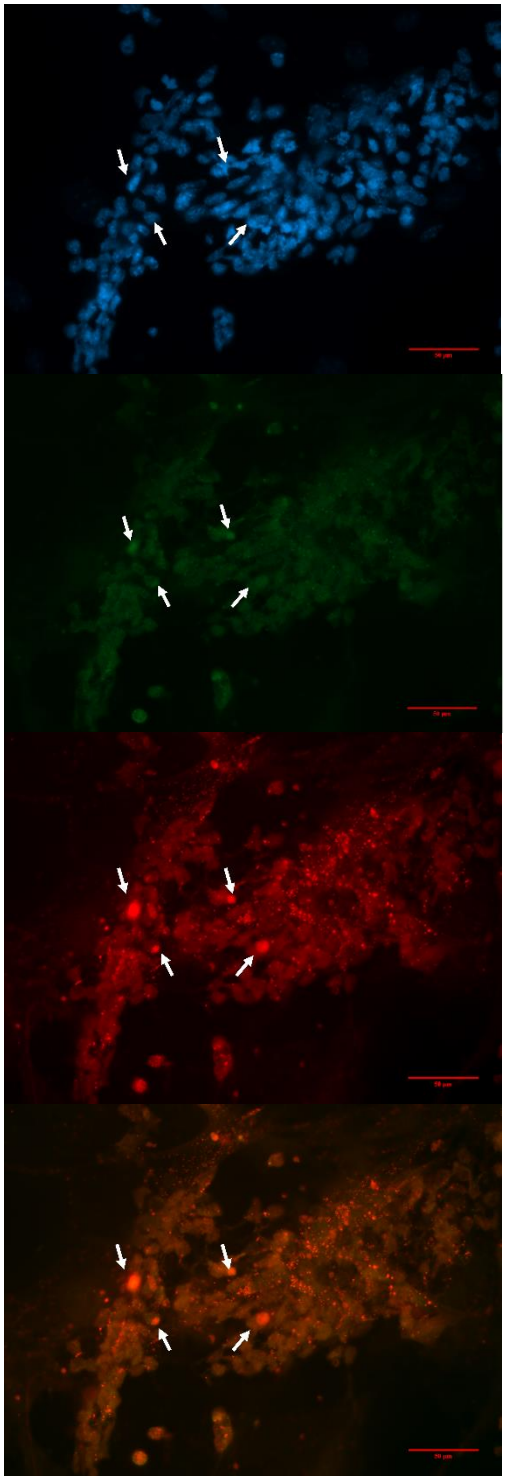

F.

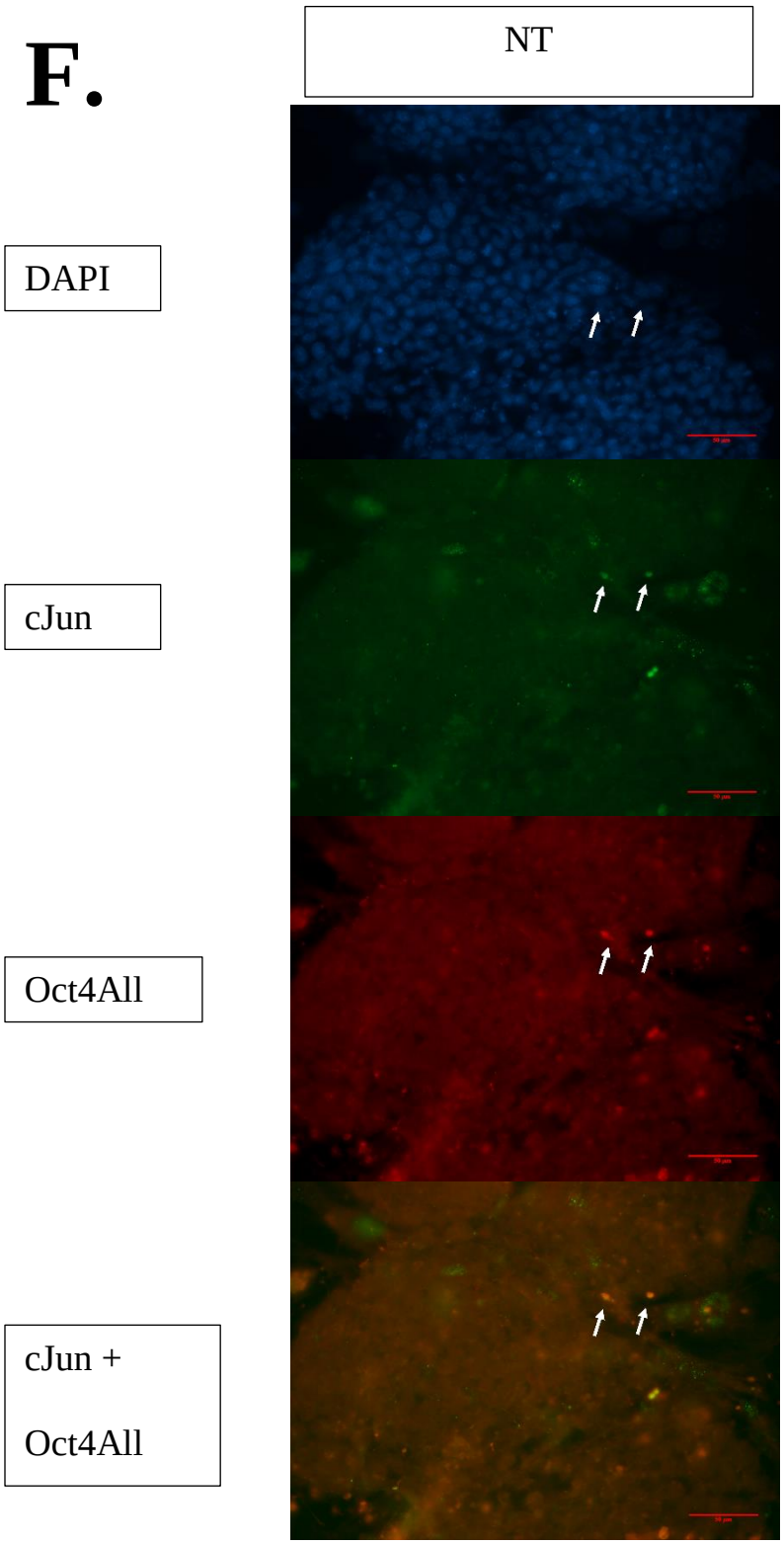

G.

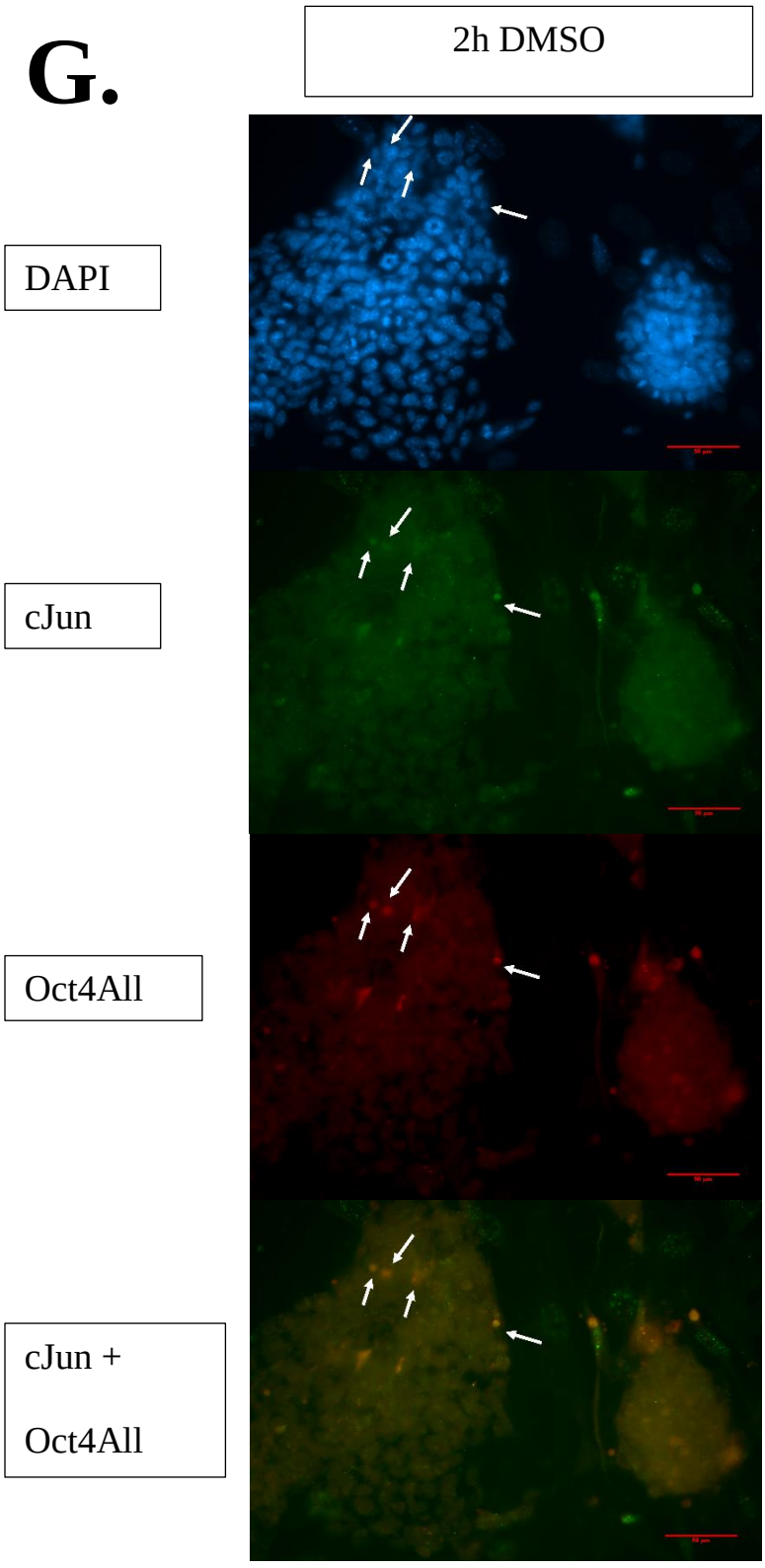

H.

4h DMSO

DAPI

cJun

Oct4All

cJun +

Oct4All

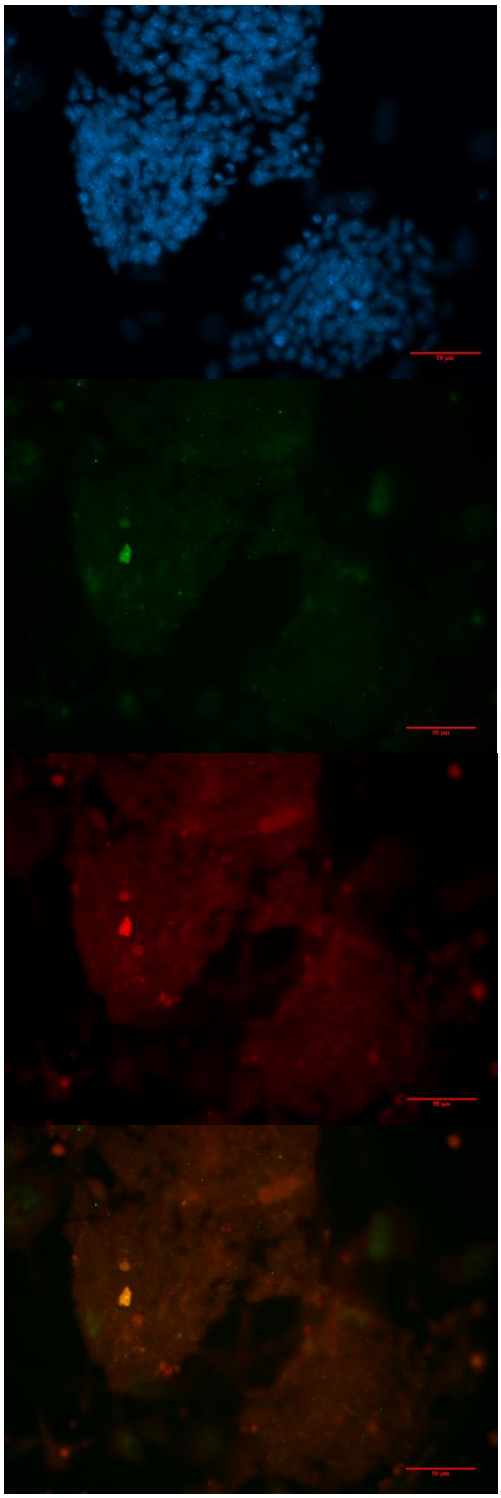

I.

2h Nocodazole (5ug/ml)

DAPI

cJun

Oct4All

cJun +

Oct4All

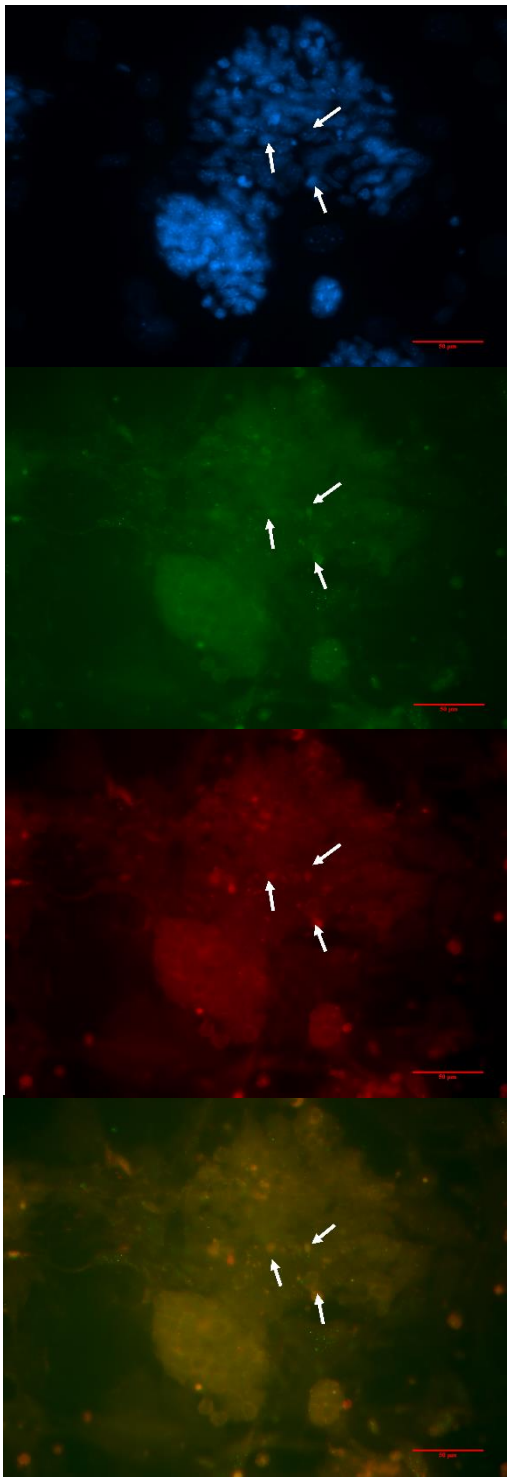

J.

4h Nocodazole (5ug/ml)

DAPI

cJun

Oct4All

cJun +

Oct4All

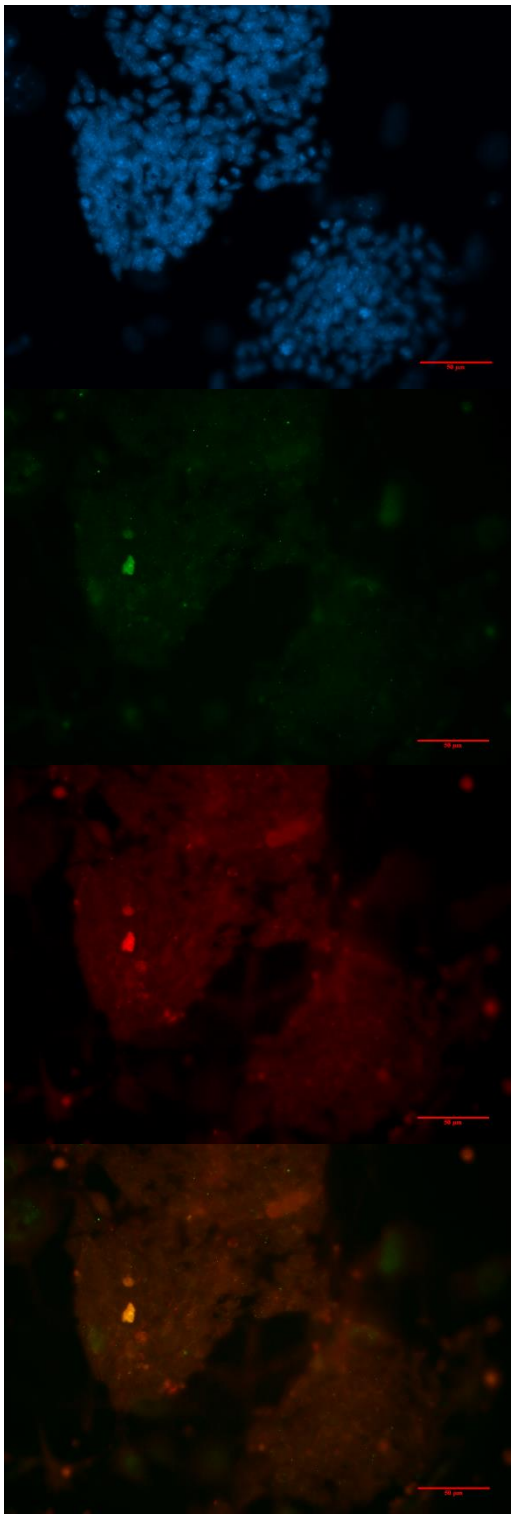

Figure 11. Nocodazole treatment increases co-localization of Oct4A/B or Oct4all with cJun. A-E. Comparison of cJun expression with Oct4A/B expression across all treatments to determine the effect of nocodazole on cJun expression as well as the co-localization of cJun to Oct4A. Generally, there is a decrease in cJun with nocodazole and an increase in Oct4A/B expression, with bright areas generally becoming very small and widely dispersed. **A.** NT. **B.** 2h DMSO. **C.** 4h DMSO. **D.** 2h nocodazole. **E.** 4h nocodazole. **F-J.** Comparison of cJun expression with all Oct4 variants (Oct4all). Nocodazole appears to increase cJun and Oct4all, but the localization changes. Similarly, to Oct4A/B, bright spots of Oct4all signal do seem to correlate to cJun. **F.** NT. **G.** 2h DMSO. **H.** 4h DMSO. **I.** 2h nocodazole. **J.** 4h nocodazole. Arrows in both images indicate a few, but not all, of the areas where co-localization was identified.

A.

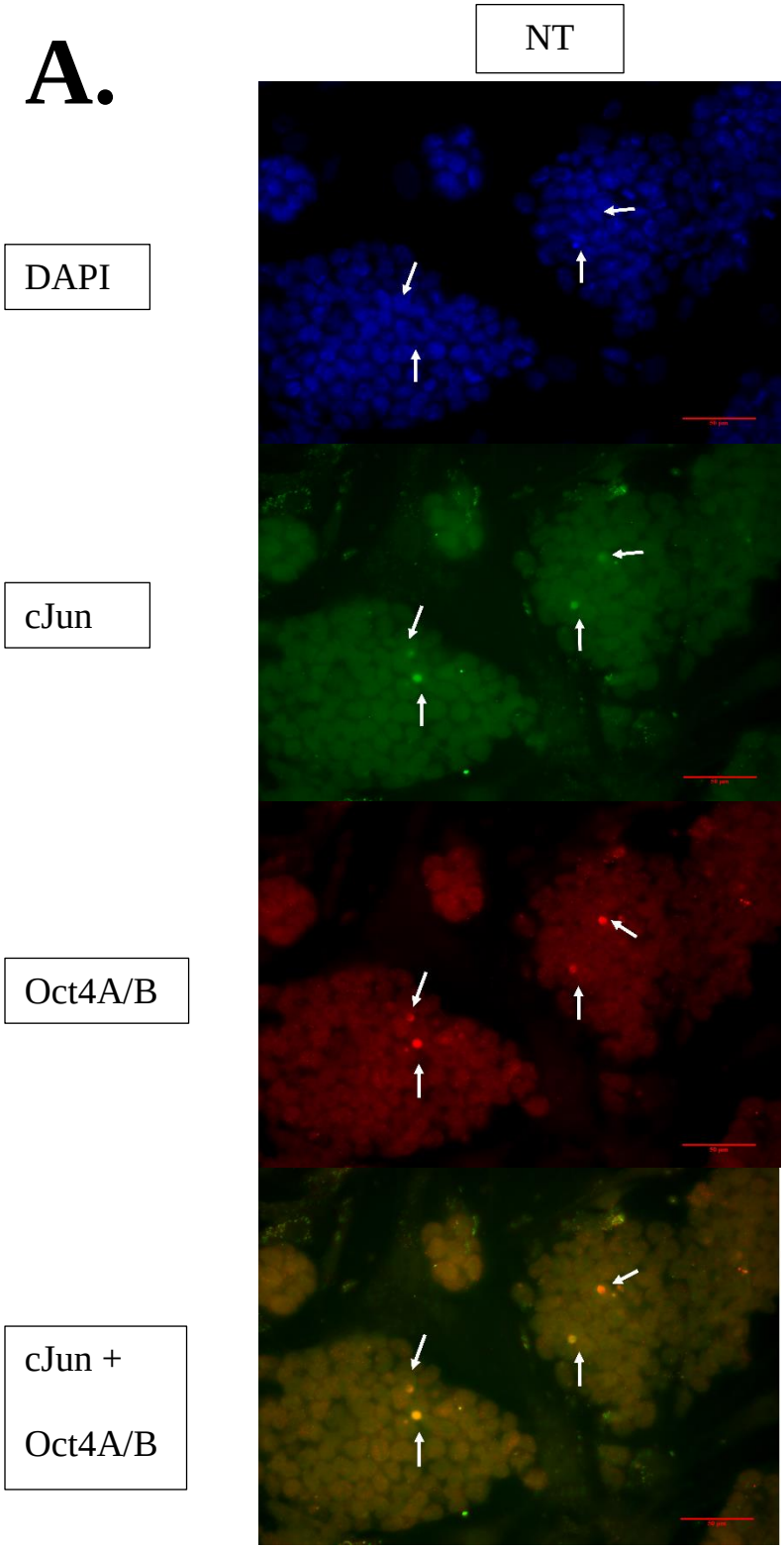

B.

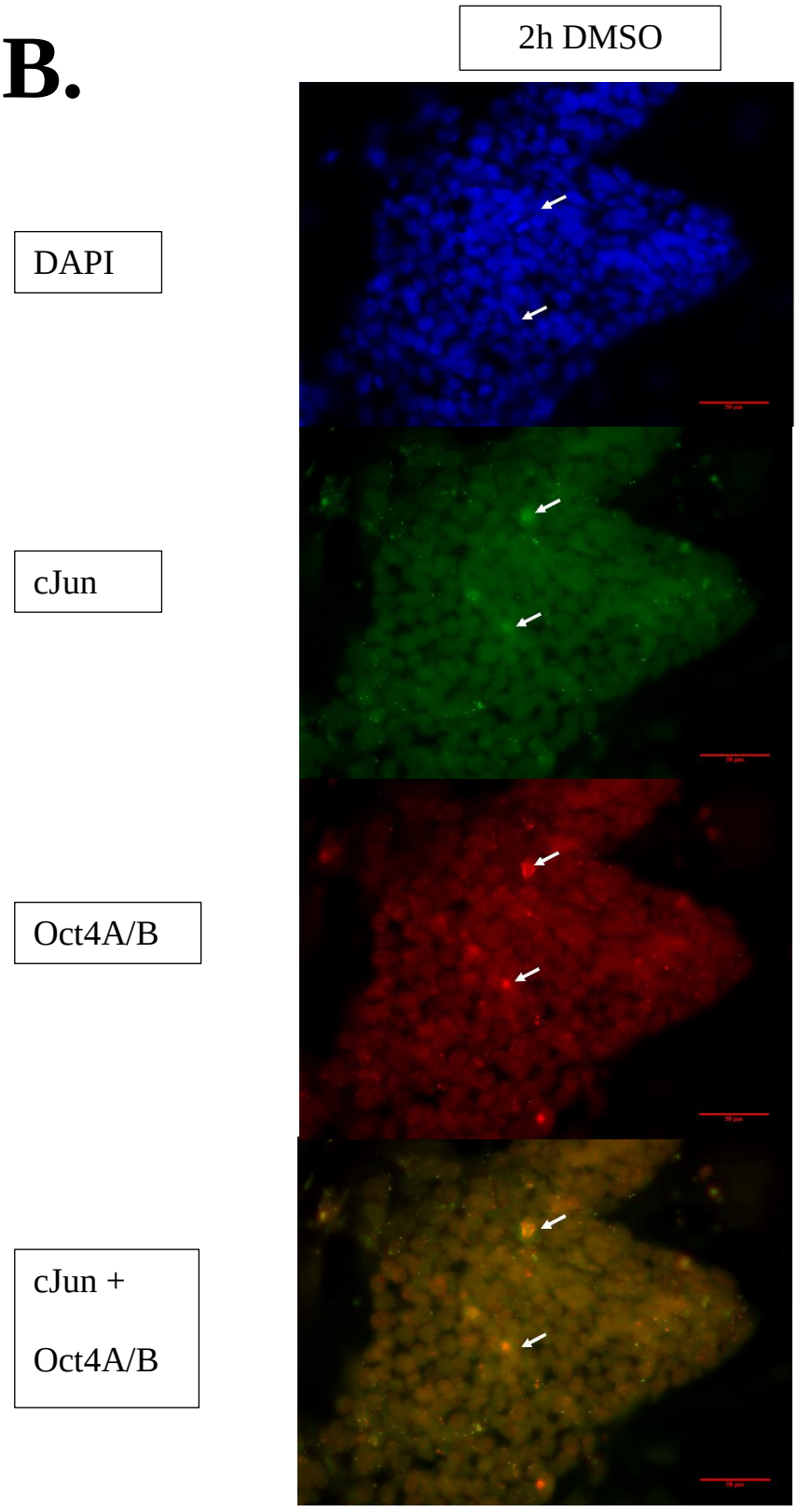

C.

4h DMSO

DAPI

cJun

Oct4A/B

cJun +

Oct4A/B

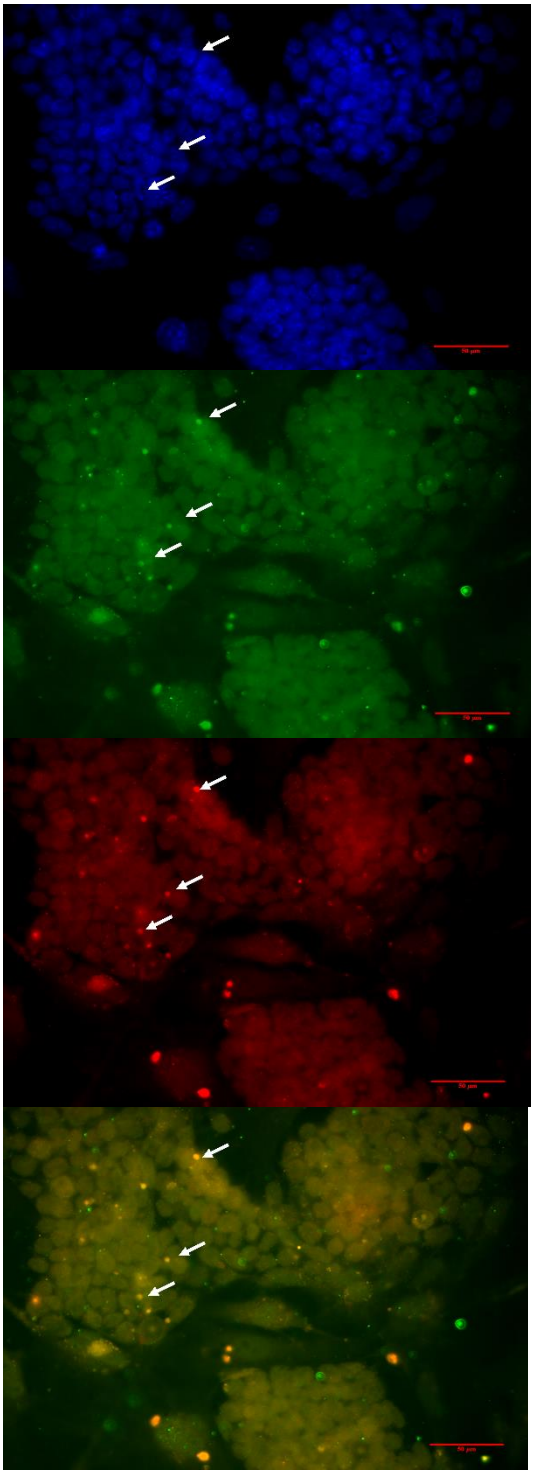

D.

2h Nocodazole (5ug/ml)

DAPI

cJun

Oct4A/B

cJun +

Oct4A/B

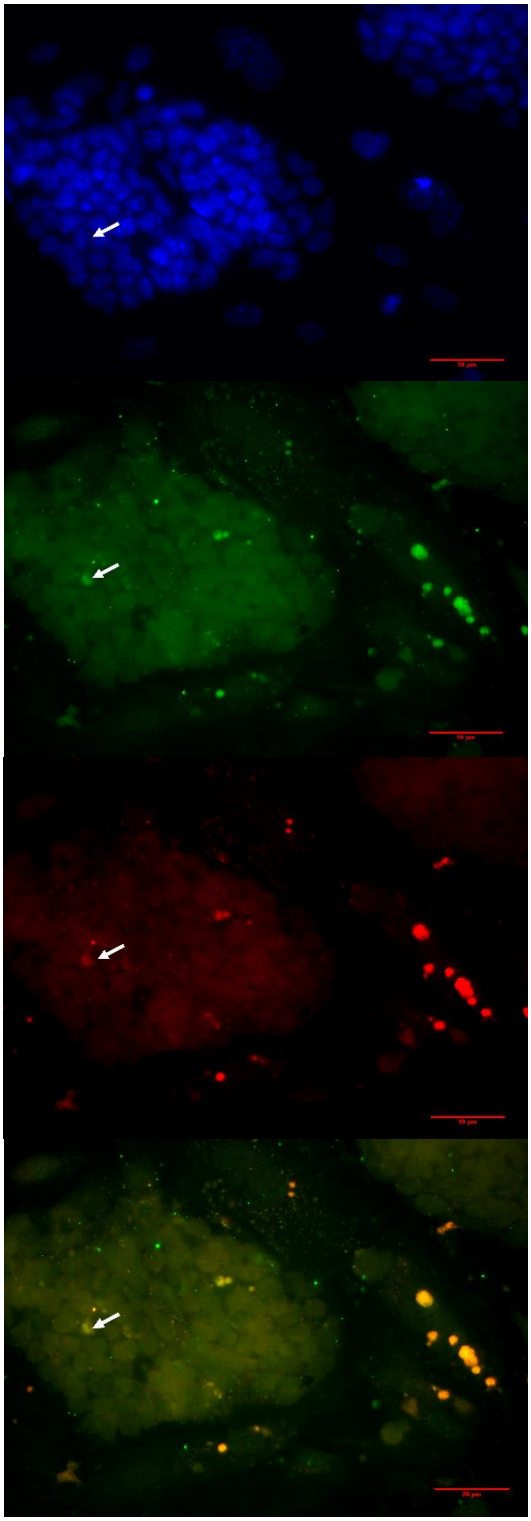

E.

4h Nocodazole (5ug/ml)

DAPI

cJun

Oct4A/B

cJun +

Oct4A/B

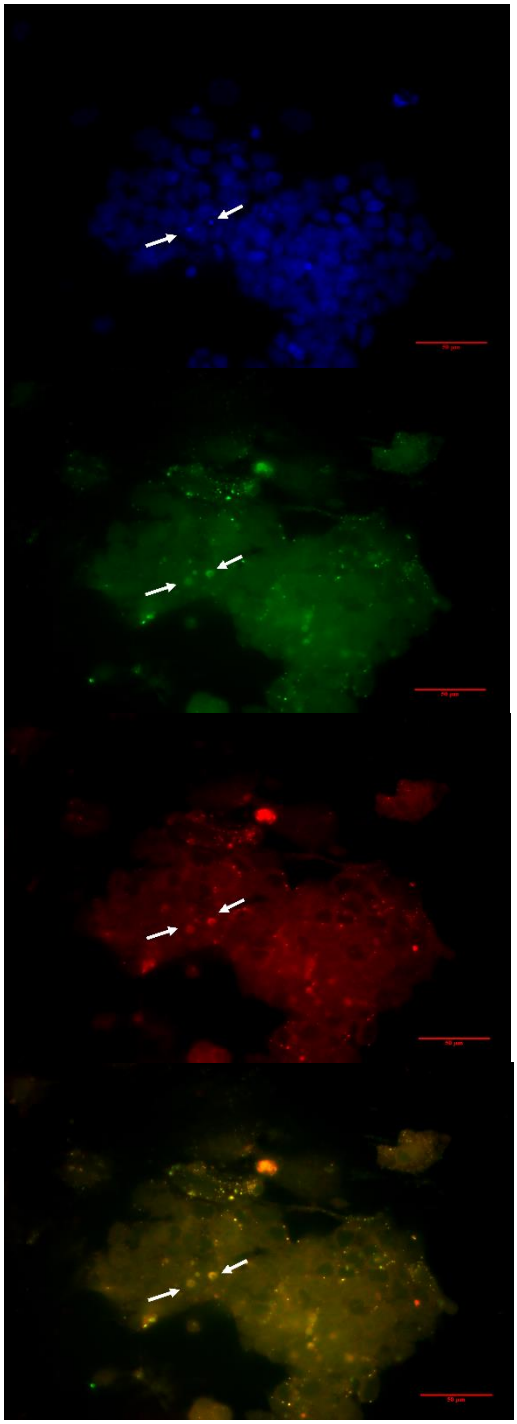

F.

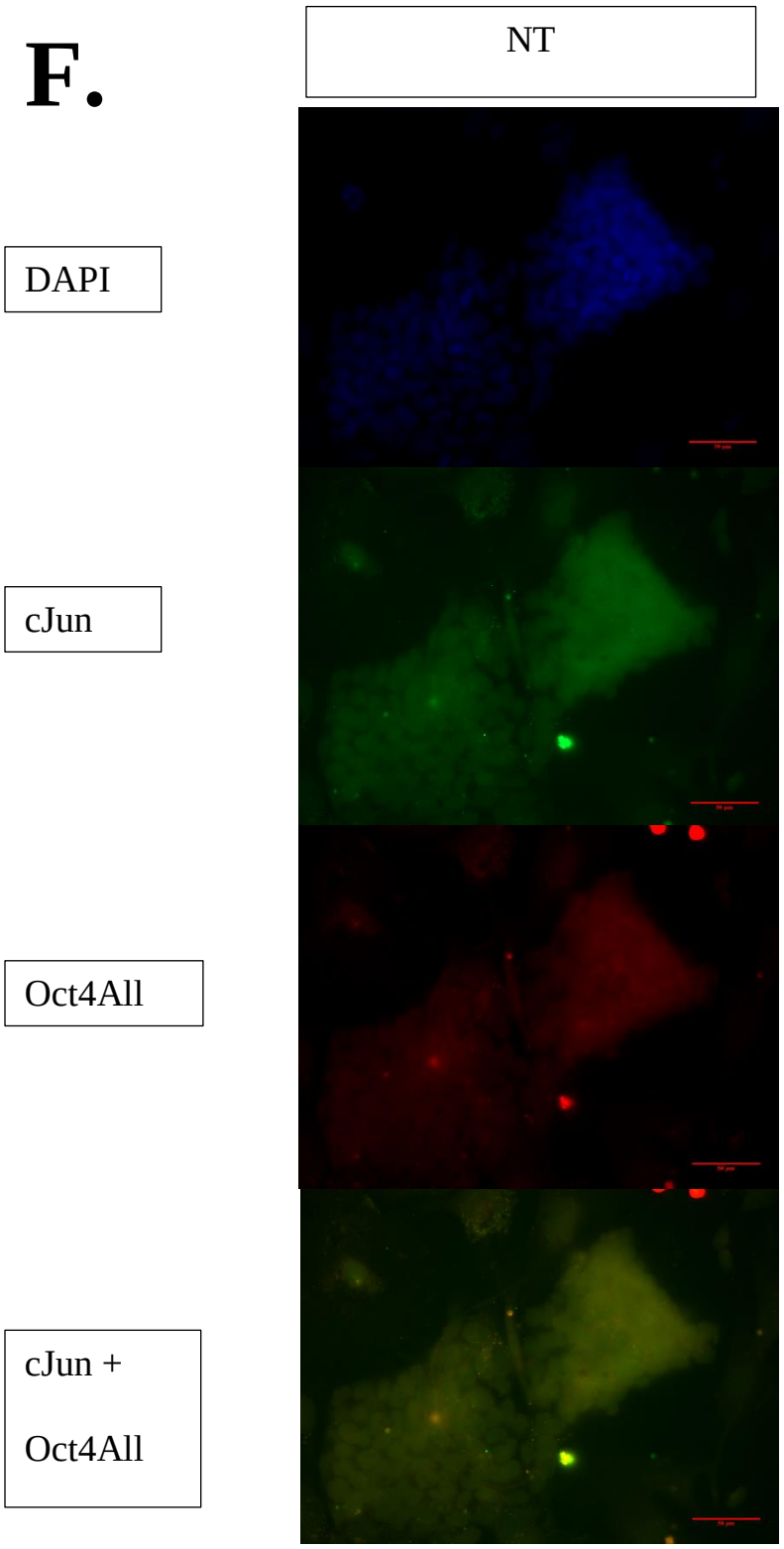

G.

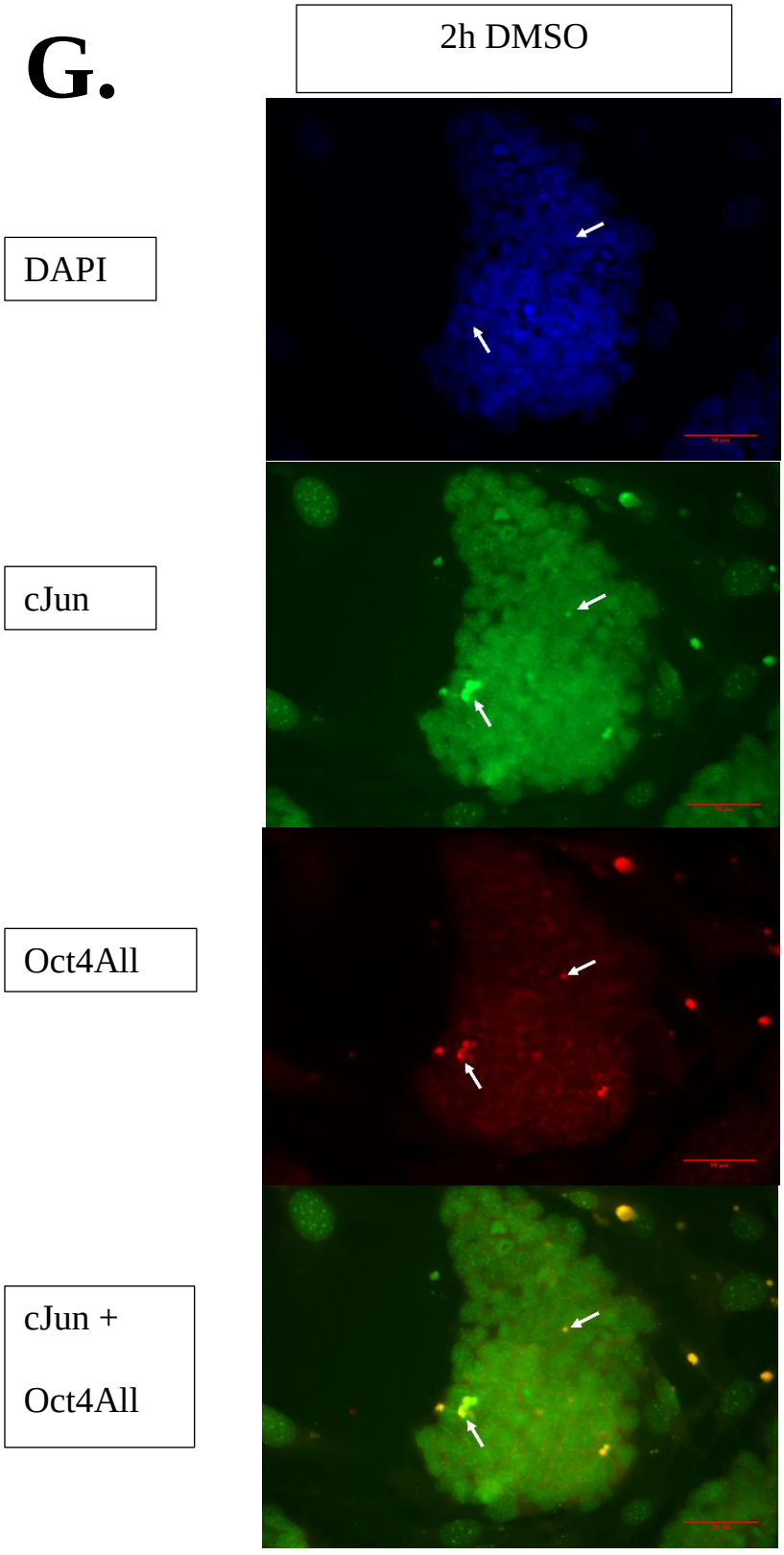

H.

4h DMSO

DAPI

cJun

Oct4All

cJun +

Oct4All

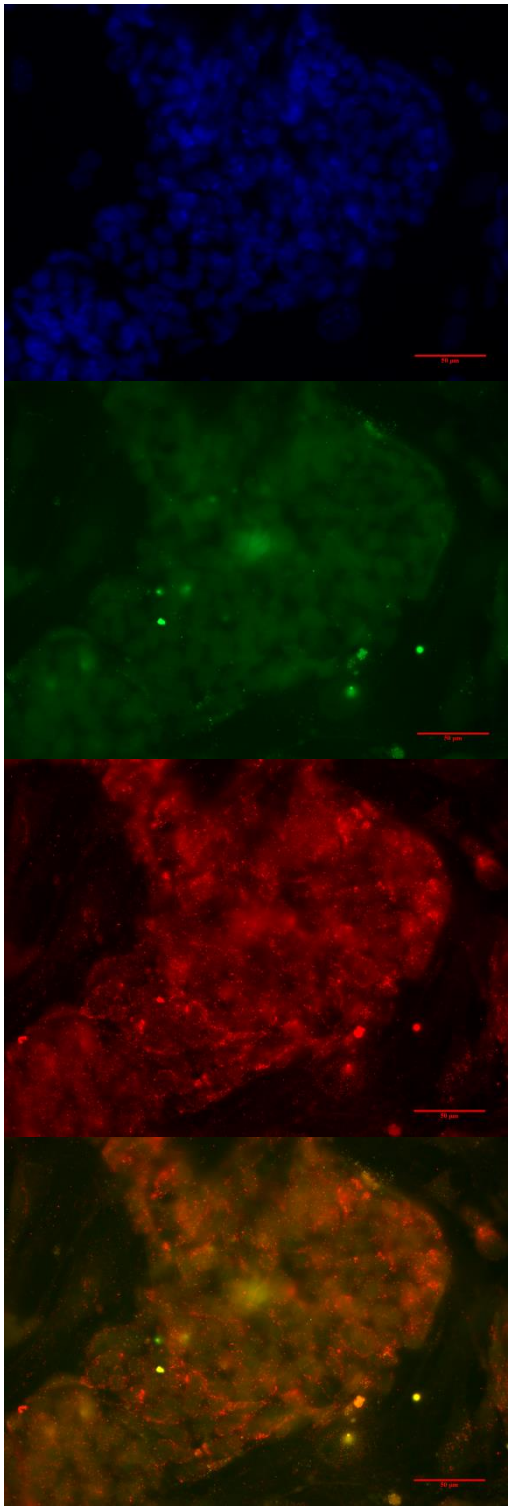

I.

2h Nocodazole (5ug/ml)

DAPI

cJun

Oct4All

cJun +

Oct4All

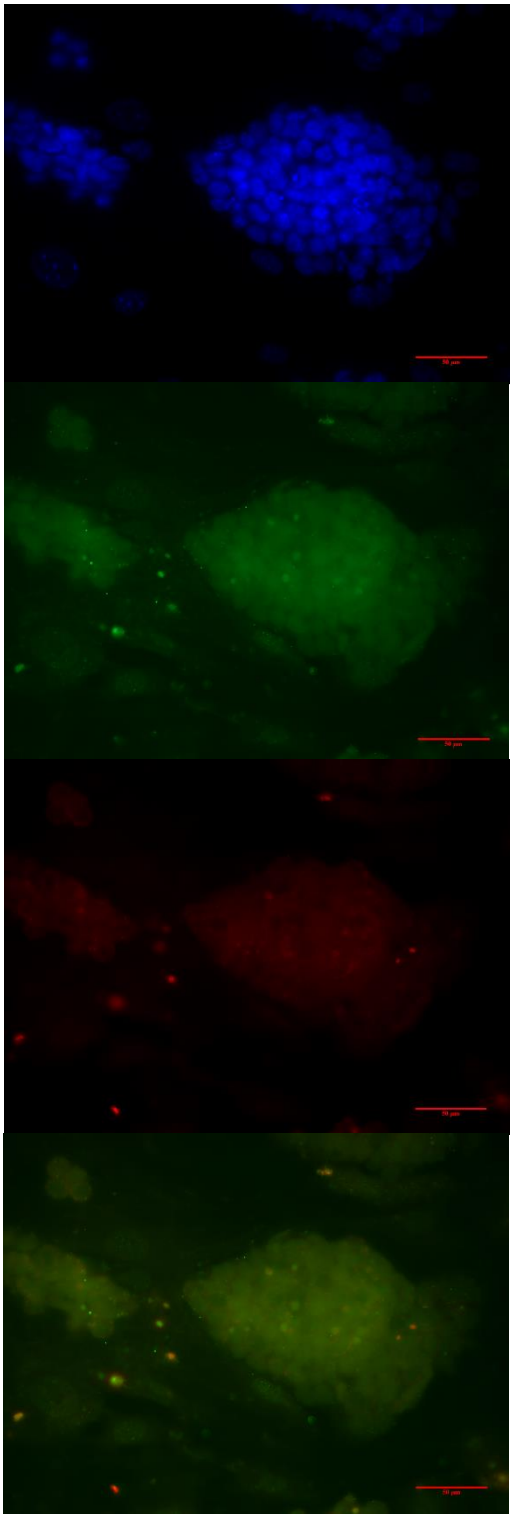

J.

4h Nocodazole (5ug/ml)

DAPI

cJun

Oct4All

cJun +

Oct4All

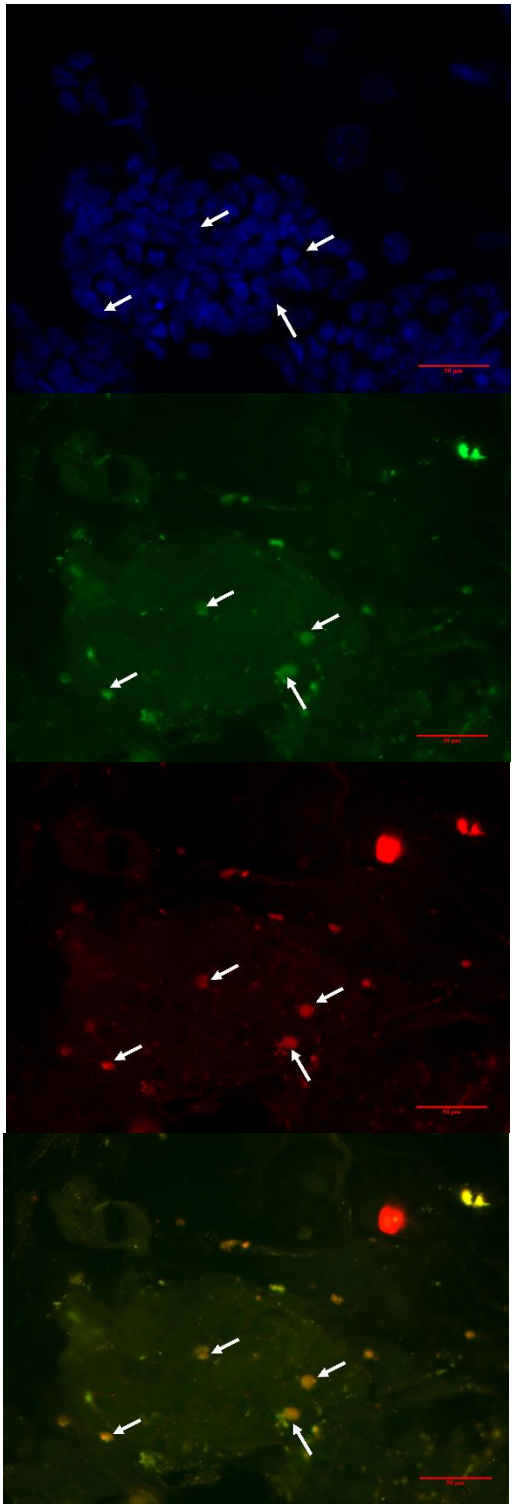

Figure 12. Nocodazole has varied affect on cJun and Oct4 protein expression. A-E. An example of variation seen between replicates for Oct4A/B. These data exhibit a more stark decrease in Oct4A/B and a larger increase in cJun expression. Bright spots of Oct4A signal still co-localize with cJun. **A.** NT. **B.** 2h DMSO. **C.** 4h DMSO. **D.** 2h nocodazole. **E.** 4h nocodazole **F-J**. An example of the variation seen between replicates for Oct4all expression. Both cJun and Oct4all expression are dramatically decreased, but the bright spots still co-localize. **F.** NT. **G.** 2h DMSO. **H.** 4hDMSO. **I.** 2h nocodazole. **J.** 4h nocodazole. Arrows in both images indicate a few, but not all, of the areas where co-localization was identified.

Table 5. Nocodazole treatments show increased co-localization of cJun with Oct4A, but a decrease in co-localization with Oct4all variants. A. Table of Oct4A co-localization with cJun for each treatment condition. Each row contains the number of co-localized spots of the total number of spots identified. Co-localized spots were evaluated on the Pearson's and Mander's coefficients provided by the Zeiss analytical software. The Mander's coefficient is the percentage of overlap between the two channels, while the Pearson's determines the correlation between pixel intensity of the two channels (Zinchuk et al. 2007). Very strong Pearson's values are those greater than 0.85, strong is 0.85 to 0.49, and moderate is 0.49 to 0.1. Weak and very weak Pearson's coefficients are 0.1 to -0.26 and -0.26 to -1. Very strong Mander's coefficients are ≥0.98, strong are 0.98 to 0.89, and moderate values are 0.89 to 0.71. Weak and very weak Mander's coefficients are 0.71 to 0.5 and 0.5 to 0. These data were then further defined by combinations of the two coefficients to provide a better co-localization picture. The greatest number of co-localized spots per colony is seen in the 4h nocodazole treatment, but the greatest percentage of co-localized spots with at least strong Pearson's and Mander's coefficients was seen in the 2h nocodazole sample. **B.** Table of Oct4all co-localization with cJun. These data were organized as previously mentioned.

A.

Oct4A co-localization	NT	2h DMSO	4h DMSO	2h Nocodazole	4h Nocodazole
Very strong Pearson's coefficient (≥0.85)	4	3	7	21	3
Strong Pearson's coefficient (≥0.49)	12	18	9	26	19
Moderate Pearson's coefficient (≥0.1)	12	11	14	5	9

Oct4A co-localization	NT	2h DMSO	4h DMSO	2h Nocodazole	4h Nocodazole
Very strong Mander's coefficient (≥0.98)	26	40	31	56	22
Strong Mander's coefficient (≥0.89)	7	3	11	2	2
Moderate Mander's coefficient (≥0.71)	0	0	2	0	0
Very strong Pearson's and Very strong Mander's	3	3	6	21	3
Very strong Pearson's and Strong Mander's	1	0	1	0	0
Strong Pearson's and Very strong Mander's	10	17	5	24	19
Strong Pearson's and Strong Mander's	2	1	3	2	0
Strong Pearson's and Moderate Mander's	0	0	1	0	0
Moderate Pearson's and Very Strong Mander's	8	9	11	5	8
Moderate Pearson's and Strong Mander's	4	2	2	0	1
Moderate Pearson's and Moderate Mander's	0	0	1	0	0
Weak Pearson's and Very Strong Mander's	4	10	8	2	9
Weak Pearson's and Strong Mander's	0	0	1	0	0
Very Weak Pearson's and Very Strong Mander's	1	1	1	4	0
Very Weak Pearson's and Strong Mander's	0	0	4	0	1
Total number of co-localized spots identified	33	43	44	58	41
Total number of cell colonies for all images	40	53	54	66	31

B.

Oct4All co-localization	NT	2h DMSO	4h DMSO	2h Nocodazole	4h Nocodazole
Very strong Pearson's coefficient (≥0.85)	5	7	1	12	5
Strong Pearson's coefficient (≥0.49)	7	6	6	9	17
Moderate Pearson's coefficient (≥0.1)	5	5	6	10	23
Very strong Mander's coefficient (≥0.98)	19	15	12	33	50
Strong Mander's coefficient (≥0.89)	0	5	8	6	8
Moderate Mander's coefficient (≥0.71)	0	0	0	0	0
Very strong Pearson's and Very strong Mander's	5	7	1	11	5
Very strong Pearson's and Strong Mander's	0	0	0	1	0
Strong Pearson's and Very strong Mander's	7	4	3	6	16
Strong Pearson's and Strong Mander's	0	2	3	3	1
Moderate Pearson's and Very Strong Mander's	5	3	4	8	17
Moderate Pearson's and Strong Mander's	0	2	2	2	6
Moderate Pearson's and Moderate Mander's	0	0	0	0	0
Weak Pearson's and Very Strong Mander's	2	1	4	7	9
Weak Pearson's and Strong Mander's	0	1	3	0	2
Very Weak Pearson's and Very Strong Mander's	0	0	0	1	2
Very Weak Pearson's and Strong Mander's	0	0	0	0	0

Oct4All co-localization	NT	2h DMSO	4h DMSO	2h Nocodazole	4h Nocodazole
Total number of co-localized spots identified	19	20	20	39	58
Total number of cell colonies for all images	36	46	27	41	45

Similarly to Oct4A co-localization, Oct4all co-localization to cJun was assessed. Generally, there was an increase in cJun and Oct4all with nocodazole treatment and a localization more towards the cytoplasm. Again, bright spots appear to be co-localized with cJun in the nucleus, but many bright areas that appear to be cytoplasmic co-localize with cJun as well (**Error! Reference source not found.**). In contrast to this, another replicate showed a dramatic decrease in Oct4all and a slight decrease in cJun. The bright spots still co-localized with cJun and appeared to be mostly in the nucleus. There was also a larger increase in cJun and Oct4all for the 4h DMSO samples, which also appeared to be cytoplasmic (**Error! Reference source not found.**). Analysis of the co-localized spots across all replicates (n=3) showed that the number of co-localized spots per colony increased with nocodazole treatment. Despite this, the degree of co-localization decreased with nocodazole treatment. Only 38% of identified co-localized spots in 4h nocodazole samples had at least a strong Pearson's and Mander's coffecient, while 54% were seen in the 2h nocodazole samples and 63% in the NT samples. This would correlate well to the data seen with Oct4A, as increases in co-localization of Oct4A with cJun would indicate that these two transcription factors have more of a relationship than cJun with other Oct4 variants.

DISCUSSION

We aimed to better characterize the effects of cJun on *Oct4* expression. To achieve this, we transiently transfected mES cells with a GFP-cJun construct and a transcriptionally inactive L40/42 mutant. Addtionally, we utilized a cytoskeleton disrupting drug, nocodazole, to determine if effects of cJun on Oct4 variants would occur when endogenous cJun expression was increased under these conditions. Overall, our data indicates overexpression of cJun by both mechanisms affects Oct4 variant expression. Previous experiments in our laboratory and the data reported here describing increased expression of GATA4 and GATA6 in mESCs ectopically expressing GFP-cJun and GFP-L/40/42A suggest these changes in Oct4 affect the potency of mESCs.

cJun Over Expression Produces an Increase in Oct4 Variants and Affects Other Pluripotency Markers

Transfection of cJun increased overall levels of cJun cDNA when analyzed by SYBR qPCR chemistry; however, these data were complicated by multiple bands on gel analysis and mulitple dissociation peaks. This only occurs in samples transfected with either cJun or the L40/42 mutant, suggesting ectopic expression of cJun from the pLVX plasmids are creating additional targets recognized by the primers. As the primers produce a single band when the purified plasmid is used as template, the most likely cause for multiple bands is that the mRNA produced from the plasmid is different than that expressed

from the genomic loci. Some bands on the gel which were too close in size to distinguish from one another were seen in a few samples which produced only one dissociation peak. Further experiments will be needed to fully understand the inconsistency. Plasmid primers did produce small additional peaks in the dissociation curves, but they only produced one band after agarose gel analysis. Becaue these data were cleaner, the plamid expression was used as an indicator of cJun over expression.

Using a SYBR-based assay, we were able to determine the trends between expression of *Oct4*A, *Nanog* and *Sox2* in relation to the cJun overexpression data. We saw a slight increase in expression of all genes in cJun transfected samples. The increase in *Oct4*A gene expression correlates with Western blot analysis of these samples (Brewer 2018). The increase in *Oct4*A gene expression is very similar in the transcriptionally inactive L40/42 samples, which suggests perhaps that the MAPK binding that ocurrs at those residues to phosphorylate S63 and S73 is not as necessary in this system.

The exon specific primer/probe analyses showed a larger increase in the the *Oct4*B variants compared to *Oct4*A expression, which allowed us to better resolve the isoform expression differences captured by others in our laboratory who looked at protein expression. Protein expression was assessed with a polyclonal antibody generated from a recombinantly produced peptide that contains all amino acids of the human Oct4 protein that are N-terminal to the POU DNA binding domain. We called Cell Signalling Technologies to verify this region contains exon 1 of Oct4A as well as amino acids of

Oct4B. When aligning the human and murine protein sequences, the Oct4B amino acid sequence is conserved (Figure 13).

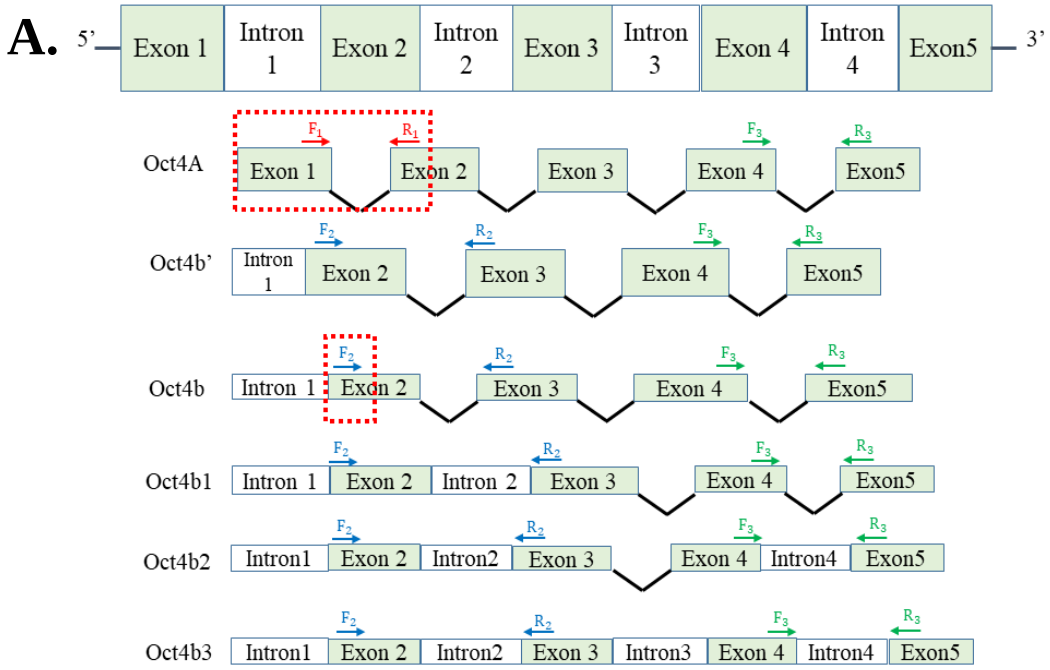

Figure 13. The polyclonal antibody used to identify Oct4A has some alignment with Oct4B. A. A graphical representation of the *Oct4*B variant transcripts with primers for exon 1 (red), exon 2 (blue), and exon 5 (green) denoted by F and R. Additional red boxes outline the approximate position in the protein where the antibody would bind. **B.** Alignment of the primary amino acid sequence of the mouse protein with the human protein up to the POU domain**.**

The Oct4 variant specific primer-probe assays reveal a large increase in the cDNA of Oct4B variants and a decrease in Oct4A. Furthermore, agarose gel electrophoresis reveal multiple products generated in each of the transfected sample using exon 2 primers. Some are of expected sizes, as the primers should amplify Oct4b, Oct4b', Oct4b1, b2, and b3 sequences recently identified by Liu et al (2017), but there are also additional bands. Those in samples expressing GFP are smaller and not as distinct. The cJun samples have a clearer band around 400bp and a faint band around 1,00bp. The L40/42 samples analyzed with primers to both exon 2 and exon 5 appear to have a range of large, distinct bands, suggesting that loss of phosphorylation of S63/73 affects their expression. One possible mode of regulation to explain the increase in products specific to L40/42 expression is through a change in Oct4 mRNA splicing. cJun has previously been shown to particiapte in splicing regulation by regulating the transcription of several genes involved in the splicing process. The loss of cJun resulted in a change in splicing pattern for 147 genes, including 8 involved in cancers and 14 involved in cell death (Katiyar et al. 2012). It would be interesting to sequence the additional products, which would reveal whether there are additional variant transcripts that have not been identified or if there is aberrant splicing occuring, which results in transcripts that differ in intron number and length. Sequencing would elucidate whether these sequences contain the probe sequence, which would define which bands contribute to the expression data.

It is also interesting to note that when optimizing the E2 primers, we used cDNA from embryoid bodies (EBs) because there was little to no product produced from the

cDNA of untransfected mES cells. Since there are changes in Oct4 expression affected by cJun over expression, we expect the delicate balance necessary for pluripotency to be shifted, as levels of 1.5 fold expression are sufficient to affect cell fates (Niwa et al. 2000). There is some evidence that *Oct4*B variants may have a function in maintaining pluripotency as well (Liu et al. 2017). There is a an increase in *Sox2* gene expression at a level that could predict biological significance, as it is highest in cells expressing cJun L40/42 when compared to cJun wild type. Though these data indicate that cJun may be regulating *Sox2* expression directly by binding the promoter, an alignment analysis of the *Sox2* gene and promoter did not reveal an AP-1 binding site motif; and thus, it is unlikely that cJun directly regulates *Sox2* expression. An alternative model is that it is the increase of *Oct4* by cJun that is responsible for this change, as Oct4 has been shown to regulate *Sox2* expression (Catena et al. 2004).

Even though none of these data were statistically significant, due to large variability and small sample size, the balance of pluripotency markers is very specific. Less than a two-fold increase in Oct4 expression can result in the formation of primative endoderm and mesoderm (Niwa et al. 2000). Sox2 has been shown to repress mesoderm formation (Wang et al. 2012) and a loss of Nanog results in a failure of the blastocyst inner cell mass to generate epiblast tissue and ES cells differentiate into extraembryonic endoderm (Yamaguchi et al. 2005). Additionally, Nanog maintains pluripotency in the absence of LIF (Yamaguchi et al. 2005).

cJun Over Expression Directs mESCs Towards an Endoderm Lineage

If slight changes in pluripotency markers have effects on potency, we would predict that there would be an effect on gene expression of germ layer markers affected by slight increases in Oct4 expression (Gata4, Gata6) and Sox2, which has been shown to repress mesoderm formation (Wang et al. 2012) in these cells. Indeed, we observed larger increases in *Gata4* and *Gata6* expression of NT normalized data. While the differences were a bit smaller, GFP normalized data also show the same trend. GFP normalized data showed that generally an increase in cJun resulted in an increase in *Gata4* and *Gata6* expression. When cJun overexpression was at its highest (331.3-fold increase), based on pLVXcJun amplification, we saw 1.3-fold increase of *Gata4* and a 1.2 increase of *Gata6*. At the lowest pLVXcJun expression (104.9-fold increase), we saw a decrease in both *Gata4* and *Gata6* with a 0.75- and 0.79-fold change for *Gata4* and *Gata6*, respectively. The intermediate overexpression values of 168.5-fold and 190.4-fold resulted in 1.4-fold and 2.4-fold increase of *Gata4*, respectively. This corresponded to a 2.6-fold and 1.9-fold increase in in *Gata6*, respectively. Western blot analyses performed by others in our laboratory showed an increase in Gata4 protein in cJun transfected samples as well (Brewer 2018). Biologically, expression of *Gata6* precedes *Gata4*, as *Gata6* drives differentiation to primitive endoderm and *Gata4* marks differentiation into definitive endoderm tissues (Plusa et al. 2008; Schrode et al. 2013). Additionally, *Gata6* is necessary for primitive endoderm formation, as *Gata6* negative ICM cells differentiate into mature epiblast tissue

prematurely (Schrode et al. 2013). This possibly explains the larger increase in gene expression for *Gata6*.

The changes in pluripotency markers seen with overexpression of *cJun* coupled with the upregulation of *Gata6* suggest cJun could be directing the cells towards - endoderm. In addition to these data, cardiomyocytes formed from cJun transfected EBs exhibited an increased number of beating colonies (Brewer 2018). This supports previous research that showed Gata4 expression in embryoid bodies directs these cells towards an endoderm fate, which produce cardiac inducing factors and enhance cardiomyocyte formation (Holtzinger et al. 2009). This does not exclude the possibility that over expression of *cJun* can be initiating the mechanism through other pathways as an increase in cJun and loss of Oct4 are typically indicators for differentiation.

Other germ layer markers, *Brachyury* and *Sox1*, were not as greatly affected by cJun over expression. When normalized to GFP the mean expression was similar to NT. Interestingly, *Sox1* expression normalized to GFP is greatly affected by L40/42 transfection. Sox1 marks ectodermal lineages and previous data from our lab has shown that cJun over expression inhibits proper differentiation of pancreatic islet-like insulin secreting clusters with reduced neural network formation, while the L40/42 transfection increased both the number of these clusters and the neural projections surrounding them (Hosawi 2016). The large increase in *Sox1* gene expression is supportive of this data and suggests that a decrease in cJun would direct cells towards ectoderm lineages. Additionally, *Brachyury* gene expression was not affected, which correlates with Western blot data that

did not show any change in protein expression as well (Brewer et al. *in prep*). This supports the idea that cJun may not be involved in *Brachyury* regulation at either the protein or the transcript level. Taken together, these data indicate that cJun over expression in mES cells begins directing cells towards an endoderm progam.

Nocodazole-Induced Expression of cJun Produces a Trend of Increased cJun that Affected the Expression of Pluripotency Genes and Oct4 Variants.

Nocodazole is a cytoskeltal disrupting drug, which can induce alternative tranlation of mRNA. It has been shown to increase cJun protein levels by intitating translation at an IRES in the cJun 5' mRNA in human and rat priamry glia, NIH3T3, HEK293T, Cos-7, and HeLa cell lines (Polak et al. 2006; Blau et al. 2012). Activation of these mechanisms has also shown that cJun protein produced in this manner has different downstream effectors than proteins produced through cap-dependent mechanisms. Our results show nocodazole treatment of mES cells produced variable expression of *cJun*. Interestingly, cJun expression is also affected by DMSO. The mechanism by which DMSO affects cellular function isn't fully understood and varies between cell type used. However, it has been shown it increases differentiation of human embryonic stem cells (hESCs) to definitive endoderm through the formation of hepatocytes (Pal et al. 2012; Czysz et al. 2015) and there has been some evidence which suggests that DMSO may affect splice sights *in vitro*

(Bolduc et al. 2001). DMSO treatment produced a similar, but less extreme pattern of cJun variation. Threfore, there is a nocodazole specific increase in *cJun* expression.

As seen in our transient transection assays, the variations in *cJun* expression observed in nocodozole-treated samples associated with variations in gene expression of *Oct4*A, *Nanog* and *Sox2* by SYBR analysis. The variation in expression levels observed between replicates may be due to a dosage affect. The increased expression of *Oct*4 may be due to cJun binding the promoter and regulating expression or it may be due to activation of the IRES present in *Oct4*. DMSO also produced an increase in *Oct4*A expression, but this was complicated by one replicate (replicate 3, table 4) producing an additional band between 1200bp and 1500bp. This band was not seen in any other sample of the replicate and could be due to the alternative translation of *cJun*.

The probe-based assays do not show as great an increase in gene expression, however the trend holds. Where there is increased *cJun* due to nocodazole, there is increased expression of *Oct4*A (exon 1) and decreased expression of *Oct4*B (exon 2). Additionally, extra bands were seen with exon 1 primers at about 250bp and 400bp. Normalization of all expression data to DMSO maintained the trends seen with NT normalized data, but indicates *cJun* expression from nocodazole may affect *Oct4* expression in a dose dependent manner. For DMSO normalized data, replicate 1 produces the highest fold change in expression for *cJun* at 169.9 and 1.6 for exon 1. Replicate 2 expressed less than half the level of *cJun* at 43.1, but has a 2.6 fold increase over DMSO for exon 1. Replicate 3 has the lowest *cJun* expression at 2.6 and produced a fold change

of 1.2 for exon 1. These data would indicate that there might be an optimal level of *cJun* expression to increase *Oct4*A, while others promote other *Oct4* variants. This would indicate that cJun regulates Oct4A expression, but does not eliminate the possibility that nocodazole could regulate protein expression translationally. Western blot analysis was as variable as the gene expression and requires further study to determine which mechanisms are functioning in this system.

Gel analysis of the Oct4 primer/probe assays produced similar results to tranfected data; multiple unexpected bands were seen. Exon 1, which only produced one band for all treatments in the over expression data, had multiple bands for DMSO- and nocodazole-treated samples. The size of these bands varied between replicate, which is most likely due to the variable cJun expression. Bands for replicate 1, which had the highest fold change of 169.9, (Figure 10) are at 250bp and 400bp, while bands for replicate 2, which had a fold change of 43.1, are only seen in nocodazole samples and are >10,000bp. Additionally replicate 3 had a fold change of 2.65 and did not produce any extra bands, except a faint 300bp band in one triplicate of nocodazole treated sample. Replicate 4 (data not shown) showed the most extreme nocodazole response, with extremely bright bands around 500-600bp (Appendix D and E) Exon 2 primers produced a large range of bands, similar to those seen in transfection data and appeared to have a larger variability between replicates. All replicates had a 350bp band, like the transfected samples; however, this is not an expected amplicon. Additionally there are many bands between 100-350bp that are also similar to the transfection data. These regions also encompass the expected amplicon sizes.

In addition to these similarities, nocodazole samples occasionally produce a 1500bp, or >10,000bp band that correspond to replicates that show similarly large bands in exon 1. Interestingly, exon 5 primers show the same trend. The same replicates produce bands >10,000bp and between 900-1,000bp. In addition to this, NT samples amplified by exon 5 primers occasionally produce bands at 250bp, 300bp, or 400bp. DMSO samples occassionally have bands at 300bp, while nocodazole samples can have the previously mentioned large bands or bands at 300bp and 400bp. All of these bands are similar bands seen with cJun and L40/42 transfected samples, except for the extremely large bands seen and the additional bands for exon 1, which only produced one band for all transfected samples. Despite different mechanisms in increasing cJun expression, there appears to be overlap in the bands produced, indicating the effect on *Oct4* variants is the same. The exceptions to this is the effect on *Oct4*A and the very large amplicons seen across primer sets (Appendix D and E)

It is possible that increased cJun from activation of the alternative translation pathway though nocodazole is affecting the splicing of the Oct4 transcripts such that many of the introns are not removed. Others have documented a role for cJun in regulation of splicing events. Studies performed in murine mamary epithilium demonstrate cJun regulates alternative exon splicing in approximately 147 genes (Katiyar et al. 2011). Further study of the *Oct4* variants and nocodazole is required to ellucidate the effect alternative translation mechanisms may have on gene expression.

Given the large changes on *Oct4* variants, we would expect the balanced network of pluripotency factors to be disrupted. While *Oct4*A expression is increased in nocodazole samples, the transcript levels may be enough to change potency and begin directing cells towards a specific fate, much like the spinfection samples. *Nanog* levels generally decreased with increased *cJun* expression and could be due to changes in expression of the other markers, or as a result of nocodazole treatment directly. Nocodazole has been shown by flow cytometry to reduce the number of Nanog positive human embryonic stem cells (Kallas et al. 2011); however they also saw a decrease in Oct4 positive cells. The authors postulated that nocodazole caused a decrease in Oct4, which decreased Nanog and thus pluripotency. Discovering how nocodazole affects cJun and the expression of Oct4 variants may explain this decrease. *Sox2* expression did not appear to be affected by nocodazole treatment. These data would appear to contradict the data produced by overexpression of cJun through transfection. However, cJun protein produced through alternative translation may be regulating expression of different genes and no longer regulates expression of *Sox2*. It is possible that nocodazole could also be initiating alternative translation of the Oct4 (Guo et al. 2012), which may also have different downstream targets that do not include *Sox2*.

Unfortunately, we could not determine the effect of nocodazole on germ layer expression, as we did with transfection samples, due to an inability to produce EBs in the presence of nocodazole. The repeated attempts resulted in large amounts of cell death by day 2. However, because gene expression is a relatively quick process, there may be the

possibility for a dosing schedule that would reduce cell exposure to the drug and still initiate a gene expression programs. Further studies will be needed to determine if these trends in gene expression of pluripotency markers results in a specific differentiation program. As there are many redundancies in cell signalling and many interconnecting parts of this system that are still unknown in ES cells, it is difficult to draw any conclusions beyond the general trends seen.

Nocodozole-Induced Changes in cJun and Oct4 Expression Co-localize to the Same Cells

Nocodazole treatment produced a varied response in protein expression by ICC analysis as well. The increases in cJun and either Oct4A or Oct4all varied from mild to large and varied within and between replicates. As each replicate was performed at different times and with different batches of nocodazole, it is possible the variation is from that. Despite this, there is a general trend consistant across all replicates. Bright spots of Oct4A or Oct4all generally co-localize in the same cell as those with high levels of cJun expression. cJun is not always the brightest at these spots, but it is there. Analysis of co-localized spots using the Zeiss software supports this trend. Evaluation of co-localization by Pearson's and Mander's coefficient shows that 2h nocodazole treatment produced the strongest cellular co-localization of Oct4A/B with cJun and 4h nocodazole treatment showed stronger co-localization than NT. However, there were a larger number of co-localized spots per colony for 4h nocodazole treated samples than 2h nocodazole.

Previous work demonastrated that nocodazole induces an increase in cJun mRNA 30 minutes post treatment; however, following this, there is no increase in mRNA for the following 24h in HeLa cells. Despite this, cJun protein increased over 24h (Polak et al. 2006). Our nocodazole samples were harvested 2h post nocodazole treatment and did show an increase in cJun transcript, which appears to contradict the previous findings. This could be explained by the transcriptional activity of mES cells, which are in a more transcriptionally active state. Because of this, mESCs may be more susceptible to gene expression changes or possibly more sensitive to the cytoskeletal disruption induced by nocodazole. Additionally, because of the more permissive chromatin structure and increased cJun, it is possible the increase in cJun cDNA expression seen might be due to regulation of its own promoter.

The number of cellular co-localization/colony also increased in cells examined with an antibody recognizing all isoforms of Oct4 (Oct4 all), but the degree of co-localization decreased with nocodazole treatment compared to NT. There was a higher degree of co-localization with 2h nocodazole samples, compared to 4h treatment. While the number of co-localized spots did not appear to increase with colony number, colony size was not taken into account and may be correlated. There appears to be a very tentative relationship between nocodazole and Oct4A co-localization with cJun versus Oct4all co-localization with cJun 2h after nocodazole treatment. In this treatment, the Oct4A/B co-localization increased, while Oct4all co-localization decreased. It is not at all a definitive relationship, but may indicate a trend that further testing would reveal. It

would also support the transcriptional data we saw. Generally speaking, there is an increase in co-localization of Oct4A/B/B1 with cJun in the same cell following nocodazole treatment, which is supported by transcript data via probe based assays. Additionally, the inconsistencies seen with ICC and Western blot analysis seem to correlate with the large variation seen in transcript data.

In addition to co-localization, we observed a few other trends with nocodazole treatment. While the sub-cellular localization of these proteins cannot be validated on our microscope, cJun expression appears to be more cytoplasmic 4h after nocodazole treatment. Oct4all also demonstrated this pattern and cytoplasmic localization of Oct4B variants has been shown previously with genotoxic, heat, and cell stress (Wang et al. 2009; Gao et al. 2012).

Generally, all co-localized spots had at least a strong Mander's coefficient. The Pearson's coefficient was more distributed from very weak co-localization to very strong. However, generally very few co-localized spots fell into the weak or very weak category. This indicates there is a large portion of overlap between these signals in general, but a more variable correlation in relative signal intensity. Further studies on the effect of nocodazole on the co-localization of cJun with Oct4 variants could include the use of a microscopy that images samples in slices, which would help account for the overlap. Because cell colonies are 3D structures, but our images are not, we cannot determine whether signal overlap is in the same Z plane. The use of confocal microscopy in conjunction with deconvolution software and the antibody techniques we utilized could

improve resolution. Additionally, transmission electron microscopy could be utilized with stains for specific organelles or structures and gold-labeled anitbodies to identify these proteins at more precise locations within a single cell.

CONCLUSIONS

cJun is an important transcription factor in development. Previous work has shown cJun inhibits expression of genes important to pluripotency, like *Sall4* and *Nanog*, and upreulates expression of *Gata4* and *Gata6* (Liu et al. 2015). Generally an increase in cJun has marked a decrease in pluripotency, but the *Oct4* promoter contains an AP-1 binding site that appears to allow cJun regulation of *Oct4* variants, including the potency marker Oct4A.

Through overexpression of cJun by transiently transfecting mES cells, we determined that cJun may regulate the expression of *Oct4* variants, with the strongest change in *Oct4*B variants. That we saw a larger increase in these variants with the transcriptionally inactive L40/42 mutant indicates there may be an alternative splicing mechanism activated by cJun overexpression. An increase was also seen for *Sox2* with this mutant, indicating a potential mechanism for cJun regulation of *Sox2* through Oct4A. With these samples, we were also able to determine that overexpression of *cJun* drives mES cells toward an endoderm lineage and the L40/42 mutant may drive mES cells towards an ectodermal lineage. The upregulation of *Gata4* correlates with *cJun* overexpression and the culmination of these data support previous works that show Gata4 expression in EBs increases cardiomyocyte formation by producing specific endoderm lineages that generate cardiac inducing factors. By using nocodazole to induce cJun expression we determined that *cJun* gene expression is increased by drug treatment and that cJun protein increased by nocodazole co-localizes strongly with Oct4A/B at 2h post

treatment and not as strongly with other Oct4 variants. More work will be necessary to determine the exact mechism by which *cJun* cDNA is increased versus protein expression using nocodazole stimulation and how that might affect Oct4 gene and protein expression, as well as potency. Additionally, we were able to determine that additional bands are produced from *Oct4* variants with nocodazole and DMSO that were not seen with transfected samples. Although more work is required to determine the identity of the Oct4 variants produced, cJun appears to regulate expression of all Oct4 variants.

REFERENCES

Abboud N, Moore-Morris T, Hiriart E, Yang H, Bezerra H, Gualazzi M-G, Stefanovic S, Guénantin A-C, Evans SM, Pucéat M. 2015. A cohesin–OCT4 complex mediates Sox enhancers to prime an early embryonic lineage. Nat. Commun. 6. doi:10.1038/ncomms7749.

Aksoy I, Jauch R, Chen J, Dyla M, Divakar U, Bogu GK, Teo R, Keow C, Ng L, Herath W, Lili, Sun, Hutchins, Andrew P, Robson, Paul, Kolatkar, Prasanna R, Stanton, Lawrence W. 2013. Oct4 switches partnering from Sox2 to Sox17 to reinterpret the enhancer code and specify endoderm. EMBO J. 32:938–953. doi:10.1038/emboj.2013.31.

Atlasi Y, Mowla SJ, Ziaee SA, Gokhale PJ, Andrews PW. 2008. OCT4 spliced variants are differentially expressed in human pluripotent and nonpluripotent cells. Stem Cells 26:3068–3074. doi:10.1634/stemcells.2008-0530.

Azuara V, Perry P, Sauer S, Spivakov M, Jørgensen HF, John RM, Gouti M, Casanova M, Warnes G, Merkenschlager M, et al. 2006. Chromatin signatures of pluripotent cell lines. Nat. Cell Biol. 8:532–8. doi:10.1038/ncb1403.

Barrero MJ, Boué S, Izpisúa Belmonte JC. 2010. Epigenetic mechanisms that regulate cell identity. Cell Stem Cell 7:565–570. doi:10.1016/j.stem.2010.10.009.

Behrens A, Sibilia M, David J-P, Mo U, Hle-Steinlein È, Ois Tronche FË, Nther GÈ, Tz SÈ, Wagner EF. 2002. Impaired postnatal hepatocyte proliferation and liver regeneration in mice lacking c- jun in the liver. EMBO J. 21:1782–1790.

Bernardo AS, Faial T, Gardner L, Niakan KK, Ortmann D, Senner CE, Callery EM, Trotter MW, Hemberger M, Smith JC, Bardwell, Lee, Moffett, Ashley, Pedersen, Roger A. 2011. BRACHYURY and CDX2 mediate BMP-induced differentiation of human and mouse pluripotent stem cells into embryonic and extraembryonic lineages. Cell Stem Cell 9:144–155. doi:10.1016/j.stem.2011.06.015.

Bernstein BE, Mikkelsen TS, Xie X, Kamal M, Huebert DJ, Cuff J, Fry B, Meissner A, Wernig M, Plath K, Jaenisch, Rudolf, Wagschal, Alexandre, Feil, Robert, Schreiber, Stuart L, Lander, Eric S. 2006. A bivalent chromatin structure marks key developmental genes in embryonic stem cells. Cell 125:315–326. doi:10.1016/j.cell.2006.02.041.

Le Bin GC, Muñoz-Descalzo S, Kurowski A, Leitch H, Lou X, Mansfield W, Etienne-Dumeau C, Grabole N, Mulas C, Niwa H, Hadjantonakis, Anna-Katerina, Nichols, Jennifer. Oct4 is required for lineage priming in the developing inner cell mass of the mouse blastocyst. Development 141:1001–1010. doi:10.1242/dev.096875.

Blau L, Knirsh R, Ben-Dror I, Oren S, Kuphal S, Hau P, Proescholdt M, Bosserhoff A-K, Vardimon L. 2012. Aberrant expression of c-Jun in glioblastoma by internal ribosome entry site (IRES)-mediated translational activation. Proc. Natl. Acad. Sci. 109:E2875–E2884. doi:10.1073/pnas.1203659109.

Bolduc L, Labrecque B, Cordeau M, Blanchette M, Chabot B. 2001. Dimethyl sulfoxide affects the selection of splice sites. J. Biol. Chem. 276:17597–17602. doi:10.1074/jbc.M011769200.

Boyer LA, Lee TI, Cole MF, Johnstone SE, Levine SS, Zucker JP, Guenther MG, Kumar RM, Murray HL, Jenner RG, Gifford, David K, Melton, Douglas A, Jaenisch, Rudolf, Young, Richard A. 2005. Core transcriptional regulatory circuitry in human embryonic stem cells. Cell 122:947–956. doi:10.1016/j.cell.2005.08.020.

Catena R, Tiveron C, Ronchi A, Porta S, Ferri A, Tatangelo L, Cavallaro M, Favaro R, Ottolenghi S, Reinbold R, Schöler, Hans, Nicolis, Silvia K. 2004. Conserved POU binding DNA sites in the Sox2 upstream enhancer regulate gene expression in embryonic and neural stem cells. J. Biol. Chem. 279:41846–41857. doi:10.1074/jbc.M405514200.

Chambers I, Smith A. 2004. Self-renewal of teratocarcinoma and embryonic stem cells. Oncogene 23:7150–7160. doi:10.1038/sj.onc.1207930.

Chen CY, Cheng YY, Yen CYT, Hsieh PCH. 2017. Mechanisms of pluripotency maintenance in mouse embryonic stem cells. Cell. Mol. Life Sci. 74:1805–1817. doi:10.1007/s00018-016-2438-0.

Chen T, Du J, Lu G. 2012. Cell growth arrest and apoptosis induced by Oct4 or Nanog knockdown in mouse embryonic stem cells: a possible role of Trp53. Mol Biol Rep 39:1855–1861. doi:10.1007/s11033-011-0928-6.

Curran T, Franza BR. 1988. Fos and Jun: The AP-1 connection. Cell 55:395–397. doi:10.1016/0092-8674(88)90024-4.

Czaja MJ. 2003. The Future of GI and Liver Research: Editorial Perspectives III. JNK/AP-1 regulation of hepatocyte death. Am J Physiol Gastrointest Liver Physiol 284:G875–G879.

Czysz K, Minger S, Thomas N. 2015. DMSO efficiently down regulates pluripotency genes in human embryonic stem cells during definitive endoderm derivation and increases the proficiency of hepatic differentiation. PLoS One 10:1–16. doi:10.1371/journal.pone.0117689.

Eferl R, Wagner EF. 2003. AP-1: a double-edged sword in tumorigenesis. Nat. Rev. Cancer 3:859–68. doi:10.1038/nrc1209.

Efroni S, Duttagupta R, Cheng J, Dehghani H, Hoeppner DJ, Dash C, Bazett-Jones DP, Le Grice S, Mckay RDG, Buetow KH, Gingeras, Thomas R., Misteli, Tom, Meshorer, Eran. 2008. Global transcription in pluripotent embryonic stem cells. Cell Stem Cell 2:437–447.

Feldman N, Gerson A, Fang J, Li E, Zhang Y, Shinkai Y, Cedar H, Bergman Y. 2006. G9a-mediated irreversible epigenetic inactivation of Oct-3/4 during early embryogenesis. Nat. Cell Biol. 8:188–194. doi:10.1038/ncb1353.

Fouse SD, Shen Y, Pellegrini M, Cole S, Meissner A, Neste L Van, Jaenisch R, Fan G. 2008. Promoter CpG methylation contributes to ES cell gene regulation in parallel with Oct4/Nanog, Polycomb binding and histone H3 lys4/lys27 trimethylation. Cell Stem Cell 2:160–169. doi:10.1016/j.stem.2007.12.011.

Gao Y, Wei J, Han J, Wang X, Su G, Zhao Y, Chen B, Xiao Z, Cao J, Dai J. 2012. The

novel function of OCT4B Isoform-265 in genotoxic stress. Stem Cells 30:665–672. doi:10.1002/stem.1034.

Grabole N, Tischler J, Hackett JA, Kim S, Tang F, Leitch HG, Magnúsdóttir E, Surani MA. 2013. Prdm14 promotes germline fate and naive pluripotency by repressing FGF signalling and DNA methylation. Nat. Publ. Gr. 14:629–63767. doi:10.1038/embor.2013.67.

Guenther MG, Levine SS, Boyer LA, Jaenisch R, Young RA. 2007. A Chromatin Landmark and Transcription Initiation at Most Promoters in Human Cells. Cell 130:77–88. doi:10.1016/j.cell.2007.05.042.

Guo C long, Liu L, Jia Y dan, Zhao X yang, Zhou Q, Wang L. 2012. A novel variant of Oct3/4 gene in mouse embryonic stem cells. Stem Cell Res. 9:69–76. doi:10.1016/j.scr.2012.04.004.

Hackett JA, Surani MA. 2012. DNA methylation dynamics during the mammalian life cycle. Phil Trans R Soc B 368. doi:10.1098/rstb.2011.0328.

Hattori N, Nishino K, Ko Y-G, Hattori N, Ohgane J, Tanaka S, Shiota K. 2004. Epigenetic control of mouse Oct-4 gene expression in embryonic stem cells and trophoblast stem cells. doi:10.1074/jbc.M309002200.

Hilberg F, Aguzzi A, Howells N, Wagner E, Nature. 1993. c-jun is essential for normal mouse development and hepatogenesis. Agric. Environ. Sci. Database pg 365.

Ho L, Ronan JL, Wu J, Staahl BT, Chen L, Kuo A, Lessard J, Nesvizhskii AI, Ranish J, Crabtree GR. 2009. An embryonic stem cell chromatin remodeling complex, esBAF, is essential for embryonic stem cell self-renewal and pluripotency. PNAS 106:5181–5186.

Holtzinger A, Rosenfeld GE, Evans T. 2009. Gata4 directs development of cardiac-inducing endoderm from ES cells. Magn Reson Imaging 31:477–479. doi:10.1016/j.immuni.2010.12.017.Two-stage.

Hu YC, Okumura LM, Page DC. 2013. Gata4 is required for formation of the genital ridge in mice. PLoS Genet. 9:1–12. doi:10.1371/journal.pgen.1003629.

Jerabek S, Merino F, Schöler HR, Cojocaru V. 2014. OCT4: Dynamic DNA binding pioneers stem cell pluripotency. Biochim. Biophys. Acta - Gene Regul. Mech. 1839:138–154. doi:10.1016/j.bbagrm.2013.10.001.

Jochum W, Passegueâ E, Wagner EF. 2001. AP-1 in mouse development and tumorigenesis. Oncogene 20:2401–2412.

Johnson RS, Van Lingen B, Papaioannou VE, Spiegelman BM. 1993. A null mutation at the c-jun locus causes embryonic lethality and retarded cell growth in culture. Genes Dev. 7:1309–1317.

Kallas A, Pook M, Maimets M, Zimmermann K, Maimets T. 2011. Nocodazole treatment decreases expression of pluripotency markers nanog and Oct4 in human embryonic stem cells. PLoS One 6. doi:10.1371/journal.pone.0019114.

Katiyar S, Jiao X, Addya S, Ertel A, Covarrubias Y, Rose V, Casimiro MC, Zhou J, Lisanti MP, Nasim T, et al. 2012. Mammary gland selective excision of c-Jun identifies its role in mRNA splicing. Cancer Res. 72:1023–1034. doi:10.1158/0008-5472.CAN-11-3647.

Lerch JK, Martinez Y, Bixby JL, Lemmon VP. 2014. cJun promotes CNS axon growth. Mol Cell Neurosci 59:97–105. doi:10.1016/j.mcn.2014.02.002.

Li J, Li J, Chen B. 2012. Oct4 was a novel target of Wnt signaling pathway. Mol. Cell. Biochem. 361:233–240. doi:10.1007/s11010-011-1148-z.

Liu J, Han Q, Peng T, Peng M, Wei B, Li D, Wang X, Yu S, Yang J, Cao S, Huang, Kaimeng, Hutchins, Andrew Paul, Liu, He, Kuang, Junqi, Zhou, Zhiwei, Chen, Jing, Wu, Haoyu, Guo, Lin, Chen, Yongqiang, Chen, You, Li, Xuejia, Wu, Hongling, Liao, Baojian, He, Wei, Song, Hong, Yao, Hongjie, Pan, Guangjin, Chen, Jiekai, Pei, Duanqing. 2015. The oncogene c-Jun impedes somatic cell reprogramming. Nat. Cell Biol. 17:856–867. doi:10.1038/ncb3193.

Liu X, Yu T, Sun Y, Wang H. 2017. Characterization of novel alternative splicing variants of Oct4 gene expressed in mouse pluripotent stem cells. :1–10. doi:10.1002/jcp.26411.

Martin GR. 1981. Isolation of a pluripotent cell line from early mouse embryos cultured in medium conditioned by teratocarcinoma stem cells. Proc. Natl. Acad. Sci. U. S. A. 78:7634–7638. doi:10.1073/pnas.78.12.7634.

Meissner A, Mikkelsen TS, Gu H, Wernig M, Hanna J, Sivachenko A, Zhang X, Bernstein BE, Nusbaum C, Jaffe DB, Gnirke, Andreas, Jaenisch, Rudolf, Lander, Eric S. 2008. Genome-scale DNA methylation maps of pluripotent and differentiated cells. Nature 454:766–770. doi:10.1038/nature07107.

Meshorer E, Yellajoshula D, George E, Scambler PJ, Brown DT, Misteli T. 2006. Hyperdynamic plasticity of chromatin proteins in pluripotent embryonic stem cells. Dev Cell 10:105–116. doi:10.1016/j.devcel.2005.10.017.

Mizuno N, Kosaka M. 2008. Novel variants of Oct-3/4 gene expressed in mouse somatic cells. J. Biol. Chem. 283:30997–31004. doi:10.1074/jbc.M802992200.

Nichols J, Zevnik B, Anastassiadis K, Niwa H, Klewe-Nebenius D, Chambers I, Schö H, Smith A. 1998. Formation of pluripotent stem cells in the mammalian embryo depends on the POU transcription factor Oct4. Cell 95:379–391.

Niwa H, Miyazaki J, Smith AG. 2000. Quantitative expression of Oct-3/4 defines differentiation, dedifferentiation or self-renewal of ES cells. Nat. Genet. 24:372–376. doi:10.1038/74199.

Okita K, Ichisaka T, Yamanaka S. 2007. Generation of germline-competent induced pluripotent stem cells. Nature 448:313–317. doi:10.1038/nature05934.

Pal R, Mamidi MK, Das AK, Bhonde R. 2012. Diverse effects of dimethyl sulfoxide (DMSO) on the differentiation potential of human embryonic stem cells. Arch. Toxicol. 86:651–661. doi:10.1007/s00204-011-0782-2.

Pan Gujin, Chang Zengyi, Er Hansrsch, Pei Du. 2002. Stem cell pluripotency and transcription factor Oct4. Cell Res. 12:321–329.

Papamichos SI, Kotoula V, Tarlatzis BC, Agorastos T, Papazisis K, Lambropoulos AF. 2009. OCT4B1 isoform: The novel OCT4 alternative spliced variant as a putative marker of stemness. Mol. Hum. Reprod. 15:269–270. doi:10.1093/molehr/gap018.

Pardo M, Lang B, Yu L, Prosser H, Bradley A, Madan Babu M, Choudhary J. 2010.

Resource An Expanded Oct4 Interaction Network: Implications for Stem Cell Biology, Development, and Disease. Stem Cell 6:382–395. doi:10.1016/j.stem.2010.03.004.

Pfaffl M. 2004. Quantification strategies in real-time PCR Michael W . Pfaffl. A-Z Quant. PCR:87–112. doi:http://dx.doi.org/10.1007/s10551-011-0963-1.

Plusa B, Piliszek, Anna, Frankenberg, Stephen, Artus J, Hadjantonakis A-K. 2008. Distinct sequential cell behaviours direct primitive endoderm formation in the mouse blastocyst. 135:3081–3091. doi:10.1242/dev.021519.Distinct.

Poh Y-C, Chen J, Hong Y, Yi H, Zhang S, Chen J, Wu DC, Wang L, Jia Q, Singh R, Yao, Wenting, Tan, Youhua, Tajik, Arash, Tanaka, Tetsuya S., Wang, Ning. 2014. Generation of organized germ layers from a single mouse embryonic stem cell. Nat. Commun. 5:1–12. doi:10.1038/ncomms5000.

Polak P, Oren A, Ben-Dror I, Steinberg D, Sapoznik S, Arditi-Duvdevany A, Vardimon L. 2006. The cytoskeletal network controls c-Jun translation in a UTR-dependent manner. Oncogene 25:665–676. doi:10.1038/sj.onc.1209114.

Rodriguez RT, Velkey JM, Lutzko C, Seerke R, Kohn DB, O'Shea KS, Firpo MT. 2007. Manipulation of OCT4 levels in human embryonic stem cells results in induction of differential cell types. Exp. Biol. Med. (Maywood). 232:1368–80. doi:10.3181/0703-RM-63.

Romito A, Cobellis G. 2016. Pluripotent stem cells: Current understanding and future directions. Stem Cells Int. 2016. doi:10.1155/2016/9451492.

Schrode N, Saiz N, Talia S Di, Hadjantonakis A-K. 2013. GATA6 levels modulate primitive endoderm cell fate choice and timing in the mouse blastocyst. Magn Reson Imaging 31:477–479. doi:10.1016/j.immuni.2010.12.017.Two-stage.

Shaulian E, Karin M. 2002. AP-1 as a regulator of cell life and death. Nat Cell Biol 4:E131-6. doi:10.1038/ncb0502-e131.

Shi G, Jin Y. 2010. Role of Oct4 in maintaining and regaining stem cell pluripotency. Stem Cell Res. Ther. 1.

Takahashi K, Yamanaka S. 2006. Induction of pluripotent stem cells from mouse embryonic and adult fibroblast cultures by defined factors. Cell 126:663–676. doi:10.1016/j.cell.2006.07.024.

Velkey JM, Sue O 'Shea K. 2003. Oct4 RNA interference induces trophectoderm differentiation in mouse embryonic stem cells. Genesis 37:18–24. doi:10.1002/gene.10218.

Veluscek G, Li Y, Yang SH, Sharrocks AD. 2016. Jun-mediated changes in cell adhesion contribute to mouse embryonic stem cell exit from ground state pluripotency. Stem Cells 34:1213–1224. doi:10.1002/stem.2294.

Wang J, Rao S, Chu J, Shen X, Levasseur DN, Theunissen TW, Orkin SH. 2006. A protein interaction network for pluripotency of embryonic stem cells. Nature 444:364–368. doi:10.1038/nature05284.

Wang X, Dai J. 2010. Concise review: Isoforms of OCT4 contribute to the confusing diversity in stem cell biology. Stem Cells 28:885–893. doi:10.1002/stem.419.

Wang X, Zhao Y, Xiao Z, Chen B, Wei Z, Wang B, Zhang J, Han J, Gao Y, Li L, Zhao, H, Zhao, W, Lin, H, Dai, J. 2009. Alternative translation of OCT4 by an internal ribosome entry site and its novel function in stress response. Stem Cells 27:1265–1275. doi:10.1002/stem.58.

Wang Z, Oron E, Nelson B, Razis S, Ivanova N. 2012. Specification roles for NANOG, OCT4, and SOX2 in human embryonic stem cells. Stem Cell 10:440–454. doi:10.1016/j.stem.2012.02.016.

Wilkinson DG, Bhatt S, Ryseck R-P, Bravo R. 1989. Tissue-specific expression of c-jun and junB during organogenesis in the mouse. Development 106:465–471.

Yamaguchi S, Kimura H, Tada M, Nakatsuji N, Tada T. 2005. Nanog expression in mouse germ cell development. Gene Expr Patterns 5:639–646. doi:10.1016/j.cell.2006.07.024.

Yan XR, Yang YH, Liu W, Geng WX, Du HC, Cui JH, Xie X, Hua JL, Yu SM, Li LW, Chen, FL. 2013. Differentiation of neuron-like cells from mouse parthenogenetic embryonic stem cells. Neural Regen. Res. 8:293–300. doi:10.3969/j.issn.1673-5374.2013.04.001.

Zeineddine D, Papadimou E, Chebli K, Gineste M, Liu J, Grey C, Thurig S, Behfar A, Wallace VA, Skerjanc IS, Pucé At, M. 2006. Oct-3/4 dose dependently regulates specification of embryonic stem cells toward a cardiac lineage and early heart development. Dev. Cell 11:535–546. doi:10.1016/j.devcel.2006.07.013.

Zinchuk V, Zinchuk O, Okada T. 2007. Quantitative colocalization analysis of multicolor confocal immunofluorescence microscopy images: Pushing pixels to explore biological phenomena. Acta Histochem. Cytochem. 40:101–111. doi:10.1267/ahc.07002.

APPENDICES

APPENDIX A

Appendix A: Whole electrophoresis gels used in Figure 4, 5, and 8. A. gel of *Gapdh* and *Sox2* primers amplifying cDNA from mESCs. *Gapdh* was used in Figure 5, but this *Sox2* set was not used. **B.** Gel of *Nanog* and pLVXcJun amplified cDNA used in Figure 5. **C.** Gel of *Sox2* used in Figure 5. **D.** Gel of *Oct4*A primers amplifying genomic and cDNA. **E.** Gel of *Gata4* and *Gata6* amplification of cDNA used in Figure 8. Lanes 1, 2, and 6 are *Gata6* and 3, 4, and 5 are *Gata4.* **F.** Gel of *Sox1* and *Brachyury* amplification of cDNA used in Figure 8. **G.** Gel of *cJun* amplification of cDNA used in Figure 5. **H.** Gel of cJun and pLVXcJun amplification of transfection samples used in Figure 4. **I.** More extreme example of multiple bands produced by *cJun* amplification of transfection samples. Used in Figure 4.

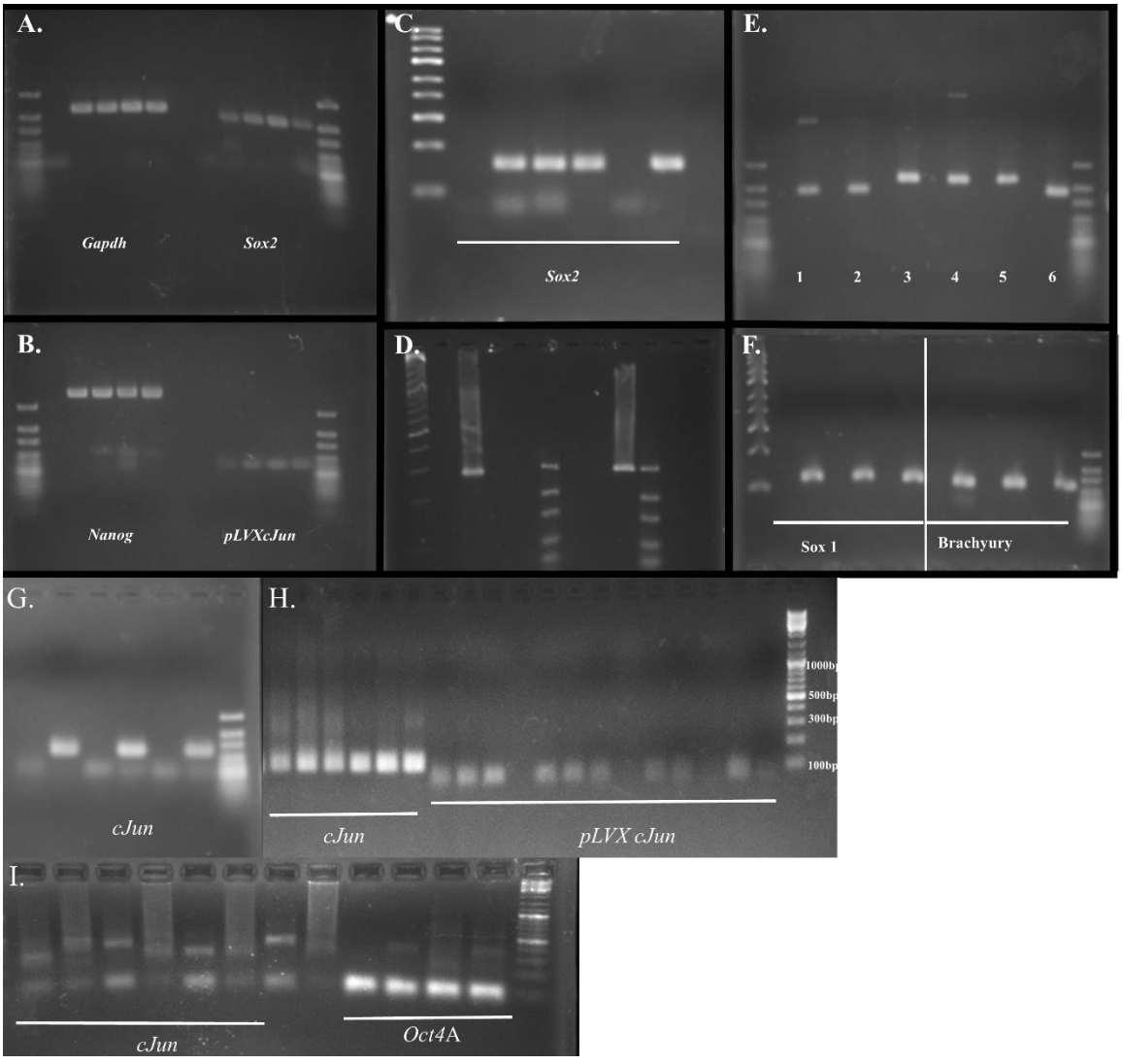

APPENDIX B

Appendix B: Primers used for RT-qPCR. The primer name, sequence, expected amplicon size, annealing temperature used, and qPCR efficiency data, r^2, slope and efficiency are given. Primers for *cJun, Sox2, Nanog, Oct4*A (exon 1), and *Oct4*all (exon 2 and exon 5) allowed us to assess the effect of cJun overexpression or nocodazole treatment on pluripotency and endogenous *cJun* transcription. The pLVXcJun primers allowed us to remove over expressed GFP-cJun mRNA from endogenous *cJun* expression in cells transfected with the GFP cJun construct and determine the autoregulatory effects of *cJun* on its own gene expression. *Gapdh* is a constitutively expressed control gene to account for unknown template concentrations. *Brachyury, Gata6, Gata4,* and *Sox1* expression provided information on whether changes in *cJun* expression initiate a differentiation program to a specific germ layer. Efficiencies determined the equation used to analyze the expression data. The Pffafl equation ($2^{-\Delta\Delta Ct}$) (Pfaffl 2004) requires that primer efficiencies be equal for the experimental gene as well as the control gene. The efficiencies below are different and analysis required a variation of the Pffafl equation which accounts for differences in primer efficiency. Expected base pair values marked with an asterisk denote the probe-based assays which produced other unexpected bands upon gel analysis.

Gene	**Sequence 5' to 3'**	**Expected bp**	**Annealing temp (°C)**	r^2	**Slope**	**Efficiency**	**Citation**
cJun-R	CACCTGTTCCCTGAGCATGTT	118	60	0.969737	-3.170345	1.067393207	Sprowles unpublished
cJun-F	CTCCAAGTGCCGGAAAAGGAA						
Nanog- R	AGGGTCTGCTACTGAGATGCTCTG	364	61	0.994614	-3.466201	0.943122998	(Chen et al. 2012)
Nanog- F	CAACCACTGGTTTTTCTGCCACCG						
Gapdh-R	CGAGTTGGGATAGGGCCTCTCTTGC	230	63 61 60	0.902912 0.952598 0.839916	-2.874308 -2.973768 -3.133186	1.227972507 1.169070714 1.085277915	(Chen et al. 2012)
Gapdh-F	GGTTGTCTCCTGCGACTTCAACAGC						
Sox2-R	TGCTGCGAGTAGGACATGCTGTAGG	207	63	0.974698	(-)3.87294	0.812181863	(Chen et al. 2012)
Sox2-F	GCACATGAACGGCTGGAGCAACG						
*Oct4*A exon 1-R	CCTCCTCTGAGCCCTGT	111bp	60	0.929277 For SYBR: 0.981957	-3.481575 For SYBR: -3.694379	0.9374313692 For SYBR: 0.8650113822	IDT predesign qPCR assays
*Oct4*A exon 1-F	AACTGTTCTAGCTCCTTCTGC						
*Oct4*A probe	TGGTTCCACCTTCTCCAACTTCACG						
*Oct4*all exon 2-R	GGTGATCCTCTTCTGCTTCAG	91, 296, 297	60	0.945009	-3.145305	1.079381572	IDT predesign qPCR assays
*Oct4*all exon 2-F	CAGATAGGAACTTGCTGGGT						
*Oct4*all exon 2 probe	CTGTTCTAGCTCCTTCTGCAGGGC						

Gene	**Sequence 5' to 3'**	**Expected bp**	**Annealing temp (°C)**	r^2	**Slope**	**Efficiency**	**Citation**
*Oct4*all exon 5-R	GTAGCCTCATACTCTTCTCGTTG	135, 274	60	0.988651	-3.209814	1.049012142	IDT predesign qPCR assays
*Oct4*all exon 5-F	CCTACAGCAGATCACTCACAT						
*Oct4*all exon 5 probe	TCGAACCACATCCTTCTCTAGCCCA						
pLVX cJun-R	TTGAGGGCATCGTCGTAGAAG	70	61				Sprowles unpublished
pLVX cJun-F	CACTAGTGATTGCGGGCC						
Sox1-R	TTGAGCAGCGTCTTGGTCTTG	134	60	0.9876	-3.276507	1.019310351	(Yan et al. 2013)
Sox1-F	GCCGAGTGGAAGGTCATGTC						
Brachyury-R	TGCGTCAGTGGTGTGTAATGTG	117	63	0.975551	-3.298003	1.010082087	(Bernardo et al. 2011)
Brachyury F	TCTCTGGTCTGTGAGCAATGGT						
Gata4-R	ACCAGGCTGTTCCAAGAGTCC	225	63	0.940442	-3.264471	1.024549247	(Hu et al. 2013)
Gata4-F	CAGCAGCAGCAGTGAAGAGATG						
Gata6-R	GCCAGAGCACACCAAGAATCC	182	63	0.883441	-3.733367	0.852911716	(Poh et al. 2014)
Gata6-F	TCTACACAAGCGACCACCTCAG						

APPENDIX C

Appendix C: Whole gel images of Oct4 amplification of transfection samples. A. and **B.** are gels of exon 1 amplification of spinfection samples for all 4 replicates. **C-E.** Gels of exon 2 amplification of transfection samples. **F-G.** Gels of exon 5 amplification of transfection samples.

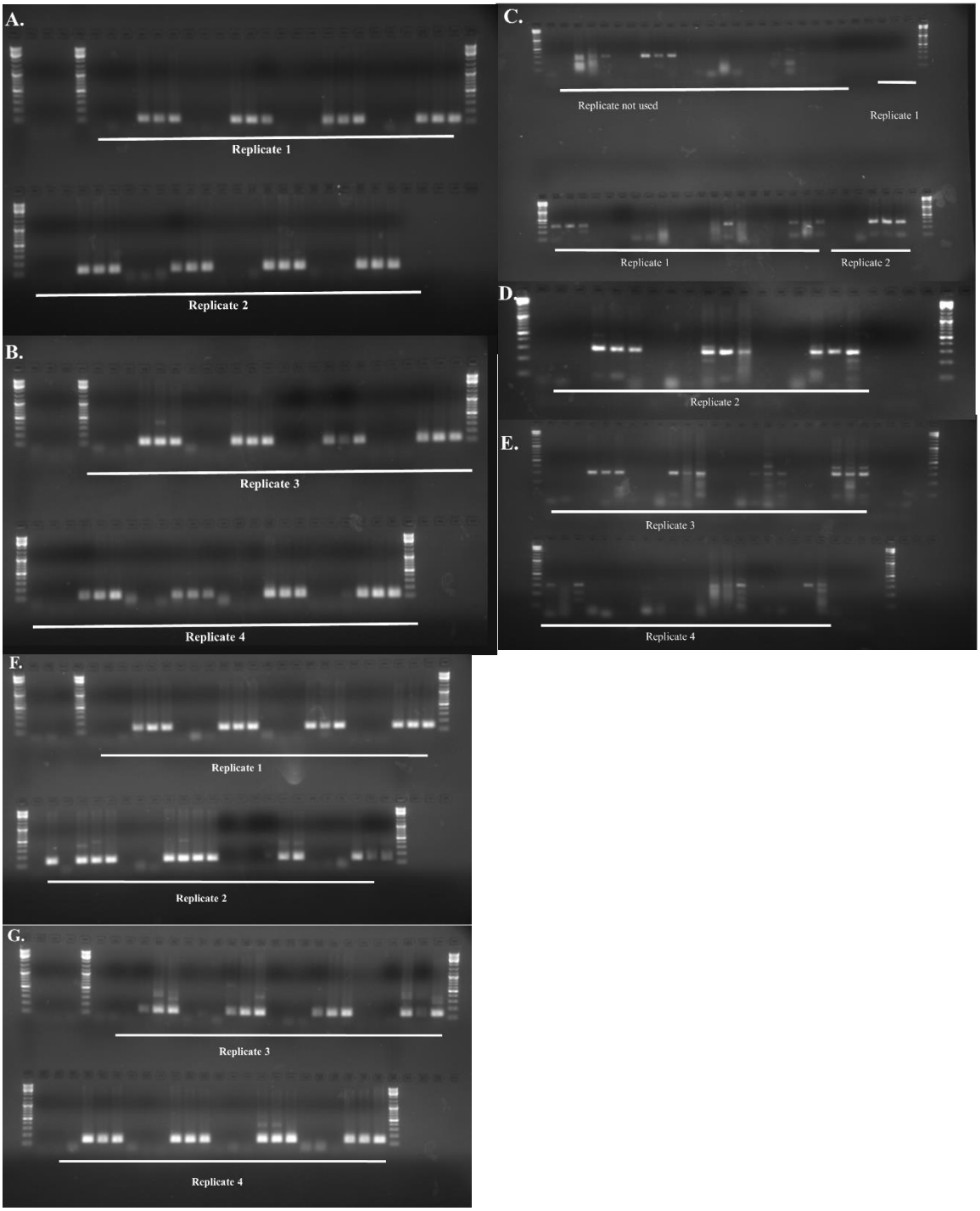
A.
Replicate 1
Replicate 2
B.
Replicate 3
Replicate 4
C.
Replicate not used
Replicate 1
Replicate 1
Replicate 2
D.
Replicate 2
E.
Replicate 3
Replicate 4
F.
Replicate 1
Replicate 2
G.
Replicate 3
Replicate 4

APPENDIX D

Appendix D: Whole gel analysis of nocodazole treated samples reveals inconsistency between replicates. A. Gel of exon 1 amplification of drug treated samples. **B.** Gel of exon 5 amplification of drug treated samples. **C.** Gel of exon 2 amplification of drug treated samples.

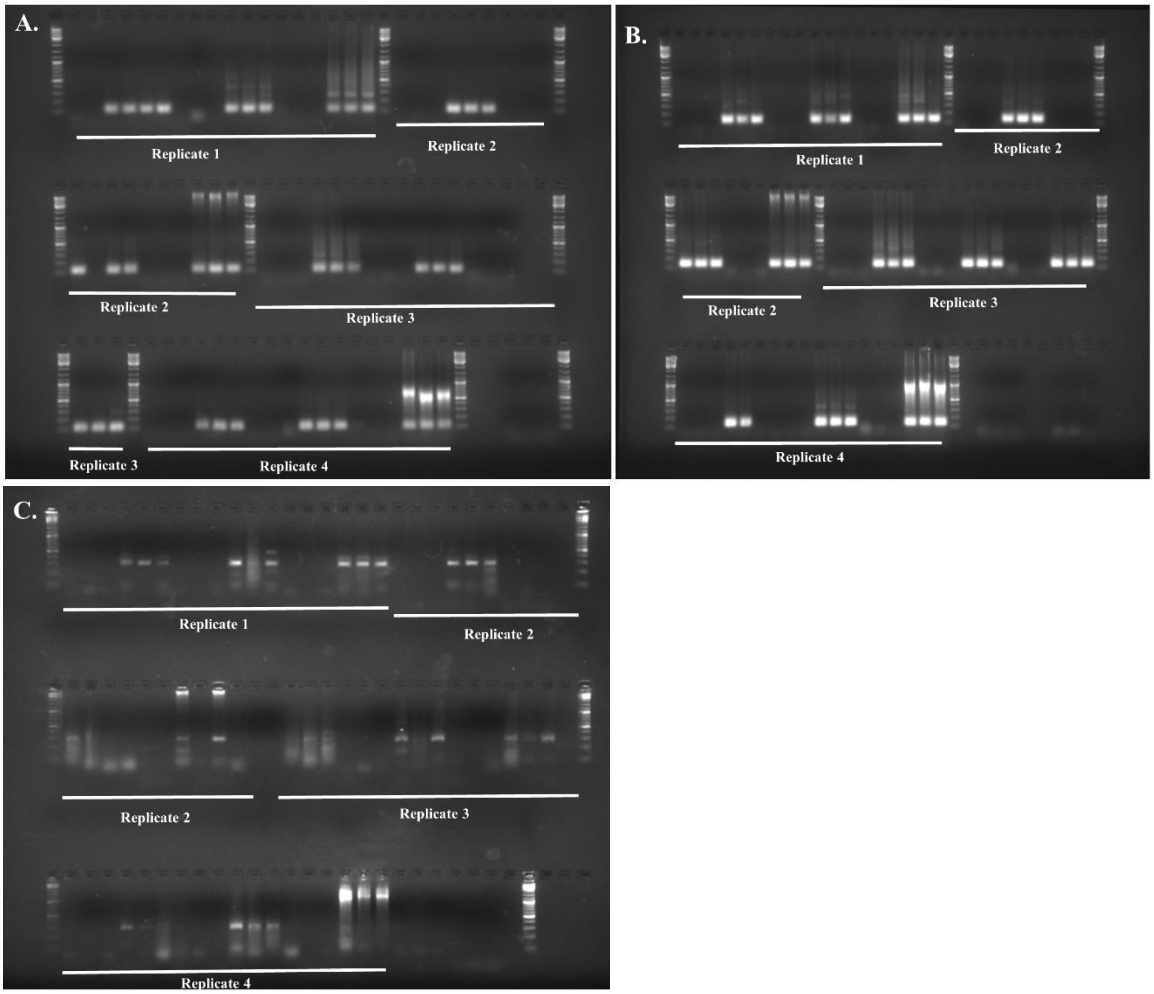

APPENDIX E

Appendix E: Table of Oct4 predicted bands, additional bands and treatment. This table highlights some of the variability in Oct4 expression seen with nocodazole treatment.

Primer set	**Expected bands**	**Bands present**	**Treatment**
Exon 1	1 band-111bp	111bp 200bp 400bp 600-700bp >10,000	All Nocodazole DMSO Nocodazole Nocodazole
Exon 2	Oct4b': 91bp Oct4b2 and 3: 296bp Oct4b and b1: 297bp	91bp-possibly 296-297bp 550bp Multiple 90-250 1,200-1,500bp >10,000	All All DMSO All Nocodazole Nocodazole
Exon 5	Oct4A, Oct4b', Oct4b and Oct4b1: 135bp Oct4b2 and 3: 274bp	135bp 274bp 250bp 300/350bp 400/450bp 900-1,000bp >10,000bp	All NT and some DMSO Some NT All but inconsistently Some NT and some nocodazole Some nocodazole Some nocodazole